

We are IntechOpen, the world's leading publisher of Open Access books Built by scientists, for scientists

6,300

Open access books available

171,000

International authors and editors

190M

Downloads

Our authors are among the

154

Countries delivered to

TOP 1%

most cited scientists

12.2%

Contributors from top 500 universities



WEB OF SCIENCE™

Selection of our books indexed in the Book Citation Index
in Web of Science™ Core Collection (BKCI)

Interested in publishing with us?
Contact book.department@intechopen.com

Numbers displayed above are based on latest data collected.
For more information visit www.intechopen.com



Enabling Optical Wired and Wireless Technologies for 5G and Beyond Networks

Isiaka A. Alimi, Ana Tavares, Cátia Pinho, Abdelgader M. Abdalla, Paulo P. Monteiro and António L. Teixeira

Abstract

The emerging fifth-generation mobile communications are envisaged to support massive number of deployment scenarios based on the respective use case requirements. The requirements can be efficiently attended with ultradense small-cell cloud radio access network (C-RAN) approach. However, the C-RAN architecture imposes stringent requirements on the transport networks. This book chapter presents high-capacity and low-latency optical wired and wireless networking solutions that are capable of attending to the network demands. Meanwhile, with optical communication evolutions, there has been advent of enhanced photonic integrated circuits (PICs). The PICs are capable of offering advantages such as low-power consumption, high-mechanical stability, low footprint, small dimension, enhanced functionalities, and ease of complex system architectures. Consequently, we exploit the PICs capabilities in designing and developing the physical layer architecture of the second standard of the next-generation passive optical network (NG-PON2) system. Apart from being capable of alleviating the associated losses of the transceiver, the proposed architectures aid in increasing the system power budget. Moreover, its implementation can significantly help in reducing the optical-electrical-optical conversions issue and the required number of optical connections, which are part of the main problems being faced in the miniaturization of network elements. Additionally, we present simulation results for the model validation.

Keywords: 5G, backhaul, centralized unit (CU), common public radio interface (CPRI), distributed unit (DU), fiber to the X (FTTX), fronthaul, functional split, optical wireless communication (OWC), passive optical network (PON), photonic integrated circuits (PICs), radio access network (RAN), radio over fiber (RoF)

1. Introduction

There have been growing concerns regarding the increasing number of unprecedented bandwidth-intensive mobile applications and services being experienced by the Internet. A notable cause of the increase in the traffic and the subsequent pressure on the network is the Internet of things (IoT) technologies. For instance, massive IoT (mIoT) schemes have caused remarkable revolutions in the amount of

mobile devices and applications in the networks. This is in an effort to enhance the user experience in delivering enhanced mobile broadband (eMBB) services and providing ultra-reliable low-latency communication (uRLLC) for critical communication and control services. In theory, IoT comprises universal existence of a collection of things like mobile PCs, tablets, smartphones, actuators, sensors, wireless routers, as well as radio-frequency identification (RFID) tags. It is remarkable that these devices are capable of cooperating not only with each other but also with their neighbors. By this approach, they are able to achieve common network goals by means of unique addressing scheme [1, 2]. Furthermore, it has been predicted that massive number of mobile devices on which various bandwidth-intensive applications and services will be operating and will be Internet connected [3]. In actual fact, there is a tremendous demand for effective systems that are capable of delivering various services in a cost-effective manner while meeting the essential network demands. Consequently, in an effort to accomplish the next-generation mobile network technical demands, there have been intensive researches on viable solutions that can satisfy the network requirements.

Additionally, to support the anticipated massive devices, there has been general consensus that the fifth-generation (5G) wireless communication system is the viable and promising solution. Meanwhile, massive multiple-input multiple-output (M-MIMO) antenna and millimeter-wave (mm-wave) technologies are anticipated to be integrated into the 5G networks, so as to enhance the wireless system bandwidth. This is due to the fact that radio-frequency (RF)-based wireless system transmission speeds are highly constrained by the regulated RF spectrum. This limitation can be attributed to numerous advanced wireless systems and standards such as UWB (IEEE 802.15), iBurst (IEEE 802.20), WiMAX (IEEE 802.16), Wi-Fi (IEEE 802.11), as well as the cellular-based 3G and 4G. On the other hand, there is a vast amount of unexploited and underutilized frequency at high bands [2, 4] as expatiated in Section 2. Nevertheless, the radio propagation at higher frequency bands is comparatively demanding. Consequently, advanced scheme like beamforming (BF) technique is essential for radio operation at the bands. The technique will help in compensating mm-wave band inherent path loss in the radio access network (RAN) [5–7].

In addition, owing to several innovative technologies that have been implemented in the optical communications, significant improvements have been noted in the network performance [8]. Among the remarkable improvements are the increase in the network reach, optical system capacity, and the number of users that can be effectively supported. This is as a result of cutting-edge optical fiber-based technologies. The optical schemes have been increasingly advancing deeper into different access networks, in order to provide various services such as mobile backhaul/fronthaul and multitenant fiber to the X (FTTX) with some variants of fiber-based broadband network architectures as discussed in Section 3. For instance, the optical broadband network architectures, such as fiber to the curb or cabinet (FTTC), fiber to the node (FTTN), fiber to the building (FTTB), fiber to the premise (FTTP), and fiber to the home (FTTH), proffer commercial solutions to the communication network performance bottleneck, by progressively delivering services in close proximity to the numerous subscribers [2].

It is noteworthy that various 5G use cases like uRLLC and eMBB can be effectively achieved by radio elements and BSs that are not far-off the end users or wireless devices. This is due to the fact that close proximity helps in facilitating better signal quality, with lower latency and higher data rates in the system [9]. This can be effectively realized by means of passive optical network (PON) technologies such as gigabit PON (GPON), 10Gbps PON (XG-PON), as well as Ethernet PON (EPON). It is noteworthy that one of the key issues is the process of supporting

different service demands with the intention of realizing ubiquitous and elastic connections. As a result, optical and wireless networks convergence is very indispensable. This is not only a cost-effective approach but also enables high-network penetration, in order to achieve the envisaged ubiquitous feature of the next-generation network (NGN) [2]. Based on this, there is a growing consensus of opinion that high-capacity optical fronthaul scheme is one of potential solutions for addressing the network demands. For instance, if the CPRI standard is to be directly employed for the transportation of a considerable number of long-term evolution-advanced (LTE-A) and/or 5G radio signals, an enormous aggregate bandwidth will be required on the backhaul/fronthaul networks [10].

Furthermore, it has been observed that the reference system architectures for the 5G standardizations are based on the notion of heterogeneous networks where mm-wave small cells are overlaid on the larger macrocells [9]. This will enable the RAN to handle the growing traffic demands. In addition, to contain the massive deployment of small-cell BSs, cloud RAN (C-RAN) has been adopted as a promising architecture to ensure effective scalability regarding deployment cost as well as energy consumption [11–14]. The C-RAN offers an innovative architecture that is really different from the traditional distributed RAN (DRAN). In the C-RAN architecture, the baseband unit (BBU) is shifted away from the cell sites where it is normally located in the DRAN. Consequently, BBU collections that are usually referred to as BBU pools are centralized at the central office (CO). With this configuration, the remote radio heads (RRHs) are left at the cell sites.

As a result, C-RAN implementation offers significant benefits such as improved system spectral efficiency and better flexibility for further RRH deployments than the DRAN. Likewise, with the centralized BBUs, C-RAN supports greener infrastructure, enhanced interference mitigation/coordination, better resource pooling, improved BS virtualization, as well as simplified management and operation. Besides, multiple technologies can be supported with smooth and scalable evolution. Furthermore, in the C-RAN architecture, the BBU pools are connected via the fronthaul network to the RRHs. It is remarkable that the de facto air interface standard that is usually employed for connecting the BBU pools to the RRHs is the common public radio interface (CPRI) protocol. This is an interface that helps in the digital baseband sample distribution on the C-RAN fronthaul. However, stringent requirements concerning jitter, latency, and the bandwidth are imposed on the fronthaul network for seamless connectivity. This makes the CPRI-based fronthaul links to be prone to flexibility and bandwidth limitations, which may prevent them from being viable solutions for the next-generation networks [11, 12]. Meanwhile, it has been noted that the 5G systems will impose higher requirements on the transport network regarding latency, bandwidth, reliability, connectivity, and software-defined networking (SDN) capability openness [15]. A number of approaches such as cooperative radio resource allocation and data compression technologies have been adopted to address the challenges; however, the fronthaul capacity demand is still considerable high [11, 12].

The viable means of addressing the capacity requirement is through the implementation of passive optical network (PON) solutions such as wavelength division multiplexed PON (WDM-PON) and ultradense WDM-PON (UDWDM-PON). The PON architectures are compatible with the 5G networks and are capable of supporting both wired and wireless services. Based on the PON architecture, individual RRH has the chance to communicate with the BBU pools using a dedicated wavelength. Besides, in the upstream direction, the aggregate wavelengths can be further multiplexed into a single shared fiber infrastructure at the remote node (RN). They can eventually be de-multiplexed at the CO [11, 12]. As aforementioned and as depicted in **Figure 1**, optical and wireless network convergence is a

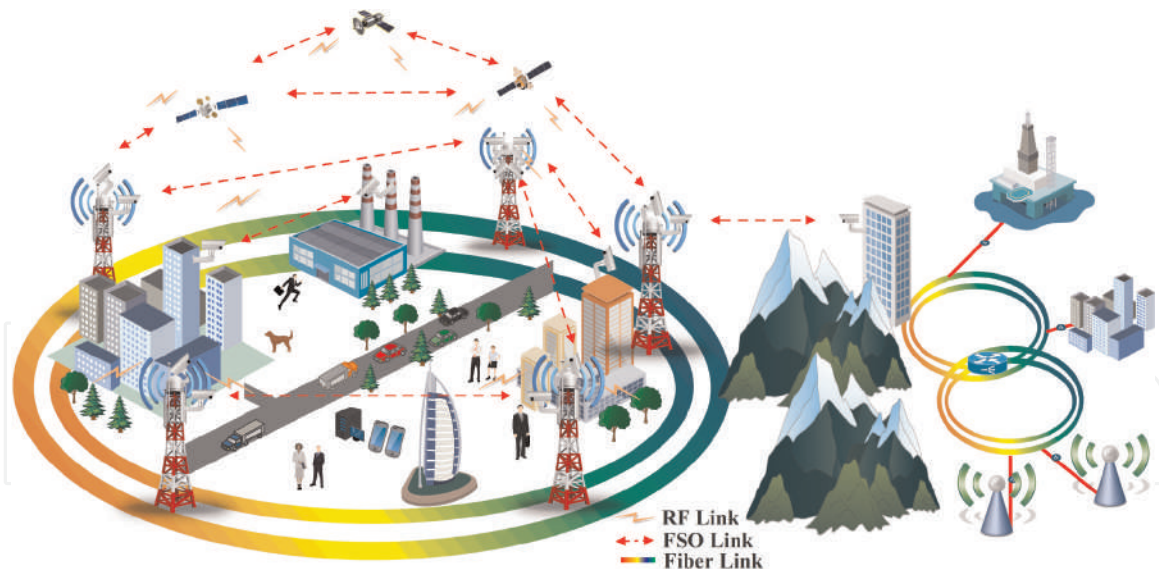


Figure 1.

A scenario for optical and wireless access networks convergence (adapted from Alimi et al. [2]).

promising scheme for exploiting the optical system inherent bandwidth and the mobility advantage of wireless connectivity, which can help in realizing the 5G network envisaged capacity and energy efficiency. In addition, optical wireless communication (OWC) is another feasible and attractive optical broadband access solution that is capable of supporting high-capacity, high-density, and low-latency networks. Therefore, it can effectively address the network requirements for different applications and services at a comparatively lower cost. So, it has been seen as an alternative and/or complementary solution for the existing wireless RF solutions [4, 16–18]. This chapter presents optical wired and wireless networking solutions for high-capacity, high-density, and low-latency networks. Furthermore, because of its potential for intense revolution and salient advantages, we focused on the second standard of the next-generation PON (NG-PON2) system. In addition, with the exploitation of notable features of photonic integration, we design and develop the physical (PHY) layer architecture of the NG-PON2 system. The proposed NG-PON2 architectures offer an enabling platform for active device integration into the chip to ensure a significantly low propagation loss. We also present simulation results for model validation. This helps in demonstrating the potential of photonic integration for optical architectures.

Furthermore, with concise information on the enabling optical wired and wireless technologies and the need for alleviating the stringent requirements in the network being introduced, we present comprehensive overview of the fronthaul transport solutions in Section 2. The salient needs for PON in the envisaged ultradense network deployments are considered in Section 3. In Section 4, a practical method for network investment optimization by the operators based on PON system coexistence is discussed. In Section 5, we present a number of viable schemes for alleviating the imposed stringent requirements in the system. The NG-PON2 PHY architecture design and development based on photonic integration are demonstrated in Section 6. In Section 7, the obtained simulation results with further discussion are presented. Section 8 concludes the chapter.

2. Fronthaul transport solutions

The fronthaul protocol can be transported by different viable means. Apart from the usually employed small form pluggable and serial constant bit rate CPRI

specification that is based on digital radio over fiber (D-RoF) implementation, there are other innovative and standard fronthaul interfaces such as Open Base Station Architecture Initiative (OBSAI), next-generation fronthaul interface (NGFI), open radio interface (ORI), and enhanced CPRI (eCPRI) that can be used [19–21]. In [11], we give an overview of various prospective and standard fronthaul interfaces. In this chapter, for reference purposes, we focus on the extensively employed CPRI protocol. However, it should be noted that the transport methods to be discussed in this section are applicable to other fronthaul interfaces. The transport methods discussed in this section are grouped into wired and wireless fronthaul solutions.

2.1 Wireless fronthaul solution

Wireless transport schemes are very viable fronthaul solutions that have resulted into tremendous evolutions in the communication systems. This is due partly to the inherent advantages such as operational simplicity, ease of deployment, scalability, roaming support, effective collaboration, and cost-effectiveness. Furthermore, it is an appropriate scheme for complementing fiber-based fronthaul solutions. However, their susceptibility to transmission channel conditions makes their implementation effective for short range. Besides, the current solution can only support few CPRI interface options. This brings about bandwidth limitation for this solution. Moreover, to alleviate this, promising wireless technologies like mm-wave and wireless fidelity (Wi-Fi) can be employed in the fronthaul [11, 22, 23].

As aforementioned in Section 1, there is a huge amount of unexploited and underutilized frequency at high bands. The fronthaul in which mm-wave is being employed is feasible due to the availability of various compact and high-dimensional antenna arrays for commercial use in the band. Besides, as a result of 60 GHz standards like 802.11ad, 802.15.3c, and WirelessHD that have been issued, considerable attention has been given to mm-wave communications. Nonetheless, the inherent high propagation losses of the mm-wave communications give rise to comparatively shorter transmission range [11, 22, 24, 25].

In addition, as stated in Section 1, RF-based system transmission speeds are substantially limited due to a number of advanced wireless systems being deployed in the network. Consequently, to meet the demands of the current and future wireless networks, many chipset suppliers and wireless operators have been paying significant attention to the unlicensed spectrum. The major focus is in the 2.4 GHz and 5 GHz frequency bands that are under implementation by the Wi-Fi. This is being used for the 5G LTE-Unlicensed communication systems [11, 26]. With this implementation, the unlicensed spectrum resources could be effectively allotted to the LTE system, in order to have more capacity for supporting the Wi-Fi users [27].

Furthermore, it is remarkable that the Wi-Fi unlicensed spectrum is a promising solution for the fronthaul network. A notable advantage of exploiting the unlicensed spectrum for the fronthaul network is due to the fact that separate frequency procurement for the fronthaul might not be necessary for the network providers. Besides, the same spectrum could be effectively reused in the access and fronthaul links. This can be accomplished by means of time-division multiplexing (TDM) and frequency-division multiplexing (FDM) schemes. Another way of achieving this is through opportunistic fronthauling, in which unlicensed spectrum can be sensed. For instance, the RRH can sense unlicensed spectrum that is available (unused unlicensed spectrum) and then employ it for fronthauling. Besides, in a situation where the active user signal is considerably lower than the predefined threshold, the RRH can also make use of the spectrum. In addition, the fronthaul link constraints could be effectively eased via the Wi-Fi. This is majorly due to the fact that it can be employed for offloading [26]. Although Wi-Fi networks are

capable of offering relatively high-data rates, they exhibit limited mobility and coverage. The drawbacks can be reduced by employing Wi-Fi mesh networks [11, 28].

2.2 Wired fronthaul solution

The wired network offers a number of advantages such as low interference, enhanced coverage, low latency, and high reliability and security. Due to these advantages, they have been able to stand the test of time and continue to be relevant despite the advent of wireless systems. Some of the fronthaul solutions that are based on wired links are dark fiber, passive WDM, WDM-PON, WDM/optical transport network (OTN), and Ethernet. In this subsection, we present potential wired-based fronthaul solutions that can support the network requirements.

2.2.1 Dark fiber solution

Dark fiber offers an attractive fronthaul solution. With this implementation, transmission equipment is not required between the BBU pools and the radio remote units (RRUs), consequently resulting in easiest deployment solution with least possible latency. Nevertheless, since dark fiber solution is based on point-to-point (P2P) direct connections, it lacks the required network protection, making it not a good candidate to support 5G use cases such as uRLLC services in which high reliability is required. Besides, its implementation demands huge amount of fiber resources. In the 5G systems in which ultradense networks are envisaged, the required amount of fiber is even more challenging. So, the fiber resources may be inadequate to support mMTC devices and other envisaged multimedia devices. Therefore, availability of fiber and the associated deployment cost may be the limiting factors for the dark fiber solution employment. This inefficiency can be addressed with the aids of different WDM and Ethernet solutions [11, 22, 23, 29].

2.2.2 Ethernet solution

In Ethernet-based fronthaul solution, packet technologies that encourage statistical multiplexing feature are employed. This helps in achieving traffic convergence and in enhancing the line bandwidth usage. Besides, considerable fiber resources can be saved due to its support for point-to-multipoint (P2M) transmission. Nevertheless, a number of issues such as identification as well as fast forwarding of low latency services deserve considerable research attention in this approach. Also, further efforts are required for backward compatibility with CPRI transmission and high-precision synchronization. Based on these, the Institute of Electrical and Electronics Engineers (IEEE) has established a task group known as time-sensitive networking (TSN) which is a part of the IEEE 802.1 working group, to study the latency-sensitive Ethernet forwarding technology. Reasoning along the same lines, the IEEE 1914 next-generation fronthaul interface (NGFI) working group has been established not only for the development of the NGFI transport architectures and the associated requirements but also for the definition of radio signal encapsulation specification into Ethernet packets [11, 29].

2.2.3 WDM-based solution

The requirement for low-latency transmission in the range of 10-Gb/s makes WDM-based network the usually adopted option for the fronthaul links. At large, WDM-based fronthaul methods can be grouped into two solutions which are active

and passive. In active solution, other protocols are used for the CPRI traffic encapsulation, before being multiplexed on the fronthaul network. Also, the solution offers robust network topologies with considerable flexibility. Moreover, with optical amplifiers, the network reach can be significantly extended. Another important distinguishing feature of an active solution is that the cell site demarcation point requires power supply for operation. On the other hand, a passive solution mainly depends on CPRI link passive multiplexing (MUX)/demultiplexing (DEMUX). Besides, this solution's demarcation point can function effectively without any battery backup and power supply. Nonetheless, active equipment can be employed for the system monitoring at the CO demarcation point [11, 22, 23, 29].

In general, the main dissimilarities between the passive and active solutions can be recognized in the nature of their routing table and switching granularity. For instance, unlike the active solution, routing table can be statically and dynamically configured as well as associated with the interface; that of passive solution is fixed and lacks configuration capability. Likewise, the passive solution switching granularity is based on spectrum or time slot as being implemented in the TWDM-PON, while an active solution presents finer switching granularity which can be based on packet or frame switching. Consequently, the active solution offers better configuration flexibility; however, it is power-consuming and relatively complicated [12]. In the following, we expatiate on different WDM-based fronthaul solutions.

2.2.3.1 Passive WDM

In this approach, a passive optical MUX/DEMUX is employed for multiplexing a number of wavelengths on a shared optical fiber infrastructure for onward transmission. Therefore, the implementation can save considerable fiber resources via the support for multiple channels per fiber. Also, the employed optical components introduce negligible latency, so, the stipulated jitter and latency requirements for CPRI transport can be effectively met. Moreover, due to the passive nature, power supply is not required for the associated equipment operation. This brings about high power efficiency in the network. Besides, this approach is not only a cost-effective solution but also offers simple maintenance. Nevertheless, the cost implication of the wireless equipment deserves significant attention. This is due to the required colored optical interfaces at the BBU and RRU. Also, factors that need consideration are the limited transmission range and inadequate optical power budget of a relatively complex topology such as chain or ring network. This can be attributed to the accumulated insertion loss owing to multiple passive WDM components. Besides, the approach offers no robust operations, administration, and maintenance (OAM) potentials, and usually, line protection is not provided. Passive WDM implementation can also be limited by the need for well-defined network demarcation points [11, 22, 23, 29].

2.1.3.2 WDM/OTN

When WDM/OTN scheme is employed, multiplexed and transparent signal transmissions can be achieved over the fronthaul link to multiple sites. Thus, the fiber capacity is increased by enabling multiple channels on a shared fiber infrastructure [11, 23, 29]. This can be realized by encapsulating the inphase and quadrature component (I/Q) data by means of OTN frame; this is subsequently multiplexed to the WDM wavelength. Consequently, any wavelength can be employed for routing the resulting frame to the destination port [12]. Apart from being able to save fiber resources, other notable advantages of this solution are provision for OAM capabilities, network protection, service reliability, as well as

service level agreement (SLA) management and network demarcation. Furthermore, this solution presents attractive features regarding low latency and high bandwidth. It is also a good approach for attending to the required colored optical interface at BBU and RRU by the passive WDM. Since colored optical interface is not demanded, wireless equipment deployment challenges are alleviated drastically by the WDM/OTN solution. Another significant advantage of the approach is the offered easy scalability. This is due to the fact that there is no need for replacing the wireless equipment optical interfaces while upgrading from non-C-RAN to the C-RAN architecture. Notwithstanding, the major drawback of the solution is the relatively higher cost of the equipment. Although power supply is not required for WDM transport in the approach, it is essential for wavelength translation and active management [11, 23, 29].

In addition, the WDM-based systems such as coarse WDM (CWDM) and dense WDM (DWDM) exhibit promising features for the fronthaul transport applications. For instance, apart from the offered high throughput and low latency, CWDM is very cost-effective regarding fiber resource usage and equipment expenses. Also, DWDM is widely known for the higher channel counts that can be efficiently supported. This can help further in increasing the number of small cells and the associated RRHs that can be deployed effectively. Furthermore, it helps in improving the fiber resource efficiency.

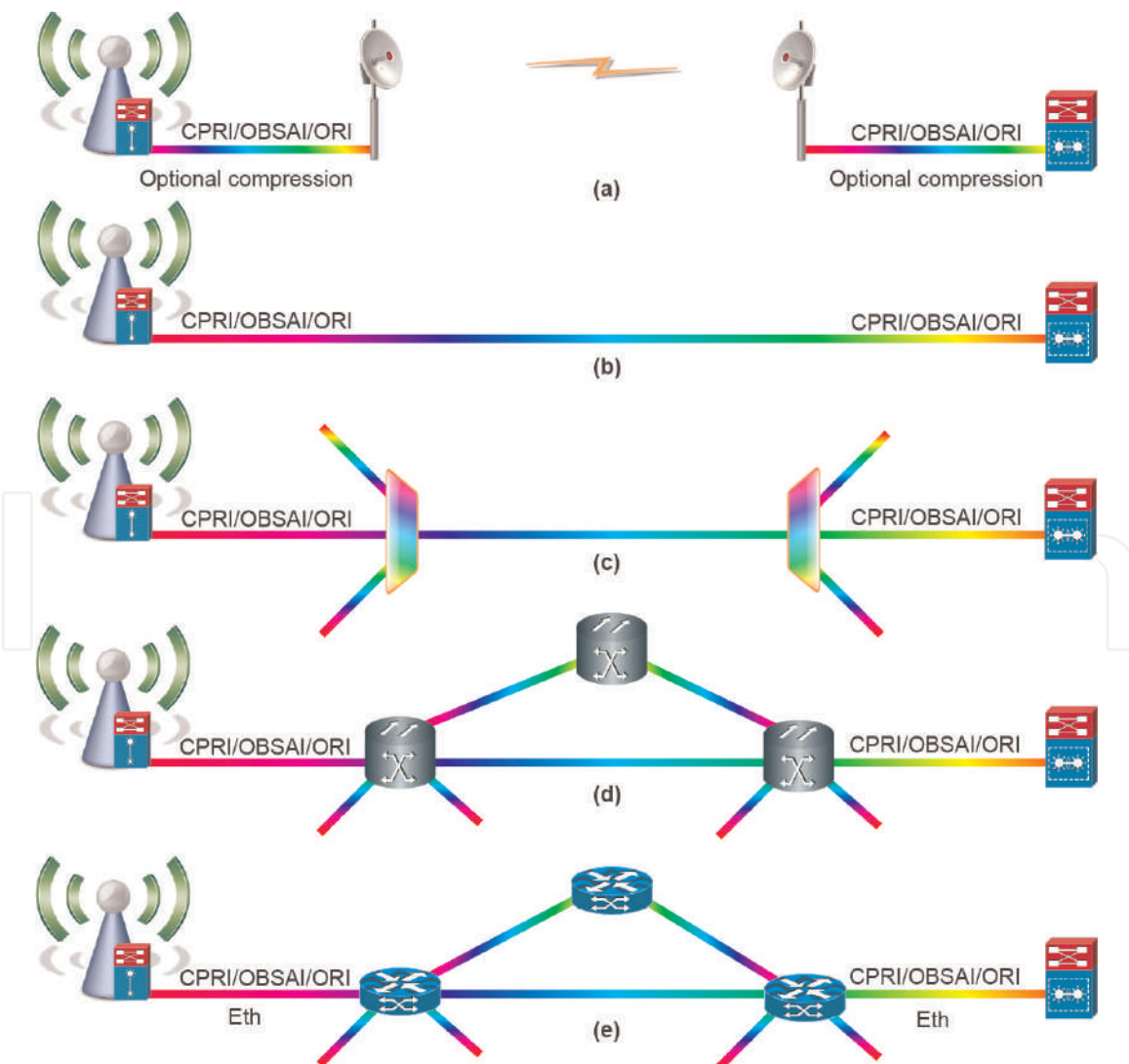


Figure 2. Potential 5G fronthaul solutions: (a) microwave, (b) point-to-point, (c) WDM-PON, (d) OTN, and (e) Ethernet.

It is remarkable that WDM-based schemes can be used in conjunction with PON technology in order to further enhance the system performance. This scheme is highly appropriate for the anticipated massive RRHs and ultradense small cell deployment as explicated in Section 3. It should be noted that, for RAN to be well deployed, especially in the urban environments, the radio elements should be, as much as possible, in close proximity to the subscribers. So, the remote elements could be mounted on different places such as buildings and street lamp poles. Therefore, the arbitrary nature of the remote element placement can be efficiently supported with the implementation of WDM schemes.

Furthermore, as discussed, there are a number of ways by which the C-RAN fronthaul can be realized; nonetheless, the imposed stringent requirements make fiber-based method the widely adopted in the C-RAN. However, optical fiber implementation for ultradense networks, besides being time-consuming, may render the C-RAN schemes uneconomical and less flexible. It is remarkable that wireless fronthaul offers attractive and flexible solutions for information exchange between the centralized unit (CU) and distributed unit (DU). This is owing majorly to the offered advantages such as higher flexibility, lower cost, and undemanding deployment when than the fixed wired fronthaul counterparts. Therefore, innovative optical wireless solutions with good scalability and operational simplicity, coupled with easy of deployment, are really desirable [11].

In addition, apart from physical fiber-based methods being discussed, OWC system, also known as a free-space optical (FSO) communication system, is another attractive and feasible optical wireless fronthaul. The FSO provides a range of benefits such as low latency and high capacity that make it viable for addressing network requirements in a cost-effective manner [4, 16–18]. The potentials for the FSO implementation in the fronthaul network and different innovative concepts that are appropriate for improving the FSO system performance, while easing the stringent system requirements, are discussed in Section 5. Different potential 5G fronthaul solutions are depicted in **Figure 2**.

3. Passive optical network (PON)

The existing fiber-based methods as well as active P2P Ethernet might unable to meet the envisaged bandwidth-intensive traffic requirements by the 5G and beyond networks. For instance, ultradense network deployments with the associated huge network resources are envisaged in the 5G network. As illustrated in **Figure 3**, PON system can make better use of the current fiber infrastructures than the existing P2P system such as CPRI. This helps considerably in reducing the required number of interfaces in the network. As a result, it aids not only in reducing the site space, but also substantial amount of system power can be saved [30]. As explained in Section 2, PON technology has been deemed as an attractive access network solution owing to the presented advantages such as low-operation cost, high bandwidth, and low-maintenance cost [11, 31, 32].

It should be noted that the PON architectures have been experiencing continuous and gradual evolution, so as to considerably enhance the service availability and the related data rates. The offered technological options and the intrinsic benefits have been attracting the operators in deploying a number of PON systems. It has been observed that the most widely deployed one is the gigabit PON (GPON) system. Moreover, the first standard 10 Gbps PON technology, the next-generation PON (NG-PON) system, known as 10-gigabit PON (XG-PON1) has also been gaining considerable attention. With continuous demand for further capacity, there are innovative PON generations such as 10-gigabit symmetric PON (XGS-PON)

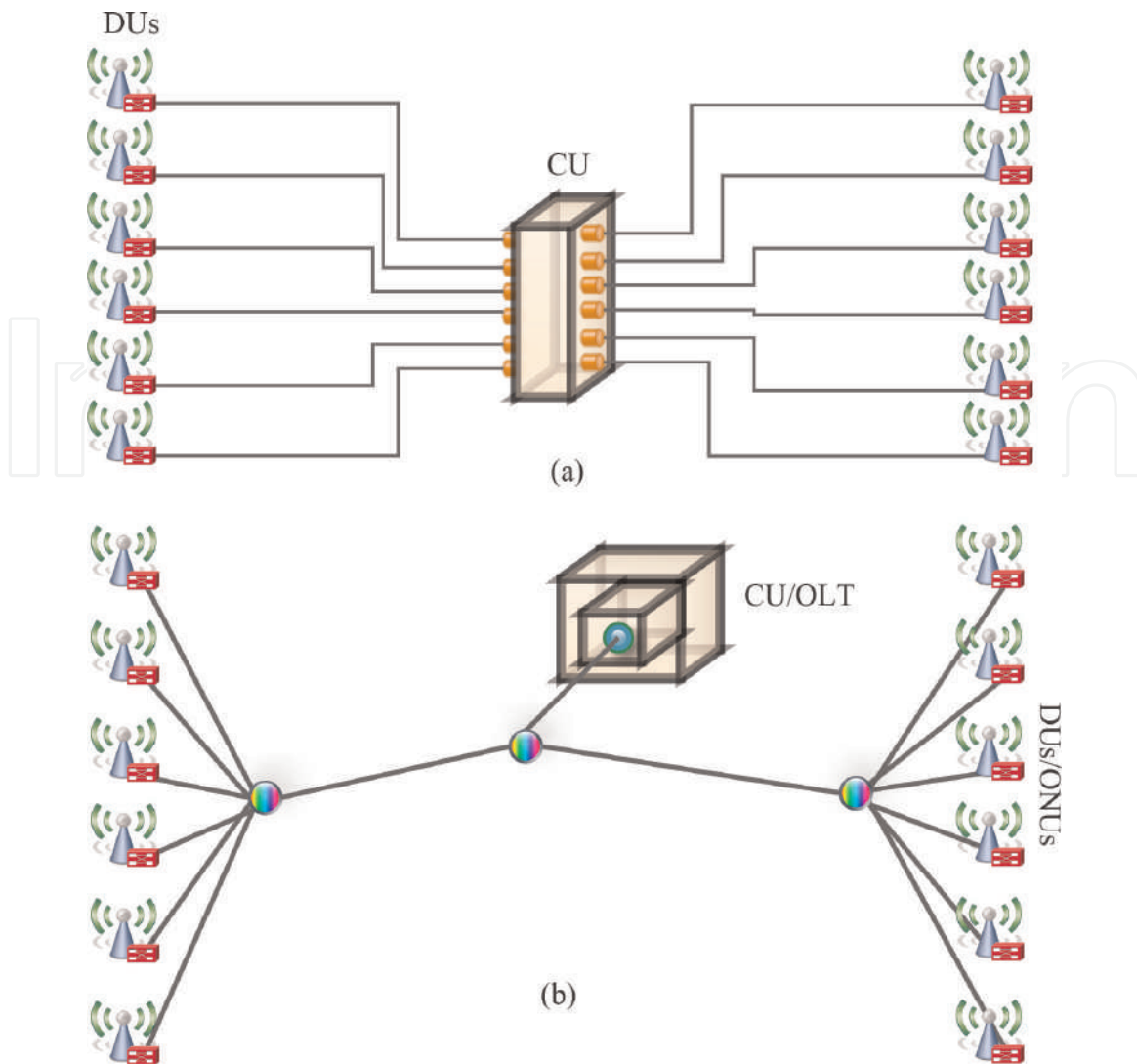


Figure 3.
Potential fronthaul solutions (a) CPRI-based and (b) PON-based schemes.

and the second standard of NG-PON (NG-PON2) that are now becoming the target of various providers [33]. In PON system, WDM and TDM techniques are normally employed to further enhance the capacity and fiber efficiency. Based on these techniques, the PON system can be broadly grouped into WDM-PON and TDM-PON.

Moreover, it is noteworthy that the TDM-PON is capable of giving considerable greater bandwidth for various data applications; however, availability of the resources that can be delivered to the end users is limited. In contrast, the issue can be effectively addressed with the WDM-PON scheme. This can be done by assigning a peculiar wavelength per subscriber. As a result of this, a distinct, high-data rate, as well as secure P2P channel, can be delivered over a high-capacity and longer optical reach, between each of the subscriber and the CU. Consequently, a WDM-PON scheme is suitable for partitioning the ONUs into a number of distinctive virtual P2P links over the shared physical optical infrastructure by multiple operators. This attribute facilitates fiber efficiency compared to P2P Ethernet. Similarly, in relation to TDM-based systems, it gives lower latency. These features make WDM-PON a disruptive solution that is very appropriate for FTTX as well as mobile backhaul and fronthaul applications. This will eventually aid the operators not only in developing converged networks but also in enhancing the current access networks. As a consequence of this, some redundant COs can be eliminated in an attempt to enhance the network performance in cost-effective ways [11, 31, 32].

Moreover, it is remarkable that advantages of both WDM-PON and TDM-PON can be effectively exploited though joint application of the schemes. This results in the TWDM-PON architecture. The potential PON architectures and their applications in telecommunication systems are presented in the subsequent subsections.

3.1 TDM-PON application

The TDM-PON can be grouped into broadband PON (BPON), asynchronous transfer mode (ATM) PON (APON), Ethernet PON (EPON), and GPON. In the existing telecommunication networks, GPON and EPON are the widely adopted schemes. Therefore, in the following, we focus on both schemes.

3.1.1 EPON application

The data traffic being encapsulated in the Ethernet frames as defined by the IEEE 802.3 standard is transported by the EPON solution. Different network elements such as optical network unit (ONU), optical line terminal (OLT), and optical distribution network (ODN) are the building blocks of a standard EPON system and other PON architectures. In the EPON solution, PON topology is exploited for getting the Ethernet access. Based on the joint schemes, EPON solution is capable of offering high bandwidth and good network scalability. Besides, due to the fact that it is highly compatible with Ethernet, network management can be supported in cost-effective manners. Likewise, as illustrated in **Figure 4**, FTTB, FTTC, and FTTH network architectures can be supported depending on the ONU deployments and demarcation point between the copper cable and optical fiber termination [32].

Typically, ONUs can be deployed beside the telegraph pole junction boxes, or else, at roadside when FTTC system is employed. Also, different types of twisted pair cables can be utilized for connecting the ONUs and the respective customer. It has been observed that FTTC technology offers a cost-effective and practical solution for delivering narrowband services. However, FTTC solution is not an ideal scheme, when broadband and narrowband services are to be incorporated [32].

Moreover, the ONU deployment can be made closer to the users in the FTTH solution. So, it can be located inside the buildings through further optical fiber penetration into customer homes. This can be achieved by means of cables, local

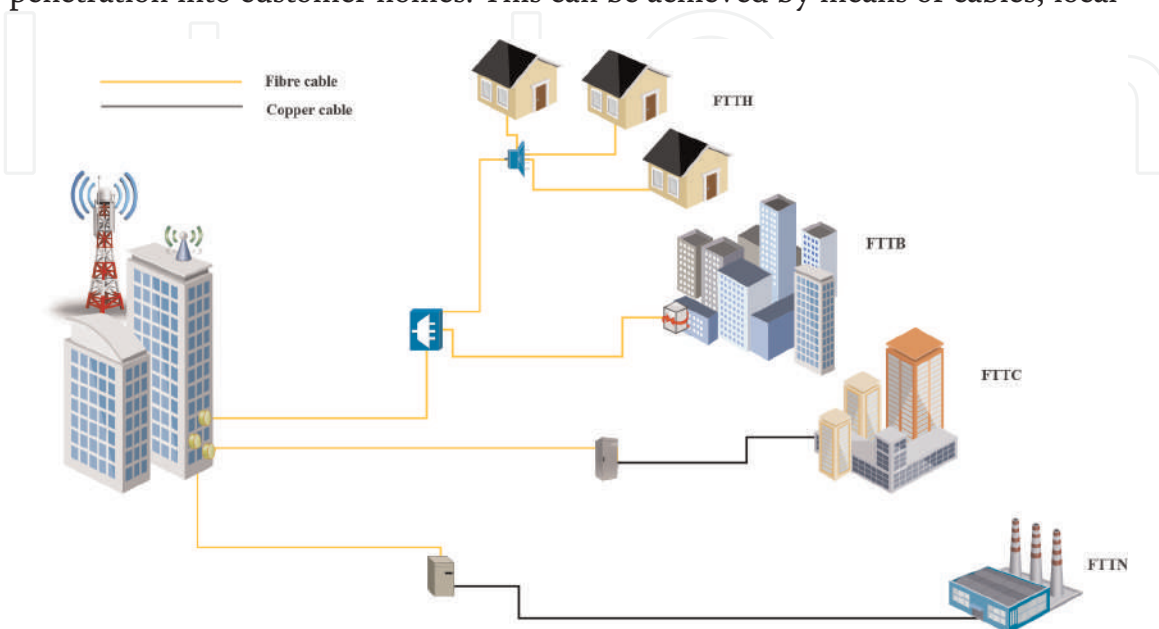


Figure 4.
FTTX architectures.

area networks (LANs), or asymmetric digital subscriber line (ADSL) broadband communication technologies. Relatively, FTTB employs more optical fiber in the connection than FTTC solution. This makes it more appropriate for broadband/narrowband service integration [32].

Furthermore, ONU deployment can take place right inside the subscribers' homes or offices in the FTTH solution. This facilitates a fully transparent network in which the ONUs are independent of the wavelength, bandwidth, as well as transmission mode and technology. These benefits enable FTTH scheme to be very ideal for access network implementations [32].

In addition, the discussed IEEE 802.3 Ethernet is a 1-Gbit/sec EPON standard. It is remarkable that there is a 10G EPON standard that is capable of supporting 10G/10G symmetric DS and US transmission. In another effort to attend to the system requirement, the IEEE 802.3ca task force has been working relentlessly on the development of 25G/50G/100G EPON standards. A notable feature of the entire EPON standards is that they are designed to be both backward and forward compatible. This is to ensure that legacy service, as well as innovative higher-speed service, can be effectively supported using the same ODN [34].

3.1.2 GPON application

Furthermore, to address the growing traffic demands, XG-PON1 has been presented. The XG-PON1 is capable of delivering higher data transmission than the legacy GPON system. Moreover, in an effort to keep the existing investments, it is backward compatible with the GPON. Also, the GPON ODN, as well as framing and management, is inherited by the XG-PON1. This encourages the reuse of the existing network elements [35].

3.2 WDM-PON application

The WDM-PON enables multiple-wavelength transmission through the multiple operators' shared optical fiber infrastructure rather than one wavelength in the PON system. This helps in ensuring that WDM-PON meets the huge subscribers' bandwidth demands. Furthermore, it presents various merits such as high wavelength efficiency and relatively simpler network management. This encourages support for various services than the TDM-PON. Besides, all anticipated services can be delivered over a shared communication network infrastructure.

In addition, it can effectively support different access networks such as FTTB, FTTH, and FTTC. Also, both small-scale and large-scale subscribers can be concurrently supported as well. Based on the inherent huge bandwidth, different types of BS bandwidth requirements can be appropriately met. Its implementation can also help in the network reach extension and in the current EPON network transition. This will help in keeping the current network investment while enhancing the network scalability [32]. In addition, UDWDM-PON offers a wavelength grid that is relatively denser for the WDM scheme. This helps not only in supporting a huge amount of aggregated wavelengths per fiber but also in accommodating higher number of RRHs per feeder fiber. Nonetheless, with the envisaged NGN stringent transport network requirements, UDWDM will be unable to maintain the high per-wavelength bit rates resourcefully. For instance, subcarriers' aggregation for high-speed services usually bring about considerable latency. Therefore, UDWDM implementation is preferred in situations where there are ultradense RRH deployments and inadequate feeder fiber accessibility. Besides, it also finds application in antenna sites which demand a low-peak but high sustainable rate [6]. As discussed in subsection 3.3, WDM-PON can be employed along with TDM-PON to achieve a

hybrid WDM-TDM-PON solution known as time and wavelength division multiplexed (TWDM-PON) scheme. Apart from being efficient for both small-scale and large-scale subscribers, the hybrid scheme offers a promising solution for applications in telecommunication environment.

3.3 TWDM-PON application

It is notable that TDM-PON implementation in the 4G networks offers a very cost-efficient solution for a wavelength channel sharing between the cell sites, by means of diverse time slot allocations for different cell sites. However, with the evolution of mobile networks, the major ITU-defined application scenarios such as eMBB, uRLLC, and massive machine-type communications (mMTC) could make TDM-PON solution unsuitable for the fronthaul transport network in the 5G and beyond networks. As aforementioned, a hybrid TWDM-PON scheme is a feasible solution with abundant bandwidth capable of supporting the fronthaul demands.

With the scheme, time slots, as well as wavelength resources, can be allocated dynamically between the RRHs. The offered centralized and virtualized PON BS can considerably help in the system energy savings. Likewise, the virtualized scheme presents a number of advantages such as low handover delay, excessive handover reduction, and better network reliability. This results in cost saving, cell-edge user throughput improvement, and enhanced mobility management [32, 36, 37]. The associated multiple wavelengths, as well as potential for wavelength tenability, give TWDM-PON unprecedented means of improving the network functionalities compared with the basic TDM-PONs [36, 37]. Likewise, orthogonal frequency-division multiplexed PON (OFDM-PON) is another promising PON solution. With OFDM, there is a comparable high potential for flexible bandwidth resource sharing as experienced in the TWDM. On the other hand, regarding the reach, the OFDM variants in which direct detection is employed usually present poor performance. Similarly, variants in which coherent detection is implemented are comparatively too expensive [6]. Furthermore, it is noteworthy that among its counterparts such as standard WDM-PON, optical code division multiplexed PON (OCDM-PON), and OFDM-PON that are capable of offering 40 Gb/s or higher (80 Gb/s) aggregated bandwidth, the full service access network (FSAN) community has chosen TWDM-PON as a major broadband solution. Apart from the inherent huge capacity with 1:64 splitting ratio, it has a long reach of 40 km. The salient features enable TWDM-PON system to meet the future broadband service requirements [37–39].

A typical TWDM-PON system architecture is depicted in **Figure 5**. In a conventional TWDM-PON solution, multiple wavelengths can effectively coexist in a shared ODN by means of WDM. Moreover, each of the wavelengths is capable of serving multiple ONUs through TDM access. With reference to the ITU-T recommendation, 4–8 wavelengths in L band (1590–1610 nm) and C band (1520–1540 nm) can be employed for the downstream (DS) and upstream (US) transmissions, respectively. Also, each of the DS wavelengths can operate at 10 Gb/s, while the US can function each at 2.5 or 10 Gb/s data rate [32, 37].

In addition, the TWDM-PON ONUs employ colorless tunable transceivers for selective transmission/reception of any US/DS wavelengths (data) via a pair of US/DS wavelengths. With this approach, the ONU inventory issue can be prevented. In essence, the transceiver features help in easing network deployment as well as inventory management. Furthermore, load balancing can be supported effectively in the TWDM-PON system. Besides, with dynamic wavelength and bandwidth allocation (DWBA) implementation, large bandwidth can be flexibly exploited. It is remarkable that TWDM-PON is a stack of four 10-gigabit PONs (XG-PONs) with

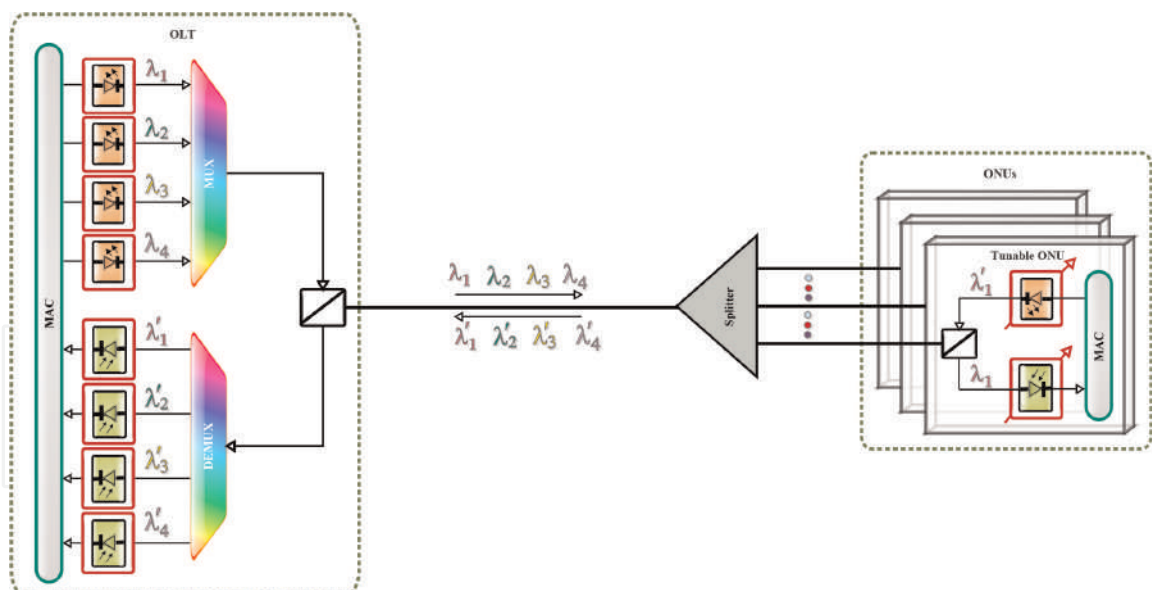


Figure 5.
Typical TWDM-PON architecture.

four pairs of wavelengths. In the stack, each XG-PON is operating on different wavelengths. Also, as stated earlier, the GPON and XG-PON GEM frames are compatible with and can be employed in the TWDM-PON solution. Based on this and the ability for coexistence with existing PON solutions, it is a viable scheme for optical access network swift evolution [11, 32, 37]. Consequently, TWDM-PON has been adopted for the NG-PON2. In NG-PON2, TWDM-PON can be employed with optional P2P WDM overlay extension. It is remarkable that DWDM scheme will enable NG-PON2 to deliver multiple unshared P2P connections, while TDM scheme simultaneously offers multiple P2M connections. This will enable the operators to efficiently support both fronthaul/backhaul and business services with the P2P WDM overlay technology, by using dedicated wavelengths [11, 40, 41].

In addition, based on the inherent colorless tunable transceivers of the TWDM-PON ONUs, three classes of wavelength channel tuning time have been specified for the NG-PON2 by the physical media dependent layer recommendation (ITU-T G.989.2). **Table 1** illustrates the specified tuning time classes by the G.989.2 recommendation. It should be noted that different innovative technologies can be exploited by the wavelength tunable devices in order to have the capability for supporting various classes. This will enable a number of potentials for the NG-PON2 system at relatively different costs. Out of the defined three classes, Class 3 is based on the slowest tunable devices. Consequently, it is applicable in scenarios with occasional tuning operations or in applications that can tolerate short service disruption. On the other hand, Class 1 wavelength tunable devices present the shortest tuning time. This feature makes them attractive for offering DWBA feature in the network. Besides, with this class implementation, the ONU transmission wavelengths can be dynamically controlled by the OLT for wavelength hopping between the transmission periods [42].

| | Class | | |
|-------------|-------------|---------------------|--------------|
| | 1 | 2 | 3 |
| Tuning time | <10 μ s | 10 μ s to 25 ms | 25 ms to 1 s |

Table 1.
Tuning time classes [42].

Although a TWDM-PON offers effective bandwidth resource allocation among multiple clients, meeting the low latency and jitter requirements of certain services may be challenging. Consequently, its implementation for the NGN RAN transport network depends mainly on the RAN use cases and deployment scenario requirements [6]. In Section 5, we present a number of viable means for alleviating the growing stringent requirements in the system. Furthermore, as aforementioned, the NG-PON2 system employs multiple wavelengths that demand for tunable transceivers at the ONUs. However, this requirement might hinder its implementation as the existing optical tunable transceivers are uneconomical. Based on this, a number of operators have been looking for ways around this by envisaging provisional scheme adoption before the full NG-PON2 migration. This will enable them to have a seamless transition with least possible or no disruption in the offered services. One of viable solution is the XGS-PON. It offers an improved commercial solution as a result of the less costly elements being employed.

3.4 XGS-PON application

The XGS-PON presents a novel technology that offers a generic solution for the NG-PON system. It can be viewed as an uncomplicated variant of TWDM-PON in which the wavelength tunability and mobility are eliminated for a more cost-effective reason. In addition, there can be an efficient coexistence between the XGS-PON and TWDM-PON using the same fiber infrastructure, since the employed wavelengths by each technology are different. Consequently, the operators can exploit the lower-cost XGS-PON for quick delivery of 10 Gbps services. This will also enable them to seize 10 Gbps services opportunities for immediate deployments. With XGS-PON, there can be cost-efficient, gradual upgrade, and well-controlled transition to a full TWDM-PON system, with minimum or no disruption to the offered services. It can also facilitate TWDM-PON system by enabling its deployment using the wavelength by wavelength approach. This will really help in pay-as-you-grow scheme for effective system upgrade and migration [33, 43].

Besides its capability for delivering 10 Gbps in both US and DS directions, XGS-PON has high potential for the dual rate transmission support as well [44]. Based on this, the 10/2.5G XG-PON ONUs and 10/10G XGS-PON ONUs can be coupled to the same OLT port via a native dual US rate TDMA scheme. It is remarkable that XGS-PON dual rate presents a comparable cost to XG-PON; nonetheless, it is capable of providing 4 times of the XG-PON US bandwidth. In addition, XGS-PON has been seen as a transitional scheme to NG-PON2 due to its ability for offering the associated NG-PON2 high-data rates in conjunction with the XG-PON1 CAPEX efficiency [33, 43]. Furthermore, it should be noted that the GPON employs 1490 and 1310 nm in the DS and UP, respectively. Likewise, XGS-PON utilizes 1578 and 1270 nm in the DS and UP, respectively. This implies that the XGS-PON service can be effectively overlaid on the same infrastructure as that of GPON. Similarly, the G.989 standard is employed in NG-PON2. The G.989 supports TWDM technologies and it is a multiwavelength access standard [44].

In addition, NG-PON2 is not only a state-of-the-art PON technology with the potential for intense revolution in the operational models of providers but also offers them flexible platform that is capable of enhancing their agility to the market demands as never before. Besides, it has the ability for cost-effective support for both the scale and capacity of the existing gigabit services while at the same time having more than enough room for the multi-gigabit bandwidth requirements of the future networks [38]. Consequently, based on the aforementioned advantages and its proficiency for multiple networks converging with outstanding

performance, in this work, we focus on the NG-PON2 system. Its PHY architecture and development are presented in Section 6.

4. PON system coexistence

Furthermore, in an effort to make considerable profit, different operators have been developing high-bandwidth demanding applications and services. Good examples of such notable ultra-broadband systems are high-definition television (TV) and mIoT. It has been envisaged that there will be a further increase in the bandwidth demand due to the innovative services such as online gaming, home video editing, interactive e-learning, next-generation 3D TV, and remote medical services. However, it should be noted that NG-PON system deployment entails huge initial investments. For instance, in the greenfield FTTH systems, out of the total network investments, the ODN deployment takes between 70 and 76%. Therefore, network investment optimization can be achieved by the operators with the existing ODN exploitation. Besides, compatibility between the NG-PON evolution and the present GPON system is highly essential [35, 44].

Moreover, efficient support for bandwidth-intensive applications and services depends on coexistence of different PON technologies. The coexistence will help in the network investment optimization when the existing ODNs are shared. For instance, a network in which service delivery is being offered by GPON and needs upgrade in order to support new FTTH access technologies can coexist with the PON technologies such as XGS-PON and NG-PON2. This can be realized with the aids of a coexistence element. Based on the desired scenario, various ONT and OLT

| | | Class | | | | | | | |
|------|-----------|-------|----|----|----|----|----|----|----|
| | | A | B | B+ | C | N1 | N2 | E1 | E2 |
| Loss | Min. (dB) | 5 | 10 | 13 | 15 | 14 | 16 | 18 | 20 |
| | Max. (dB) | 20 | 25 | 28 | 30 | 29 | 31 | 33 | 35 |

Note: The degree of severity of specific class requirements could vary from one system category to another.

Table 2.
ODN optical path loss classes [42, 46].

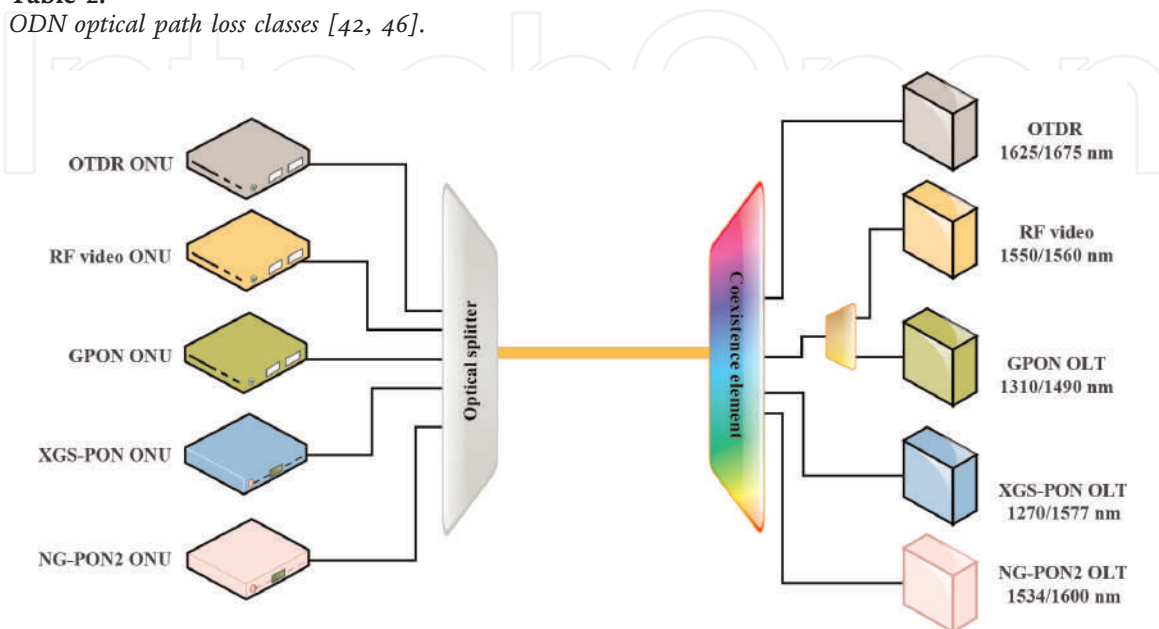


Figure 6.
PON system coexistence.

generations can effectively coexist over a shared ODN fiber infrastructure. Besides, optical time-domain reflectometer (OTDR) and RF signals can also coexist with the PON systems. This is mainly due to the fact that there is no wavelength overlap between each of the technologies. So, this permits in-band measurement without any service interruption [34, 45]. Different ODN optical path loss classes are presented in **Table 2**.

It is remarkable that, apart from the fact that the existing GPON subscribers can be kept together with higher-bandwidth services, the coexistence will also give the operators the profound chance to take advantage of different approaches such as asymmetrical and symmetrical data rates. They also have deployment flexibility by operating on fixed or tunable wavelengths in order to offer appropriate operations and services at suitable costs. It will also assist the operators in the NG-PON evolution path not only by allowing them to upgrade their networks accordingly but also for gradual migration to the evolving PON technologies that are capable of offering the full optical potential. Thus, they have the liberty of adopting the cost and deployment pace that best fit their precise business requirements [43]. Moreover, this will enable the operators in making further revenue by exploiting flexible bandwidth and wavelength plans in order to support any service type as well as any business need. **Figure 6** depicts a PON system coexistence for a gradual and pay-as-you-grow expansion [33].

5. System requirement alleviation schemes

As explained in Section 1, C-RAN is envisioned to be a promising candidate for efficient management of the access network and the associated emergent complexity. This is due in part to its cost-effectiveness and remarkable flexibility for the network element deployments. Normally, the inphase and quadrature (I/Q) component stream transmission in this architecture is via the D-RoF-based CPRI. It is remarkable that CPRI-based fronthaul demands huge bandwidth which could be a limiting factor in the 5G and beyond networks in which mm-wave and massive MIMO are anticipated to be implemented. Consequently, an advanced optical transmission technology such as analog RoF (ARoF) has to be employed for an efficient fronthaul solution realization [11, 13, 14].

5.1 RoF schemes

The RoF schemes offer efficient and economical methods for modulated RF signal transmission. For instance, it can be used for transmission from the CO, to a number of distributed RRHs, through low-loss optical fiber networks, by employing an optical carrier. In addition, as aforementioned in Section 1, optical and wireless network convergence is highly imperative for scalable and cost-effective broadband wireless networks. The envisaged convergence for the next-generation mobile communication networks can be efficiently achieved with the implementation of RoF. This is due to its simplicity and efficiency in conveying wireless signal via an optical carrier. Furthermore, the inherent low attenuation and huge bandwidth of optical link can effectively support multiple wireless services on a shared optical fronthaul network. Moreover, with RoF implementation, the CUs and DUs can be well-supported. This offers effective centralized network control that subsequently presents advantages such as easy upgrade, simple maintenance, and efficient resource sharing [11, 47, 48].

It should be noted that there are various RoF options that can be employed in the network. Furthermore, each of the viable options presents related distinct merits

and demerits. Out of the variants, the highly spectrally efficient scheme is the ARoF. Besides, its implementation results in a most power-efficient and least complex RRH design. Nevertheless, it is susceptible to intermodulation distortion which is as a result of optical and microwave component nonlinearity. This results in relatively shorter operating distance. Moreover, the transmitter components such as oscillators, digital to analog converters (DACs), and mixers consume a considerable amount of power. On the other hand, with D-RoF implementation, the ARoF-associated nonlinearity issue can be effectively mitigated. However, in a scenario where high baud rates and high carrier frequencies are required, the DAC power consumption and expenditure are excessively high. Also, if upconversion is required or implemented at the RRHs, it turns out to be substantially high. Consequently, having a fixed phase relation among various RRHs is really challenging. Besides, digitized sample transmission, rather than the analog signal, brings about a significantly low spectral efficiency. The aforementioned drawbacks can be more challenging when densely distributed RRHs are to be supported [11, 47, 48]. Therefore, to address the challenges, a hybrid scheme that is capable of exploiting the ARoF and D-RoF schemes can be employed. One of notable techniques for a hybrid scheme is based on the implementation of sigma-delta-over-fiber (SDoF). This scheme helps in ensuring digital transmission that can support simple and power-efficient RRHs. Besides, there is no need for high-resolution and high-speed DACs with its implementation [47].

It is noteworthy that the RoF scheme employment is contingent on physical optical fiber availability. On the other hand, for the envisaged ultradense small-cell deployment, fiber deployment is not only time-consuming but also capital intensive. Likewise, there could be inappropriate system deployment due to the associated right-of-way acquisition. For these reasons, as well as limited number of the deployed fiber, the FSO system practicability has been considered [11, 13, 14].

5.2 FSO scheme

FSO communication presents an alternative technology for optical fiber systems. It is based on RF signal transmission between the CU and the DU apertures via the free space. Therefore, being an optical wireless technology, the fiber media are not required, and, consequently, trenches are unnecessary for its implementation. Moreover, like a well-developed, viable, and widely employed RoF technology, FSO scheme is capable of supporting multiple RF signal transmission. Apart from having inherent optical fiber features like RoF, FSO scheme offers additional merits regarding time-saving and cost-effectiveness, since there is no need for physical fiber deployment. This makes it to be very applicable in scenarios where physical network connectivity through optical fiber media is challenging and/or unrealistic. Besides, it is capable of delivering broadband services in rural area where there is an inadequate fiber infrastructure [11, 13, 14]. It is noteworthy that, when employed as a complementary solution for fronthauling, FSO can be a promising mobile traffic offloading scheme for alleviating the stringent requirements of bandwidth-intensive services transmission via the mobile networks.

In addition, the FSO scheme offers a number of benefits such as high bit rates, ease of deployment, full duplex transmission, license-free operation, improved protocol transparency, and high-transmission security. These salient merits enable the FSO scheme to be considered as a viable broadband access technology. It is capable of addressing various services and applications' bandwidth requirements at low cost for the NGNs. Based on these, the RF signals over FSO (RoFSO) idea have been presented. This is in an effort to exploit the inherent massive transport

capacity of optical systems and the related deployment simplicity of wireless networks [11, 13, 14].

Furthermore, a DWDM RoFSO scheme implementation has the capability of supporting concurrent multiple wireless signal transmission [49]. Nevertheless, the FSO systems have some drawbacks due to their susceptibility to the atmospheric turbulence and local weather conditions. The effects of these can cause beam wandering, as well as scintillation, which in due course results in the received optical intensity fluctuation. Consequently, the system reliability and availability can be determined by the extent of the effects. As a result, FSO technology is relatively unreliable like the normal optical fiber technology. Therefore, apart from the fact that these can limit the RoFSO system performance, its employment for uRLLC applications might also be limited as well. Consequently, the drawbacks hinder the FSO scheme as an effective standalone solution. Therefore, for the FSO scheme to be effective, the associated turbulence-induced fading has to be alleviated [2, 17, 18, 50]. Based on this, several PHY layer ideas like maximum likelihood sequence detection, diversity schemes, adaptive optics, and error control coding with interleaving have been presented to address the issue [11, 50, 51]. Besides, innovative schemes such as relay-assisted transmission and hybrid RF/FSO technologies can be implemented to enhance the system performance regarding capacity, reliability, and availability [11].

5.3 Hybrid RF/FSO scheme

A hybrid RF/FSO scheme exploits the inherent high-transmission bandwidth of the optical wireless system and the related deployment simplicity of wireless links [2]. In addition, the hybrid RF/FSO system idea does not only base on concurrent means of attending to the hybrid scheme related limitations, but it also entails ways of exploiting both approaches for a reliable heterogeneous wireless service delivery. The hybrid scheme is able to achieve this by incorporating the RF solutions' scalability and cost-effectiveness with the FSO solutions' high data rate and low latency. Consequently, the technology is able to address the high throughput, cost-effectiveness, and low-latency requirements of the system. Besides, it presents a heterogeneous platform for wireless service provisioning for the envisaged 5G and beyond networks [11, 13, 14, 52, 53].

5.4 Relay-assisted FSO scheme

One of feasible methods of turbulence-induced fading mitigation is the spatial diversity scheme. In this technique, there are multiple deployed apertures at the receiver and/or transmitter sides. This is in an effort to realize extra degrees of freedom in the spatial domain. It is remarkable that spatial diversity is an appealing fading mitigation scheme, owing to the presented redundancy feature. On the other hand, multiple-aperture deployment in the system causes a number of challenges like an increase in the cost and system complexity. Moreover, in order to prevent the spatial correlation detrimental effects, the aperture separation should be sufficiently large. Furthermore, a notable approach for simplified spatial diversity implementation is a dual-hop relaying scheme. It is noteworthy that there has been extensive implementation of the scheme in the RF and wireless communication systems. Application of the scheme in these fields not only aids in improving the receive signal quality but also helps considerably in the network range extension [2, 11, 13, 14].

Conceptually, multiple virtual aperture systems are generated in the relay-assisted transmission with the intention of realizing salient MIMO technique

features. The architecture takes advantage of the RF and FSO features for an efficient and reliable service delivery. In addition, a relay-assisted transmission system is an innovative communication technique known as a mixed RF/FSO dual-hop communication system. The dual-hop scheme meaning can be easily understood from its architecture. In the architecture, the transport networks from the source to the relay system are RF links; however, the transport networks between the relay system and the associated destination node(s) are FSO links. Hence, in a dual-hop system, RF is used for signal transmission at one hop, while FSO transmission is implemented at the other. The FSO link mainly functions to facilitate the RF users' communication with the backbone network. This is purposely for filling the connectivity gap between the backbone and the last-mile access networks. Accordingly, the offered architecture can efficiently address the system-related last-mile transmission bottleneck. This can be effectively achieved by supporting multiplexed users with RF capacities. The users can also be aggregated onto a shared high-capacity FSO link. This will help in harnessing the inherent huge bandwidth of an optical communication system. Another outstanding advantage of this scheme is that any kind of interference can be easily inhibited via its implementation. This is due mainly to the fact that the RF and FSO operating frequency bands are completely different. Consequently, it offers better performance than the traditional RF/RF transmission schemes [2, 11, 13, 14].

5.5 RAN functional split

The RAN functional split is another innovative and practical scheme for alleviating the imposed fronthaul requirements by the C-RAN architecture [11, 54]. For instance, to address the drawbacks of CPRI-based fronthaul solutions, an eCPRI specification presents additional physical layer functional split options and a packet-based solution. Consequently, unlike the conventional constant data rate CPRI in which the stream significantly depends on the carrier bandwidth, as well as the number of antennas, the eCPRI stream does not depend on either of the factors but on the actual traffic load. In essence, apart from being able to alleviate the stringent bandwidth demands, multiple eCPRI stream can also be multiplexed onto a wavelength for onward transmission over the fronthaul network [12].

In addition, with recent network architecture development, the traditional BBU and RRU have been reformed into different functional entities which are the CU, DU, and RRU/active antenna unit (AAU). With the configuration, the CU majorly focuses on non-real time and part of the traditional Evolved Packet Core functionalities. This involves high-level protocol processing like dual connectivity and radio resource management. In addition, the DU is responsible for the real-time media

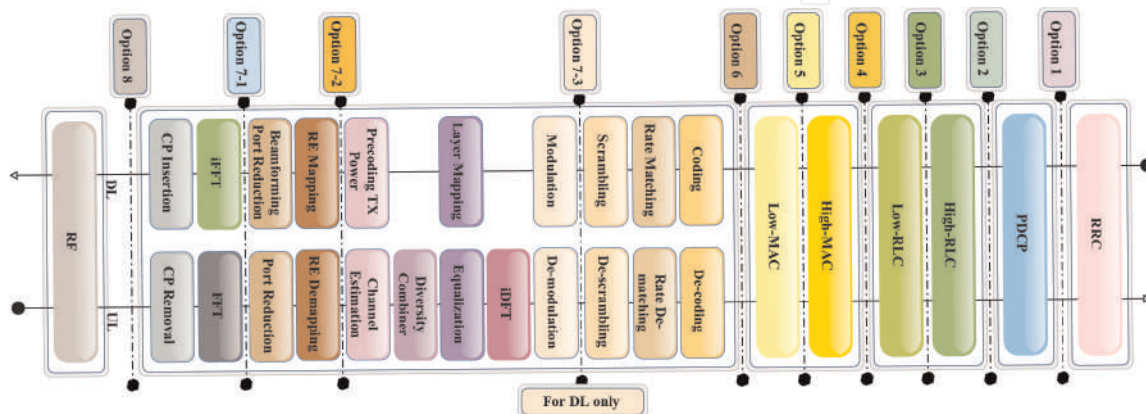


Figure 7. Functional split options between CU and DU with emphasized PHY layer.

access control layer functions like HARQ flow and physical layer function processing. Also, when massive MIMO antennas are to be employed, certain parts of the physical layer functions can also be shifted to the RRU/AAU. The implementation will not only aid in lessening the associated transmission bandwidth between the RRU/AAU and DUs but will also help in reducing the transmission cost considerably. Therefore, a number of functional split options have been presented in order to reduce the processing and network resource cost considerably. As shown in **Figure 7**, each of the option is categorized according to the demarcation point between the CU and the DU. Therefore, depending on the deployment scenarios and use cases, each option offers different degrees of flexibility regarding resource allocation for different service requirements [12, 29].

6. NG-PON2 physical layer architecture design and development

The NG-PON2 physical layer requirements are very challenging. Besides, the requirements are even more strict than the legacy PON technologies. For instance, when compared with the GPON taken into consideration the related spectrum, GPON employs only one channel for the transmission and one for the reception, with a very wide wavelength allocation (up to 100 nm). On the other hand, in NG-PON2, there are <4 nm to accommodate four channels. Consequently, this means that the thermal control must be very precise in order to keep each channel inside the specified channel space (which is ± 20 GHz). As aforementioned, there are multiple channels in NG-PON2 transmission; therefore, the receiver must be tunable so as to work for any one of them at a particular time while others are rejected. This requirement implies that there is a need for a very tight band-pass filter too for efficient operation. Also, the tuning time classes, already presented in **Table 1** in Section 3, are likewise strict and difficult to achieve on the hardware side. Besides, one of the major related issues is the amount of the required optical-electrical-optical (OEO) conversions, which can bring about an unviable and unsustainable system [55].

6.1 Photonic integrated circuit

The optical communications evolution has initiated enhanced photonic integrated circuits (PICs) that present a cost-effective alternative to data transmission. With PIC technology implementation, a number of optical components such as modulators, lasers, amplifiers, detectors, etc. can be merged/integrated on a single chip. Consequently, it helps in optical system design simplification, system reliability enhancement, as well as significant power consumption and space reduction. In addition, there can be considerable reduction in the amount of OEO converters required for the system implementation. This subsequently results in the total network cost reduction [55]. Thus, it is anticipated to be an enabling and viable technology with immense flexibility and reconfigurability in a number of fields [56]. A PIC has numerous advantages over the traditional optical sub-assemblies (OSAs). For instance, considering the occupied volume, the PICs allow a very dense architecture in a small area, passing also by the optical losses; however, the losses in the OSAs are higher because of the internal free-space alignment between each optical component. Also, other notable advantages of the PICs compared with the OSAs are lower power consumption, lower footprint, and cost-effectiveness. Therefore, PICs have the capability of permitting flexible and high data rate solutions [39, 55].

In the following, for the system realization, we propose three different architectures: the ONU architecture, the OLT architecture, and the architecture that can perform both functions just by hardware selection. It should be noted that all of these architectures have the transmit and the receive parts.

6.1.1 NG-PON2 ONU transceiver architecture

The ONU transceiver architecture is represented in **Figure 8**. This is a very simple structure regarding the optical setup, but the electrical control is very tough, mostly because of the tunability (both on the transmitter and on the receiver). In this example, there is one tunable laser. The laser can be tuned by temperature and can be directly or externally modulated (the latter would also need a modulator after the laser). On the receiver part, there is an optical band-pass filter which has to be tunable to allow one of the downstream channels and cut the rest of the spectrum. The tunable band-pass filter is followed by an optical receiver.

6.1.2 NG-PON2 OLT transceiver architecture

As explained before, the OLT is not tunable; both transmitter and receiver should work on the same fixed wavelength pair, as depicted in **Figure 9**. Consequently, four pairs of optical devices will be needed. Since it is very difficult to encapsulate everything on the same transceiver, the solution that is being followed commercially is having four different transceivers, one for each wavelength pair, and the wavelength multiplexer (WM) device is external. This WM should, in each port, allow one wavelength pair, meaning that in each port, it should pass only one downstream and the respective upstream channel.

6.1.3 NG-PON2 OLT/ONU transmission architecture

The architectures presented in **Figures 8** and **9** are the basic ones to have functional devices for NG-PON2. But taking advantage of photonic integration, it is possible to develop a much more complex circuit with more functionalities, which is being presented next. **Figure 10** illustrates the block diagram of an architecture that can be used both as ONU and OLT. This helps in exploiting the advantage of both functionalities on a single chip. The purpose (OLT or ONU) to be served can be achieved just by hardware selection. This proposed architecture fits inside a 4 × 4.6 mm indium phosphide (InP) PIC. In the following subsection, we present the final design and some obtained simulation results.

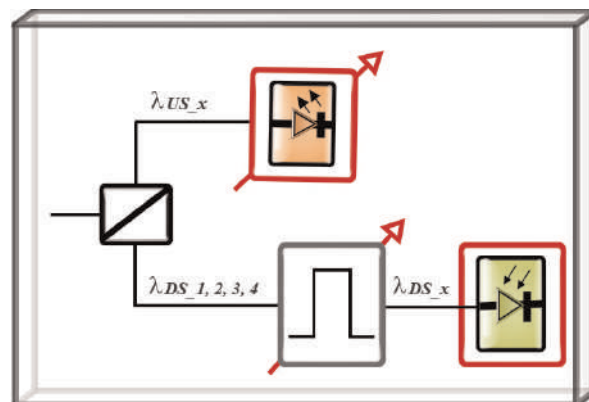


Figure 8.
ONU transceiver architecture.

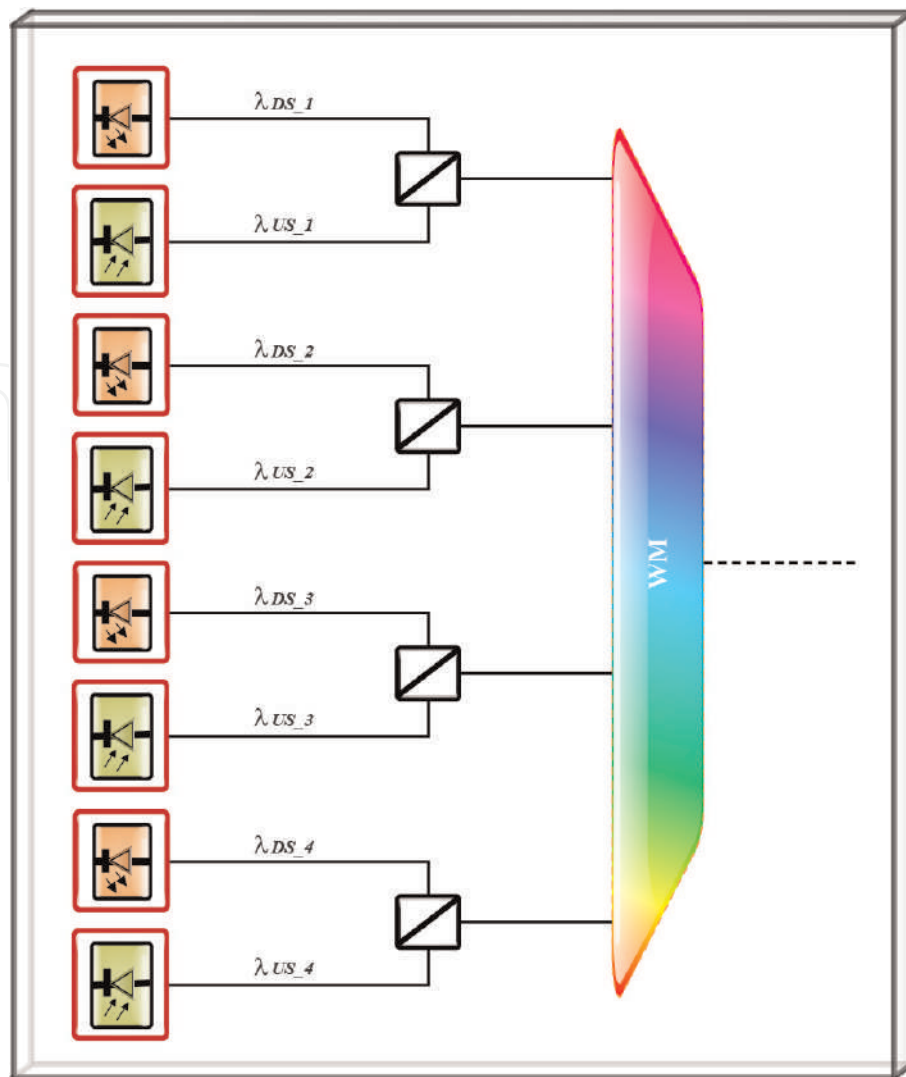


Figure 9.
 OLT transceiver architecture.

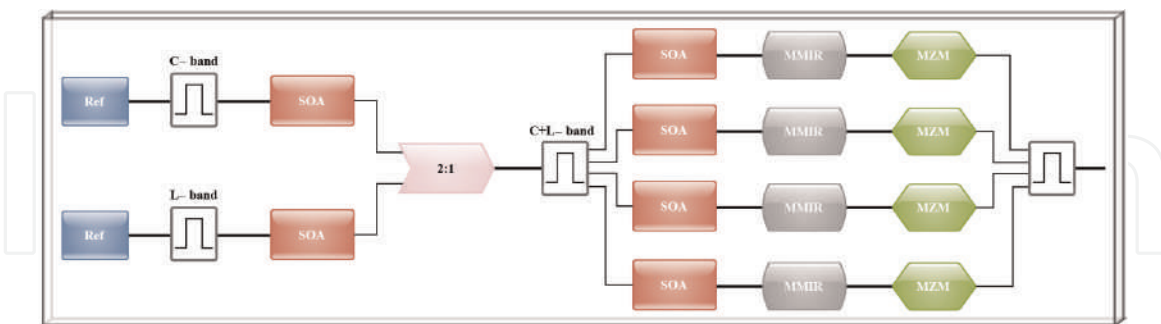


Figure 10.
 Block diagram of OLT/ONU transmission architecture.

6.2 PIC implementation of OLT/ONU and receiver circuits

The architecture comprises four lasers, four Mach-Zehnder modulators (MZM), and a number of filters. Two of the filters are for changing the operational frequency band (C band for upstream transmission and L band for downstream). Also, one filter is employed for tuning the four lasers to the correct wavelength. Besides, at the output, there is one filter working as a combiner of the four lasers. The band selection is made using the two semiconductor optical amplifiers (SOAs) that are placed after the band filters. It is noteworthy that the two SOAs are working as

switches and determine the chip's operating mode (i.e., OLT or ONU). Therefore, one of the SOAs is amplifying the light (active SOA), while the other is absorbing (passive SOA). Consequently, by this configuration, only one band filter is contributing to the setup. The employed lasers are built using laser cavities which contain SOAs that are being used for gain purposes, filters, and reflectors on both sides. The C + L band filter helps in the selection of the downstream or upstream channel [39].

Moreover, the architecture includes also a multimode interferometer reflector (MMIR) before the band selection and another one after each gain SOA. These reflectors define the laser cavity limits. The second MMIR, after the gain SOAs, only reflects 50% of the light, and the remaining 50% is the laser cavity output and is sent to the MZM for modulation. After the modulation on the MZMs, all four channels are combined in just one, and the resulting light signal is sent to the output

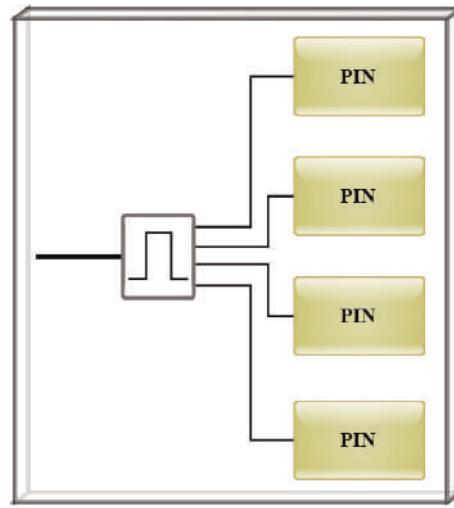


Figure 11.
Receiver block diagram.

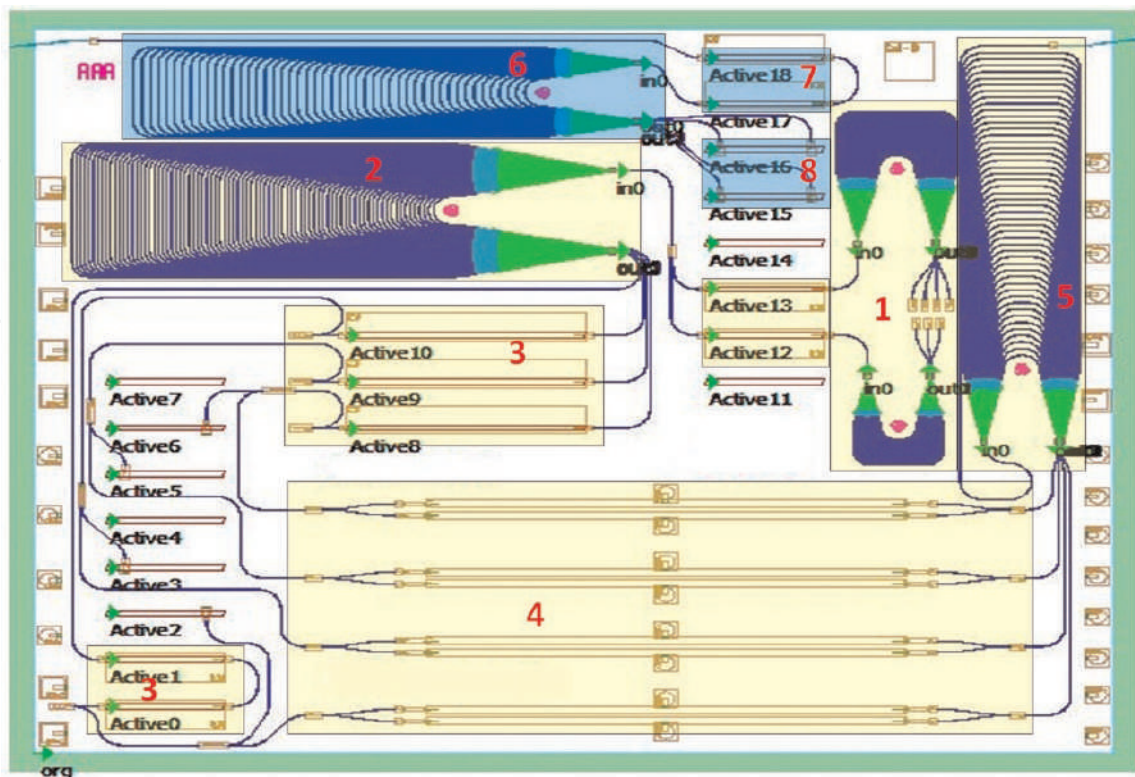


Figure 12.
OLT/ONU integrated transceiver design masks.

of the PIC, where a fiber will be aligned to collect the light, and subsequently, it will be sent to the network [39].

6.2.1 PIC implementation of receiver circuit

This PIC has also a receiver circuit, but it is a simple one, with just a wavelength division multiplexer (WDM) filter which receives the light from the network and routes each NG-PON2 channel for a different PIN. The receiver circuit schematic is depicted in **Figure 11**.

6.2.2 PIC implementation of OLT/ONU circuit

Using the photonic design kit (PDK) from the foundry Smart Photonics and a software for PIC design (Phoenix Software at the time, meantime bought by synopsis) for the implementation, the final circuit masks of the chip are shown in **Figure 12**.

7. Results and discussion

In this section, we present the obtained simulation results with further discussion on NG-PON2 physical layer architecture design and development based on PICs. **Figure 13** shows the spectral simulation results obtained using advanced simulator for photonic integrated circuits (Aspic) software from filarete. On the left figure, there is the downstream operation (L band selected), and on the right there is the upstream (C band selected). In the figure, the spectra in blue, pink, orange, and green are the four channels. In both cases, it is possible to conclude that there is about 30 dB of suppression of replicas. The suppression facilitates smooth operation of the system by preventing intra-channel interference.

The reason for using laser cavities is due to the limitations on the foundry. During the chip's design period, the Smart Photonics did not offer lasers on their process design kit (PDK). Consequently, improvements in the architecture can be undertaken to potentiate the results. For instance, the laser cavities could be replaced by distributed feedback (DFB) or distributed Bragg reflector (DBR) lasers that have narrow linewidth and a stable single mode operation. In this case, the cavity would disappear, and the filtering should be done after the lasing. In addition, the architectures can be simplified using only one modulator; nevertheless, it

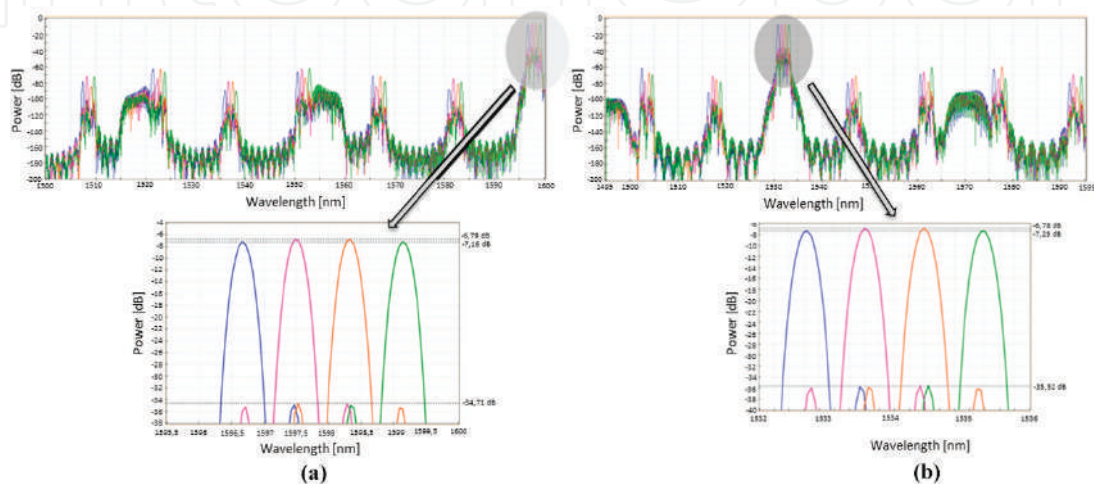


Figure 13.
Optical spectra at the transmitter output (a) downstream and (b) upstream.

would not be possible to transmit the four channels simultaneously; this implies that only one channel can be transmitted at a time. The proposed and developed architectures demonstrate the potential of photonic integration for optical architectures. Consequently, the architectures not only have the ability of supporting high data rates, high density, and flexible solutions but also offer advantages such as low power consumption, improved functionality, low footprint, and cost-effectiveness.

8. Conclusion

The 5G based system is a promising solution for attending to the growing concerns about the traffic pressure on the network. Also, the envisaged massive number of deployment scenarios and use cases to be supported brings about high-bandwidth and low-latency requirements for the 5G networks. The small-cell-based C-RAN approach can efficiently attend to the associated ultradense deployment. However, the C-RAN-based approach imposes stringent requirements regarding jitter, bandwidth, and latency for the mobile transport networks. In this book chapter, we have presented wired and wireless transport solutions that are capable of addressing the C-RAN-based stringent requirements and, consequently, the 5G mobile transport network demands. Furthermore, owing to its significant and inherent advantages for the 5G and beyond networks, we have focused on the NG-PON2 system. We have exploited the salient advantages and the low footprint platform offered by the PICs in the NG-PON2 system design and implementation. Based on these technologies, the proposed architectures are capable of alleviating the associated losses in the system while also helping in increasing the system power budget. In addition, employment of the proposed architectures can help the device makers, service/network providers, and infrastructure and chip vendors, in lowering the footprint of network elements.

Acknowledgements

This work is funded by Fundação para a Ciência e a Tecnologia (FCT) through national funds under the scholarships PD/BD/105858/2014. It is also supported by the European Regional Development Fund (FEDER), through the Regional Operational Programme of Lisbon (POR LISBOA 2020) and the Competitiveness and Internationalization Operational Programme (COMPETE 2020) of the Portugal 2020 framework, Project 5G (POCI-01-0247-FEDER-024539), ORCIP (CENTRO-01-0145-FEDER-022141), and SOCA (CENTRO-01-0145-FEDER-000010). It is also funded by Fundação para a Ciência e a Tecnologia (FCT) through national funds under the project COMPRESS-PTDC/EEI-TEL/7163/2014 and by FEDER, through the Regional Operational Program of Centre (CENTRO 2020) of the Portugal 2020 framework [Project HeatIT with Nr. 017942 (CENTRO-01-0247-FEDER-017942)] and [Project Virtual Fiber Box with Nr. 033910 (POCI-01-0247-FEDER-033910)]. Additional support is provided by the COST action CA16220 European Network for High Performance Integrated Microwave Photonics (EUIMWP) and IT (UID/EEA/50008/2013).

IntechOpen

Author details

Isiaka A. Alimi^{1*}, Ana Tavares^{1,2}, Cátia Pinho¹, Abdelgader M. Abdalla¹,
Paulo P. Monteiro¹ and António L. Teixeira¹

1 Department of Electronics, Universidade de Aveiro, Instituto de
Telecomunicações, Telecommunications and Informatics, Aveiro, Portugal

2 PICadvanced, University of Aveiro Incubator, Portugal

*Address all correspondence to: iaalimi@ua.pt

IntechOpen

© 2019 The Author(s). Licensee IntechOpen. This chapter is distributed under the terms of the Creative Commons Attribution License (<http://creativecommons.org/licenses/by/3.0>), which permits unrestricted use, distribution, and reproduction in any medium, provided the original work is properly cited. 

References

- [1] Yu C, Yu L, Wu Y, He Y, Lu Q. Uplink scheduling and link adaptation for narrowband internet of things systems. *IEEE Access*. 2017;5:1724-1734
- [2] Alimi I, Shahpari A, Sousa A, Ferreira R, Monteiro P, Teixeira A. Chapter 2: Challenges and opportunities of optical wireless communication technologies. In: Pinho P, editor. *Optical Communication Technology*. Rijeka: IntechOpen; 2017
- [3] Ejaz W, Anpalagan A, Imran MA, Jo M, Naeem M, Qaisar SB, et al. Internet of things (iot) in 5g wireless communications. *IEEE Access*. 2016;4: 10310-10314
- [4] Alimi I, Shahpari A, Ribeiro V, Kumar N, Monteiro P, Teixeira A. Optical wireless communication for future broadband access networks. In: 21st European Conference on Networks and Optical Communications (NOC); June 2016; pp. 124-128
- [5] Laraqui K, Tombaz S, Furuskär A, Skubic B, Nazari A, Trojer E. Fixed Wireless Access on a Massive Scale with 5G. *Ericsson Technology Review*. Vol. 94. Stockholm, Sweden: Ericsson; 2017
- [6] Skubic B, Fiorani M, Tombaz S, Furuskär A, Mårtensson J, Monti P. Optical transport solutions for 5G fixed wireless access [invited]. *IEEE/OSA Journal of Optical Communications and Networking*. 2017;9(9):D10-D18
- [7] David Schnauffer. 5 Things to Consider When Designing Fixed Wireless Access (FWA) Systems. United States of America: Qorvo; 2018
- [8] Pinho C, Shahpari A, Alimi I, Lima M, and Teixeira A. Optical transforms and cgh for sdm systems. In: 2016 18th International Conference on Transparent Optical Networks (ICTON); July 2016; pp. 1-4
- [9] mmw 5G-eMBB use cases and small cell based HyperDense networks. Document, version: 197.10.01, Small Cell Forum, December. UK: Small Cell Forum; 2017
- [10] Torres-Ferrera P, Straullu S, Abrate S, Gaudino R. Upstream and downstream analysis of an optical fronthaul system based on dsp-assisted channel aggregation. *IEEE/OSA Journal of Optical Communications and Networking*. 2017;9(12):1191-1201
- [11] Alimi IA, Teixeira AL, Monteiro PP. Toward an efficient c-ran optical fronthaul for the future networks: A tutorial on technologies, requirements, challenges, and solutions. *IEEE Communications Surveys Tutorials*. 2018;20(1):708-769
- [12] Yu H, Zhang J, Ji Y, Tornatore M. Energy-efficient dynamic lightpath adjustment in a decomposed awgr-based passive wdm fronthaul. *IEEE/OSA Journal of Optical Communications and Networking*. 2018;10(9):749-759
- [13] Alimi IA, Monteiro PP, Teixeira AL. Analysis of multiuser mixed rf/fso relay networks for performance improvements in cloud computing-based radio access networks (cc-rans). *Optics Communications*. 2017;402: 653-661
- [14] Alimi IA, Monteiro PP, Teixeira AL. Outage probability of multiuser mixed rf/fso relay schemes for heterogeneous cloud radio access networks (h-crans). *Wireless Personal Communications*. 2017;95(1):27-41
- [15] Fuchuan Z. Challenges and trends for 5G transport. *ZTE Technologies*. 2018;20(2):19-21

- [16] Ghassemlooy Z, Popoola W, Rajbhandari S. *Optical Wireless Communications: System and Channel Modelling with MATLAB®*. Boca Raton, London New York: CRC Press; 2012
- [17] Alimi I, Shahpari A, Ribeiro V, Sousa A, Monteiro P, Teixeira A. Channel characterization and empirical model for ergodic capacity of free-space optical communication link. *Optics Communications*. 2017;**390**:123-129
- [18] Alimi IA, Abdalla AM, Rodriguez J, Monteiro PP, Teixeira AL. Spatial interpolated lookup tables (luts) models for ergodic capacity of mimo fso systems. *IEEE Photonics Technology Letters*. 2017;**29**(7):583-586
- [19] Transport network support of IMT-2020/5G. Technical report gstr-tn5g. Canada: ITU-T; February 2018
- [20] Common Public Radio Interface: eCPRI Interface Specification. Interface specification, ecprl specification v1.1, eCPRI specification. CPRI cooperation; January 2018
- [21] View on 5G Architecture. Architecture white paper version 2.0, 5G PPP architecture working group, July 2018
- [22] Guiomar FP, Alimi IA, Monteiro PP, and Gameiro A. Flexible infrastructure for the development and integration of access/fronthauling solutions in future wireless systems. In: 2018 IEEE 19th International Workshop on Signal Processing Advances in Wireless Communications (SPAWC); June 2018; pp. 1-5
- [23] Nokia Optical Anyhaul as an enabler of C-RAN: Accelerating the delivery of 5G networks. White paper, document code: Sr1803022985en, Nokia, March 2018
- [24] Kalfas G, Pleros N, Alonso L, Verikoukis C. Network planning for 802.11ad and mt-mac 60 ghz fiber-wireless gigabit wireless local area networks over passive optical networks. *IEEE/OSA Journal of Optical Communications and Networking*. 2016;**8**(4):206-220
- [25] Stephen RG, Zhang R. Joint millimeter-wave fronthaul and ofdma resource allocation in ultra-dense cran. *IEEE Transactions on Communications*. 2017;**65**(3):1411-1423
- [26] Zhang H, Dong Y, Cheng J, Hossain MJ, Leung VCM. Fronthauling for 5g lte-u ultra dense cloud small cell networks. *IEEE Wireless Communications*. 2016;**23**(6):48-53
- [27] Chen Q, Yu G, Maaref A, Li GY, Huang A. Rethinking mobile data offloading for lte in unlicensed spectrum. *IEEE Transactions on Wireless Communications*. 2016;**15**(7):4987-5000
- [28] Aijaz A, Aghvami H, Amani M. A survey on mobile data offloading: Technical and business perspectives. *IEEE Wireless Communications*. 2013; **20**(2):104-112
- [29] 5G-oriented Optical Transport Network Solution. White paper, ZTE Technologies, June 2017
- [30] Otaka A. Flexible access system architecture: Fasa. In: NTT Tsukuba Forum 2016 Workshop Lectures. Tokyo, Japan: NTT; Vol. 15. 2017. pp. 1-7
- [31] De Betou EI, Bunge C-A, Åhlfeldt H, Olson M. WDM-PON is a key component in next generation access. Nashua, USA: Lightwave; Article, Lightwave, March 2014
- [32] The Application of TDM-PON and WDM-PON. Article, Fiber-Optical-Networking, May 2015

- [33] Bogataj T. Safe Migration to Next-Gen Optical Broadband Access: A gradual and controlled journey to XGS-PON and NG-PON2. Kranj, Slovenia: Executive whitepaper, Iskratel, January 2018
- [34] Xu Q. What the future holds for next-generation PON technologies. Nashua, USA: Article, Cabling Installation and Maintenance, October 2017
- [35] Next-Generation PON Evolution. Shenzhen, China: Manual, Huawei Technologies. 2010
- [36] Wang X, Wang L, Cavdar C, Tornatore M, Figueiredo GB, Chung HS, et al. Handover reduction in virtualized cloud radio access networks using twdm-pon fronthaul. *IEEE/OSA Journal of Optical Communications and Networking*. 2016;**8**(12):B124-B134
- [37] Cheng N, Gao J, Xu C, Gao B, Liu D, Wang L, et al. Flexible twdm pon system with pluggable optical transceiver modules. *Optics Express*. 2014;**22**(2):2078-2091
- [38] The Future of Passive Optical Networking is Here: NG-PON2. Marketing report, Broadband Forum
- [39] Jesus Teixeira AL, Maia Tavares AC, Silva Lopes AP, Rodrigues CE. Photonic integrated tunable multi-wavelength transmitter circuit. USA: United States Patent; 2017
- [40] Nettet D. Ng-pon2 technology and standards. *Journal of Lightwave Technology*. 2015;**33**(5):1136-1143
- [41] Monteiro PP, Viana D, da Silva J, Riscado D, Drummond M, Oliveira ASR, et al. Mobile fronthaul rof transceivers for c-ran applications. In: 2015 17th International Conference on Transparent Optical Networks (ICTON); July 2015. pp. 1-4
- [42] Wey JS, Nettet D, Valvo M, Grobe K, Roberts H, Luo Y, et al. Physical layer aspects of ng-pon2 standards—Part 1: Optical link design [invited]. *IEEE/OSA Journal of Optical Communications and Networking*. 2016;**8**(1):33-42
- [43] Thomas D. XGS-PON makes NG-PON simpler. Technical report, Nokia, June 2016
- [44] Challenges in Next-Gen PON Deployment. White paper, Viavi Solutions, 2017
- [45] WaveCEX: WDM module for PON coexistence-GPON, XGS-PON, NG-PON2, RF, OTDR. Wavecex family: 180409 data sheet, TELNET Redes Inteligentes, October 2017
- [46] OBA000100 GPON Fundamentals. Technical report, Huawei
- [47] Breyne L, Torfs G, Yin X, Demeester P, Bauwelinck J. Comparison between analog radio-over-fiber and sigma delta modulated radio-over-fiber. *IEEE Photonics Technology Letters*. 2017;**29**(21):1808-1811
- [48] Thomas VA, Ghafoor S, El-Hajjar M, Hanzo L. A full-duplex diversity-assisted hybrid analogue/digitized radio over fibre for optical/wireless integration. *IEEE Communications Letters*. 2013;**17**(2):409-412
- [49] Dat PT, Bekkali A, Kazaura K, Wakamori K, Matsumoto M. A universal platform for ubiquitous wireless communications using radio over fso system. *Journal of Lightwave Technology*. 2010;**28**(16):2258-2267
- [50] Alimi IA, Shahpari A, Monteiro PP, Teixeira AL. Effects of diversity schemes and correlated channels on owc systems performance. *Journal of Modern Optics*. 2017;**64**(21):2298-2305
- [51] Navidpour SM, Uysal M, Kavehrad M. Ber performance of free-space

optical transmission with spatial diversity. *IEEE Transactions on Wireless Communications*. 2007;**6**(8): 2813-2819

[52] Dahrouj H, Douik A, Rayal F, Al-Naffouri TY, Alouini M. Cost-effective hybrid rf/fso backhaul solution for next generation wireless systems. *IEEE Wireless Communications*. 2015;**22**(5): 98-104

[53] Kazaura K, Wakamori K, Matsumoto M, Higashino T, Tsukamoto K, Komaki S. Rofso: A universal platform for convergence of fiber and free-space optical communication networks. *IEEE Communications Magazine*. 2010;**48**(2):130-137

[54] Harutyunyan D, Riggio R. Flex5g: Flexible functional split in 5g networks. *IEEE Transactions on Network and Service Management*. 2018;**15**(3): 961-975

[55] Tavares A, Lopes A, Rodrigues C, Mäocheia P, Mendes T, Brandão S, et al. Photonic Integrated Transmitter and Receiver for Ng-pon2. *Proc. SPIE 9286, Second International Conference on Applications of Optics and Photonics*, 928605 (22 August 2014)

[56] Pinho C, Gordon GSD, Neto B, Morgado TM, Rodrigues F, Tavares A, et al. Flexible spatial light modulator based coupling platform for photonic integrated processors. *International Journal on Advances in Telecommunications*. 2018;**11**(1):20-31

Role of Optical Network in Cloud/Fog Computing

Kiran Deep Singh

Abstract

This chapter is a study of exploring the role of the optical network in the cloud/fog computing environment. With the growing network issues, unified and cost-effective computing services and efficient utilization of optical resources are required for building smart applications. Fog computing provides the foundation platform for implementing cyber-physical system (CPS) applications which require ultra-low latency. Also, the digital revolution of fog/cloud computing using optical resources has upgraded the education system by intertwined VR using the fog nodes. Presently, the current technologies face many challenges such as ultra-low delay, optimum bandwidth, and minimum energy consumption to promote virtual reality (VR)-based and electroencephalogram (EEG)-based gaming applications. Ultra-low delay, optimum bandwidth, and minimum energy consumption. Therefore, an Optical-Fog layer is introduced to provide a novel, secure, highly distributed, and ultra-dense fog computing infrastructure. Also, for optimum utilization of optical resources, a novel concept of *OpticalFogNode* is introduced that provides computation and storage capabilities at the Optical-Fog layer in the software defined networking (SDN)-based optical network. It efficiently facilitates the dynamic deployment of new distributed SDN-based *OpticalFogNode* which supports low-latency services with minimum energy as well as bandwidth usage. Therefore, an EEG-based VR framework is also introduced that uses the resources of the optical network in the cloud/fog computing environment.

Keywords: cloud/fog computing, optical resources, virtual reality, cyber physical system, electroencephalogram (EEG)

1. Introduction

Optical transmission is the most cost-effective technology to implement high-bandwidth-based communication in the fog/cloud computing environment. The passive optical network (PON) uses optical line terminals (OLT) and optical network units (ONU) for delivering fog/cloud-based services effectively [1]. Introducing this technology with the present information technology, Internet of Things (IoT), cloud computing, 5G wireless networking, and embedded artificial intelligence have tremendous potential to assist the development of smart applications that demand a large amount of data to be processed locally and operate on-premise with minimum latency and network congestion [2]. Optical technology has supported IoT-based applications for transferring massive information in a

virtual frictionless fashion by using the optical network elements. It has provided new ways for various business applications to move over the latest technologies such as big data analytics, machine learning, etc. in the era of the 5G network.

Fog computing is a new distributed architecture which brings computing, storage, and networking services closer to the proximity of the end user [3]. As compared to the traditional cloud computing techniques, it processes real-time applications and data at the edge with minimum latency, minimum network congestion, and lower energy consumption which are the key demand of many industries such as manufacturing, e-health, education, oil and gas, smart cities, smart homes, and smart grids [4]. Fog nodes aggregate the computing resources of edge devices to perform the critical data-sensitive computations where the data of analysis part is directly sent to the cloud for further processing because traditional fog nodes have limited storage and computing power.

The integration of fog computing and PON is an inexpensive, scalable, and simple technology to provide a most promising solution for building e-learning-based smart educational applications [5]. The dynamic capabilities of SDN combined with the state-of-the-art optical technologies have the ability to modernize the optical transport network through its primary feature, i.e., programmability [6]. The purpose of this chapter is to explore efficient techniques to combine SDN-based optical technology at different levels of design and development of smart VR-based applications.

2. Utilization of optical resources in cloud/fog computing environment

In order to handle real-time and bandwidth-intensive applications, fog leverages the computing resources of the SDN-based optical network. **Figure 1** shows that the Optical-Fog layer [7] uses ONUs in the middleware of the cloud and IoT layer. In a typical PON channel with multiple OLTs, each OLT is connected with multiple ONUs (16–256) [8]. The Optical-Fog layer is designed by using their residual processing, storage, and interconnection capabilities. It can enable fast service provisioning, dynamic service restoration, network automation, and network optimization at different layers of the underlying network infrastructure. It makes optical network

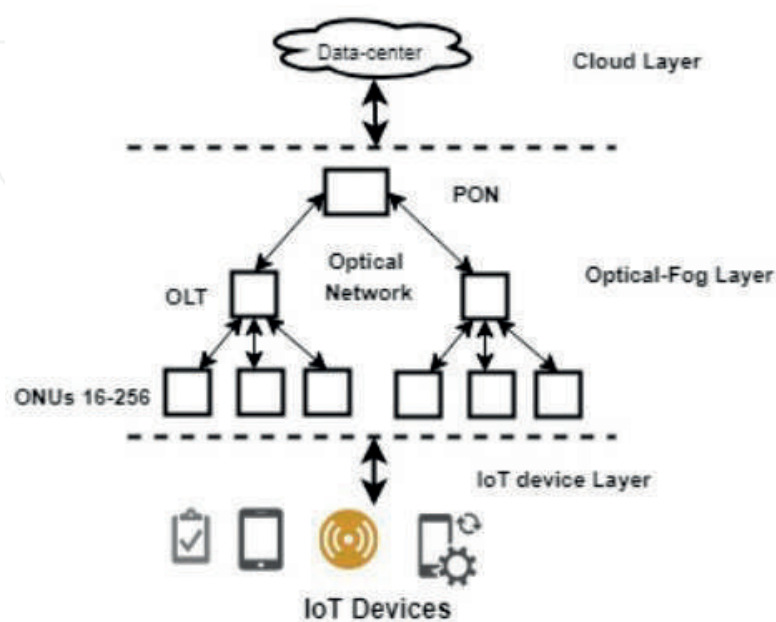


Figure 1. Utilization of optical resources in cloud/fog computing environment.

centralized, intelligent, and controlled (real time) which can serve application-level services efficiently in the heterogeneous IoT, machine learning, big data, and cloud computing paradigms. The acronyms used in this paper are defined in **Table 1**.

2.1 SDN-based optical network

Presently, SDN is supporting wide area network to deal with many more technologies for delivering several benefits. It has adopted a hierarchical approach in which domain controllers collect information and delegate the control (real time) over the network layers and geographic clusters to support applications and provide higher levels of service orchestrations. Initially, SDN was used in data centers for separating the data plane, control plane, and management plane from each other [9]. The interface like OpenFlow is used by the centralized controller to deliver computing infrastructure for making better communication. While applying this concept to the optical network, optical domain controller (ODC) plays an important role. As shown in **Figure 2**, it provides a more programmatic and abstract view of the underlying optical network through the northbound interface [10]. The programming feature of SDN makes it capable of fulfilling customized demands for manipulating network infrastructure. To handle real-time, bandwidth-intensive applications, fog uses the computing resources of the SDN-based optical network.

The SDN-based optical network infrastructure fulfills the demand of increasingly high-performance and network-based applications with flexibility and efficiency. The key security issues in fog/cloud computing over optical network lies at both downstream and upstream channels of PON. PON uses broadcasting in the downstream channel which is prone to eavesdropping attacks where an attacker can modify the behavior of ONUs at its media access control (MAC) layer. On the other hand, the traffic in the upstream channel is only visible to the OLT rather than other ONUs that can also be exploited for attacks. In PON network, OLT uses time division multiplexing access (TDMA) that provides sharing of the upstream channel among

| | |
|------|-----------------------------------|
| PON | Passive optical network |
| OLT | Optical line terminal |
| ONU | Optical network unit |
| CPS | Cyber physical systems |
| VR | Virtual reality |
| EEG | Electroencephalogram |
| QoE | Quality of experience |
| QoS | Quality of service |
| ONV | Optical network virtualization |
| SDN | Social-defined network |
| FAR | Free available resource |
| TDMA | Time division multiplexing access |
| MPCP | Multipoint control protocol |
| ODC | Optical domain controller |
| MAC | Media access control |

Table 1.
List of acronyms.

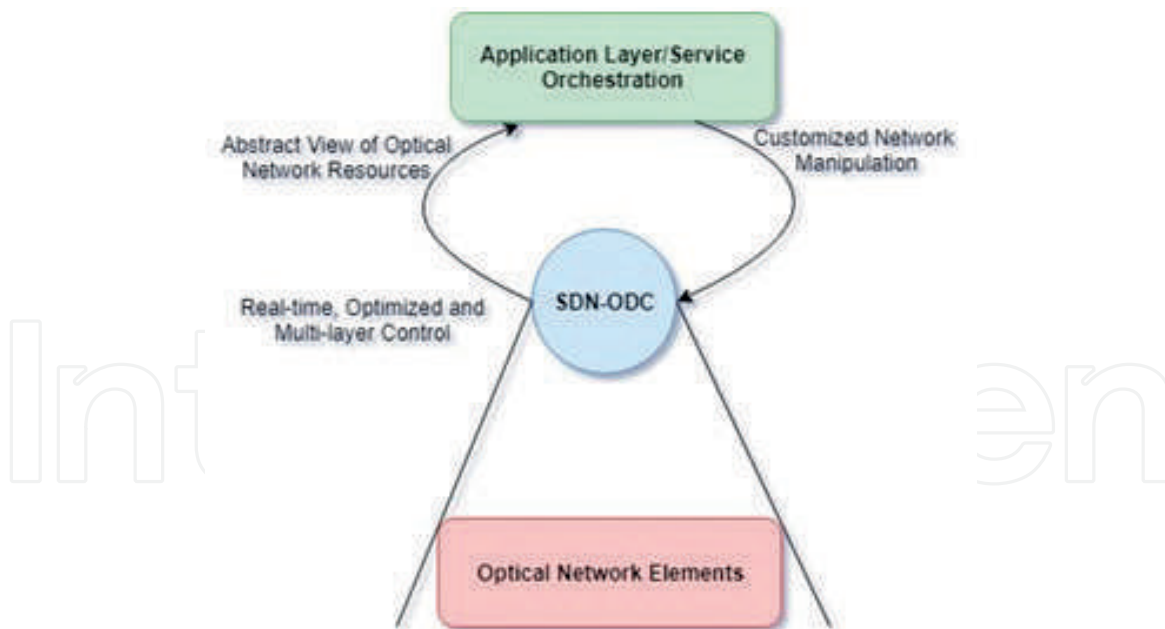


Figure 2.
SDN-based optical network.

ONUs [11]. It assigns static or dynamic nonoverlapping time slots to connected ONUs. Here, OLT and all connected ONUs are well synchronized that result in the collision-free transmission of the traffic or data frames. In the security aspects of PON, more research work is required that can restrict the ONUs to send data frames outside of their preassigned time-slots. In case if a malicious ONU intends to send data frames outside its preassigned time slot, the collision can encounter with the data-frames of other ONUs that degrade the quality of service (QoS) of the optical channel.

To ensure QoS and quality of experience (QoE) to the end-user for various real-time CPS-based applications, Optical-Fog layer is utilized. To handle real-time processing, this layer uses the optical network resources by creating *OpticalFogNode*. The optical network can effectively realize the interconnected optical resources (PON, OLTs, and ONUs) across the 5G network. It provides ultralow delay and less energy consumption for IoT devices and uses the majority of the computing resources of the optical layer rather than the cloud layer.

2.2 *OpticalFogNode* for implementing CPS system

CPS enables the integration of cyber components such as sensors, computational and control units, and network devices into the physical components (such as objects, end-users, and infrastructures) by connecting them to the Internet and each other. It also has shown tremendous progress in many fields like communication, healthcare, education, manufacturing, robotics, transportation, military, etc. It has also encouraged many innovative and ever-growing projects in the application domain of cloud and fog computing. CPS requires a novel, highly distributed, secure fog computing infrastructure in the heterogeneous network for strengthening its position for the mobile and wireless network in the new 5G era [12]. It can provide unified and cost-effective computing services for smart cities, vertical industries, and IoTs at the extreme edge of the new 5G network.

Further, the concept of an *OpticalFogNode* is proposed that supports low-cost and on-demand access to the computing infrastructure of the Optical-Fog layer in the 5G network. The main challenge is to run the CPS-based applications on the *OpticalFogNode*. The optical network virtualization (ONV) and SDN provide a

novel solution to deploy *OpticalFogNode* at the edge of the network. All free available resources (FARs) of the optical elements are grouped together to form an *OpticalFogNode* with the computing capabilities like processor, memory, and bandwidth. ONV converts the free available physical resources of the optical network elements into the virtual resources as infrastructure-as-a-service (IaaS) model. Initially, each submitted task is categorized as CBS-based or non-CPS-based task on the basis of requested resources in terms of processing power, storage, bandwidth, acceptable security level, etc. The Optical-Fog manager can dynamically reconfigure the *OpticalFogNode* which provides the desired reliability and QoS for the CPS. An algorithm is proposed that identify all possible created *OpticalFogNode* on the SDN path and assign them CPS-based tasks for further processing. The non-CPS-based tasks are directly sent to the cloud layer only if the resources of *OpticalFogNode* are not free.

Algorithm Task placement algorithm for the proposed framework.

```

Data:  $T$ 

while  $P \in$  Across all SDN paths do
    List RunningTasks;
    while OpticalFogNode  $\in$   $P$  do
        List TaskToPlaced;
        while task  $T \in$  CPS do
            if All predecessors of  $T$  are in TaskToPlaced then
                Add  $T$  to TaskToPlaced;
            end
        end
    end
    while Task  $T \in$  TaskToPlaced do
        if ( $Resources_T^{req} < Resources_{OpticalFogNode}^{Avail}$ ) then
            Allocate  $T$  on OpticalFogNodeAvail;
            if (!OpticalFogNodeAvail) then
                Allocate  $T$  on OpticalFogNodeDC;
            end
        else
            Allocate  $T$  on OpticalFogNodeDC;
            if (!OpticalFogNodeDC) then
                Choose  $T'$  such that ( $T' > T$  AND  $T' =$ non-CPS) if
                    (!NULL) then
                        Allocate  $T'$  on cloud data-centers;
                        Allocate  $T$  on OpticalFogNodeDC;
                    else
                        Allocate  $T$  on cloud data-centers;
                    end
                end
            end
        end
    end
end
    
```

In the proposed algorithm, the resources required by the new task are evaluated and then allocated on the *OpticalFogNode*. This node is scalable to provide the required computing resources dynamically by using the concept of ONV.

If the computing resources of *OpticalFogNode* are already occupied, then there are two options to execute the task on the basis of its preference. If the requested new task is a non-CPS task, it can be directly allocated to the cloud. Otherwise, CPS-centric task can be executed.

- T represents the requirements of submitted task for the framework along with its category as CPS-based or non-CPS-based task.
- *RunningTask* represents the already running tasks.
- *OpticalFogNode* is virtual and a dynamically configurable smart node using the concept of ONV at the Optical-Fog layer.
- *TaskToPlaced* all coming task to be allocated to the *OpticalFogNode* for further processing.
- $OpticalFogNodeNode^{Avail}$ is a free available resource at the OpticalFog.
- $OpticalFogNode_{DC}^{Avail}$ is a free available resource at the dynamically configured *OpticalFogNode*.

Further, this layer uses the SDN-based controller for optimizing the distribution of the flow among various redundant paths. In order to increase the QoS, the shortest path is chosen that minimizes the delay. In the optical network in the 5G environment, the *OpticalFogNode* has a flow table which is used to match the routing information of the received packet in the path. If there is no entry found in the flow table, the received packet is forwarded to the SDN controller for finding the shortest path so that the particular packet can be forwarded. Thus, a new entry is added (once the path is chosen) in the flow table of the *OpticalFogNode* for the coming future packets. Hence, the proposed SDN controller identifies the shortest path with the least congestion among all possible paths.

2.2.1 Architecture of *OpticalFogNode*

In SDN-based Optical-Fog/cloud network, the key challenge with the deployment of a fog node is to make it secure from the attackers. However, attackers are capable to create malicious programs with the ability to detect and evade their targets in distributed computing environments. **Figure 3** shows that optical network virtualization provides a novel solution to deploy *OpticalFogNode* in the middleware of IoT devices and the cloud rather than deploying at cloud data centers.

SDN technology combined with optical network virtualization allows for running the control logic of each tenant on a virtual SDN controller rather than deploying and running at the cloud data centers.

The resources to the proposed *OpticalFogNode* can be provisioned on demand from geographically distributed optical elements specially ONUs. The architecture of *OpticalFogNode* is shown in **Figure 4** where it can be deployed and configured virtually. The architecture has southbound and northbound interface along with SDN controllers which belong to different tenants of *OpticalFogNode* to emulate them for different IoT applications. It has the capability to control optical network elements for processing the configuring demand of different *OpticalFogNode* tenants such as computing resources, topology, address scheme, node mapping options, etc. Hence, virtual *OpticalFogNode* can be created in the form of infrastructure-as-a-service for providing real-time control to each *OpticalFogNode* tenant over its virtual

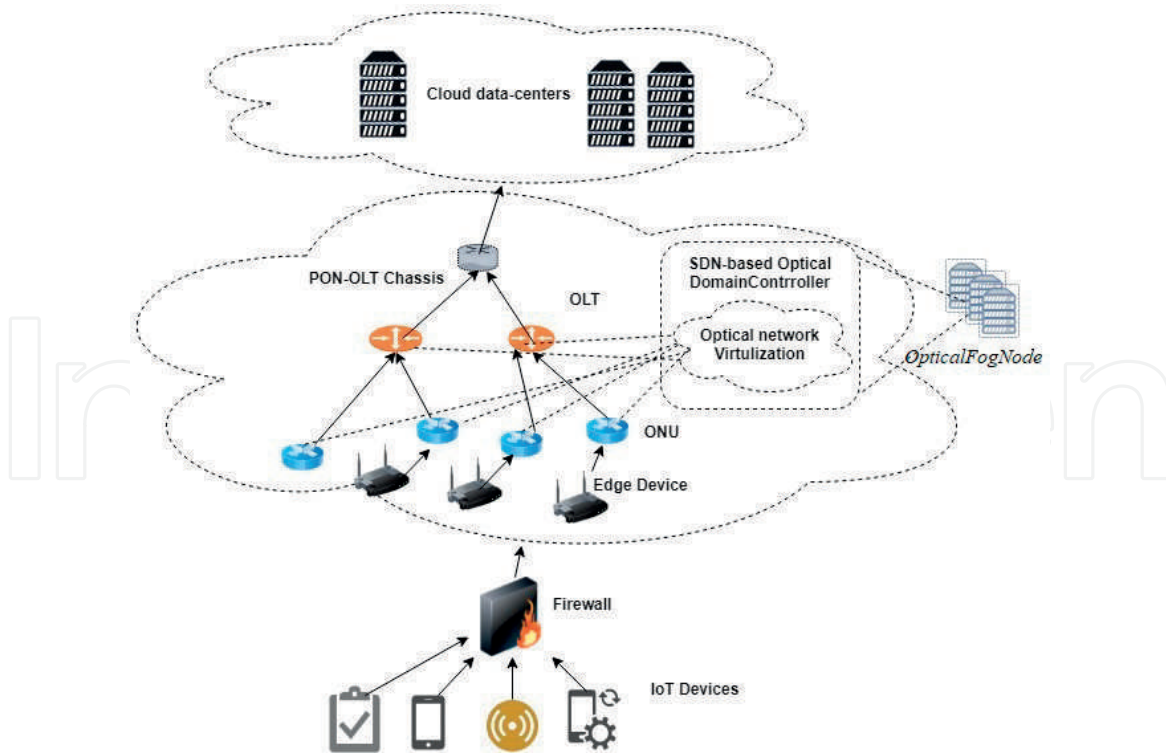


Figure 3.
 Deployment scenario of *OpticalFogNode* at *Optical-Fog* layer.

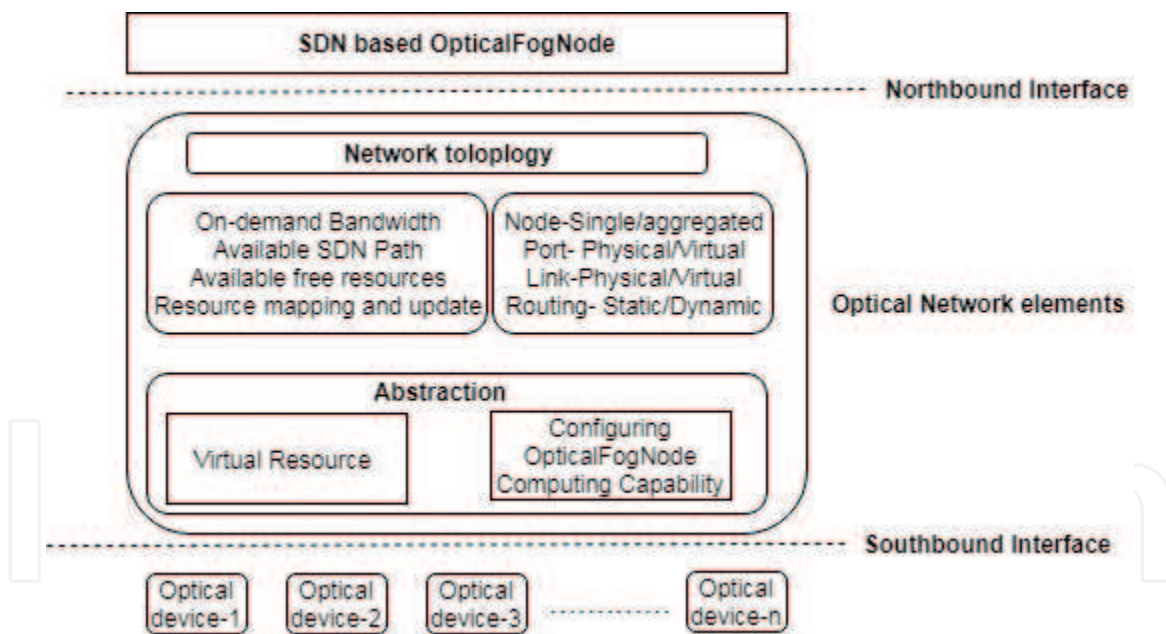


Figure 4.
 SDN-based *OpticalFogNode* architecture.

network. In order to form virtual infrastructure, a free-available-resource concept is proposed which uses the freely available resources of the optical network elements that lie at the *Optical-Fog* layer. Since routers and switches have limited resources, only optical elements such as optical network units and optical line terminals are taken into account for implementing FAR. Optical elements like ONUs and OLTs have their own processing, storage, and interconnection capabilities that are not fully utilized by the present network scenario. Thus, as shown in **Figure 5**, each optical element has some amount of running resources as well as FAR. Our proposed *OpticalFogNode* aggregates those FARs for facilitating the computing capability to each *OpticalFogNode* tenant.

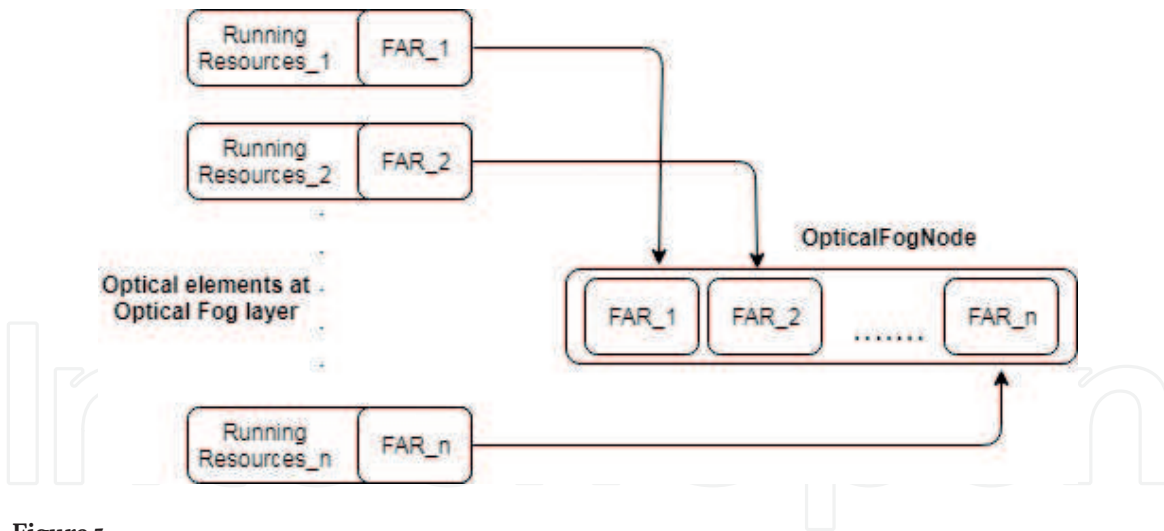


Figure 5.
Free available resource.

Hence, all FARs of optical network are grouped together to form virtual data centers with computing resources such as processor, memory, and bandwidth. ONV converts the physical resources of optical network elements into the virtual resources as infrastructure-as-a-service (IaaS) model to build virtual honeypots that prevents vulnerability and its identity from the attacker.

2.3 EEG-based VR gaming applications

SDN-based Optical-Fog network introduced as shown in **Figure 3** provides optimum bandwidth and ultralow delay for EEG-based VR gaming applications. The Edge-Fog layer and Optical-Fog layer provide rich gaming experience and QoE for EEG-based VR gaming applications by utilizing the optical resources than the cloud resources [13]. The Optical-Fog layer executes the game logic where the VR scenes can be encoded and streamed at the Edge-Fog layer. SDN-based controller improves the QoE and supports the playing of a game across the distributed geo-locations with minimum delay. It optimizes the flow distribution among the various redundant paths inside the Optical-Fog network to reduce the delay. In contrast to a traditional controller, the proposed SDN controller provides the shortest path with the least congestion among all possible paths

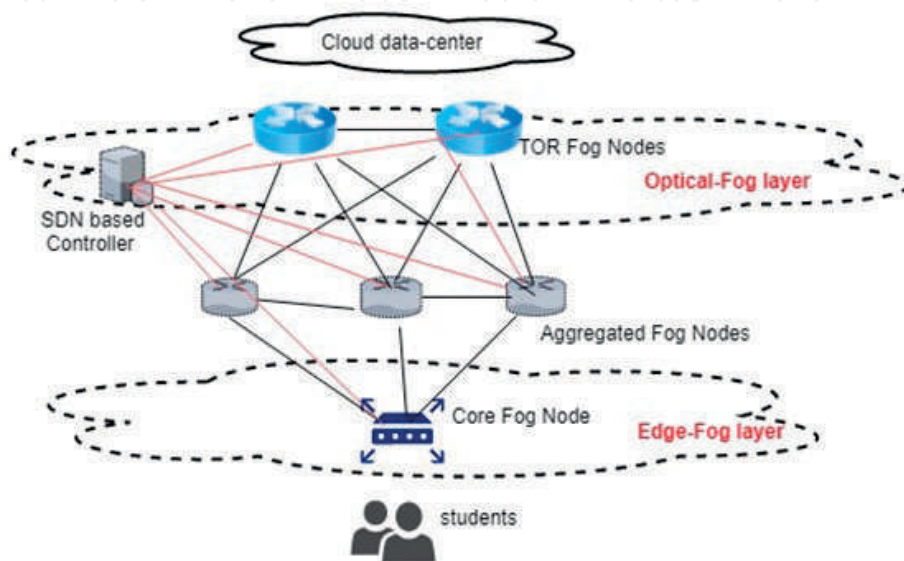


Figure 6.
SDN-based Optical-Fog network.

from the requesting Core Fog nodes to the Top of Rack (TOR) Fog nodes in the optical network which is shown in **Figure 6**. It uses an open-loop congestion control mechanism to employ congestion aware direct routing. Each node of the SDN network keeps the estimation cost $C_n^c(t)$ for delivering packets to their destination node c [14]. It helps to find the shortest path with least congestion by using the historical knowledge of the connection to node c and the waiting time of packets to c in the node n 's queue. It is assumed that all nodes broadcast a request for the cost frequently to their neighbors. Also, all neighbor nodes keep updating their cost table on the basis of the received request for the cost. To find the shortest path with the least congestion, the node with minimum delivery cost is selected as shown in **Figure 7**. The convoluted parameters are referred to as *Proximity Measure* $\Theta_n^c(t)$ and *Net Destination Queue Waiting Time* $\Omega_n^c(t)$ are used to compute the delivery cost [13].

$$\Theta_n^c(t) = \frac{Q_n^c(t)}{T_n^c(t)} \quad (1)$$

The value of $\Theta_n^c(t)$ lies between 0 and 1. The value 1 indicates the connection between n and c , whereas 0 shows that they were never connected. Here, $T_n^c(t)$ is the time increment, and $Q_n^c(t)$ is the time duration while c and n remains connected.

2.3.1 Net destination queue waiting time

$$\Omega_n^c(t) = \sum_{i=0}^N (\tau - a_{n,i}^c) \quad (2)$$

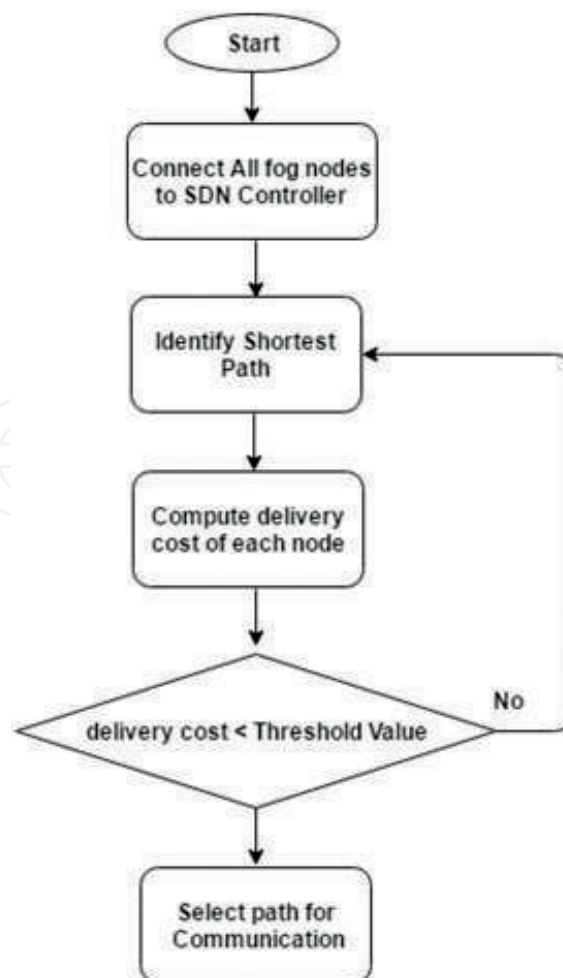


Figure 7.
 Workflow to find the shortest path.

Here, τ is the present time and $a_{n,i}^c$ is the arrival time of packets i . Since the queue waiting time is used to predict the congestion, delivery cost can be considered as an exponentially increasing function. Hence, the delivery cost to c via n is computed as:

$$C_n^c(t) = \Omega_n^c(t) \cdot [1 - \Theta_n^c(t)] + C_n^c(t - 1) \quad (3)$$

Thus, the shortest path with least congestion is identified by pulling packets toward the neighbors that have the smallest queue. It helps the SDN controller to set the threshold value for decision making.

2.3.2 Modules placement strategy in the Optical-Fog network

In order to deploy gaming modules, an algorithm is proposed that utilizes the Edge-Fog layer and Optical-Fog layer in the Optical-Fog network. The proposed algorithm places gaming modules using the SDN topology and iterates over all paths. Here, it places modules on the devices in incremental fashion starts from edge devices d_{Edge} to the optical devices $d_{Optical}$ and to the cloud data-centers. The modules that can be placed for each fog device in the path $\varepsilon_{d_{Edge}} \cup d_{Optical}$ are identified by computing the processing requirement against the available capacity of fog devices.

A module M is placed on a fog device d_{Edge} or $d_{Optical}$ only if all other modules are already placed in the bottom-up path.

| Algorithm | Optical-Fog-based gaming modules placement |
|-----------|---|
| Data: | M |
| | <pre> while $P \in$ Across all SDN paths do List PlacedModules; while Fog devices ($d_{Edge} \cup d_{Optical}$) \in P do List ModulesToPlaced; /* Bottom-up traversal*/ while module $g \in$ GamingApp do if All predecessors of g are in PlacedModules then Add g to ModulesToPlaced; end end end end while module $M \in$ ModulesToPlace do if ($CPU_M^{req} < CPU_{d_{Edge}}^{Avail}$) then Allocate M on d_{Edge}; if ($CPU_{d_{Edge}}^{Avail}$) then Allocate M on $d_{Optical}$; end else Allocate M on $d_{Optical}$; if ($CPU_{d_{Optical}}^{Avail}$) then Choose M' such that ($M' > M$ AND $M' = \text{Less-Delay-Sensitive}$) if (!NULL) then Allocate M' on cloud data-centers; Allocate M on $d_{Optical}$; else Allocate M on cloud data-centers; end end end end end end </pre> |

3. Performance analysis

The real-time gaming applications and CPS systems require ultralow latency, minimum energy consumption, and optimum bandwidth. The proposed Optical-Fog layer provides the desired QoE by evaluating the following parameters such as latency measure, energy consumption and bandwidth usage in contrast to the traditional cloud computing.

3.1 Latency measure

The proposed system utilizes the Optical-Fog layer that reduces the delay and improves QoE. The latency measured in the context of delay is the most concerning issue. The communication between ONU and OLT is supported by the multi-point control protocol (MPCP) which is a frame-based protocol [15]. Here, only GATE and REPORT messages are exchanged between OLT and ONU. So, in the Optical-Fog network, the delay is measured as the time between the arrival of its last bit at ONU and the arrival of its last bit at OLT. The delay $tD(f_i)$ is the computation of adding three basic components shown as:

$$tD(f_i) = \Gamma_i + t_p + T_R \quad (4)$$

Alternatively, it is the time during which the respective REPORT message reaches at the OLT completely, where Γ_i represents the one-way propagation time of ONU_i , t_p represents the time between the request arriving at ONU_i and the start of the next REPORT message, and T_R represents the time duration of REPORT message [16]. Thus, the Optical-Fog layer processes more smart applications which require ultralow delay as well as efficient QoS requirements.

3.2 Energy consumption analysis

For computing energy consumption, only the edge devices of the network is a concerning issue because energy consumption by the PON channel is negligible. Thus, the total energy consumption is computed as:

$$\Delta E = E_{Edge-Fog} + E_{Optical-Fog} + E_{cloud} \quad (5)$$

- $E_{Edge-Fog} = \Sigma(E_{Edge-devices})$ represents the energy consumed by all edge devices.
- $E_{Optical-Fog} = \Sigma(E_{ONU} + E_{OLT} + E_{PON})$ represents the energy consumed by the optical elements which is negligible.
- E_{cloud} is the energy consumption of cloud data centers.

The proposed framework computes most of the computations at the Optical-Fog layer which reduces the overhead on the cloud data centers. Thus, QoE is improved by minimizing the overall energy consumption.

3.3 Bandwidth measure

Real-time applications require more bandwidth to process the extraordinarily huge volume of data. Thus, the traditional cloud system increases the overhead on communication bandwidth which results in increasing delay and poor QoE. To

compute the communication bandwidth constraint, the traffic rate is assumed to be dispatched from the fog node i located at Edge-Fog layer to the server j located at cloud data center through the transmission path [17]. There is a limitation $\lambda_{i,j}^{max}$ on the bandwidth capacity of each path which is computed as:

$$0 \leq \lambda_{i,j} \leq \lambda_{i,j}^{max} \quad \forall_i \in N_{fog} \text{ and } \forall_j \in M_{cloud} \quad (6)$$

Here, N_{fog} represents the set of fog devices where M_{cloud} is the set of cloud data center servers. The optimum utilization of Optical-Fog network is more effective than the traditional cloud.

4. Conclusion

The utilization of optical resources provides several benefits such as high scalability, optimum bandwidth capacity, ultralow delay, and very less energy consumption. A novel concept of FRF and ONV is used to create *OpticalFogNode* in SDN-based optical network technology. In the realization of the SDN-based optical network in fog/cloud environment, the optical network uses SDN controller efficiently to identify the shortest path (with the least congestion) to minimize delay. Also, the proposed framework effectively enhances the QoE by using the proposed module placement algorithm which enhances the QoE and makes applications more entertaining. The realization of CPS-based tasks requires optimum placement strategy which is one of the concerning issues. The proposed algorithm efficiently finds the shortest path by utilizing the concept of SDN over the optical network. The novel concept of configuring *OpticalFogNode* successfully implemented to fulfill the requirements of the CPS system. Further, the performance of the proposed system is evaluated by effectively interpreting the delay measure, bandwidth usage, and energy consumption. Finally, Optical-Fog-based deployment provides an effective platform which enhances the QoE for smart applications.

Author details

Kiran Deep Singh

Department of Computer Science and Engineering, Khalsa College of Engineering and Technology, Amritsar, Punjab, India

*Address all correspondence to: kdkirandeep@gmail.com

IntechOpen

© 2019 The Author(s). Licensee IntechOpen. This chapter is distributed under the terms of the Creative Commons Attribution License (<http://creativecommons.org/licenses/by/3.0>), which permits unrestricted use, distribution, and reproduction in any medium, provided the original work is properly cited. 

References

- [1] Chanclou P, Cui A, Geilhardt F, Nakamura H, Nessel D. Network operator requirements for the next generation of optical access networks. *IEEE Network*. 2012;**26**(2):8-14
- [2] Gubbi J, Buyya R, Marusic S, Palaniswami M. Internet of things (IoT): A vision, architectural elements, and future directions. *Future Generation Computer Systems*. 2013;**29**(7):1645-1660
- [3] Bonomi F, Milito R, Zhu J, Addepalli S. Fog computing and its role in the internet of things. In: *Proceedings of the First Edition of the MCC Workshop on Mobile Cloud Computing*. ACM; 2012. pp. 13-16
- [4] Chen S, Xu H, Liu D, Hu B, Wang H. A vision of IoT: Applications, challenges, and opportunities with China perspective. *IEEE Internet of Things Journal*. 2014;**1**(4):349-359
- [5] Yang B, Zhang Z, Zhang K, Hu W. Integration of micro data center with optical line terminal in passive optical network. In: *2016 21st OptoElectronics and Communications Conference (OECC) Held Jointly with 2016 International Conference on Photonics in Switching (PS)*. IEEE; 2016. pp. 1-3
- [6] Nunes BAA, Mendonca M, Nguyen X-N, Obraczka K, Turletti T. A survey of software-defined networking: Past, present, and future of programmable networks. *IEEE Communication Surveys and Tutorials*. 2014;**16**(3):1617-1634
- [7] Sood SK, Singh KD. SNA based resource optimization in optical network using fog and cloud computing. *Optical Switching and Networking*. 2017
- [8] Luo Y, Effenberger F, Sui M. Cloud computing provisioning over passive optical networks. In: *2012 1st IEEE International Conference on Communications in China (ICCC)*. IEEE; 2012. pp. 255-259
- [9] Feamster N, Rexford J, Zegura E. The road to SDN: An intellectual history of programmable networks. *ACM SIGCOMM Computer Communication Review*. 2014;**44**(2):87-98
- [10] Sood SK, Singh KD. Identification of a malicious optical edge device in the SDN-based optical fog/cloud computing network. *Journal of Optical Communication*. 2018. DOI: 10.1515/joc-2018-0047. [Retrieved 19 Feb, 2019]
- [11] Banerjee A, Park Y, Clarke F, Song H, Yang S, Kramer G, et al. Wavelength-division-multiplexed passive optical network (WDM-PON) technologies for broadband access: A review. *Journal of Optical Networking*. 2005;**4**(11):737-758
- [12] Khan S, Parkinson S, Qin Y. Fog computing security: A review of current applications and security solutions. *Journal of Cloud Computing*. 2017;**6**(1):19
- [13] Sood SK, Singh KD. An optical-fog assisted EEG-based virtual reality framework for enhancing e-learning through educational games. *Computer Applications in Engineering Education*. 2018;**26**(5):1565-1576
- [14] Yassine A, Rahimi H, Shirmohammadi S. Software defined network traffic measurement: Current trends and challenges. *IEEE Instrumentation and Measurement Magazine*. 2015;**18**(2):42-50
- [15] Luo Y, Ansari N. Bandwidth allocation for multiservice access on EPONS. *IEEE Communications Magazine*. 2005;**43**(2):S16-S21
- [16] Wan C-Y, Campbell AT, Krishnamurthy L. PSFQ: A reliable

transport protocol for wireless sensor networks. In: Proceedings of the 1st ACM International Workshop on Wireless Sensor Networks and Applications. ACM; 2002. pp. 1-11

[17] Deng R, Lu R, Lai C, Luan TH, Liang H. Optimal workload allocation in fog-cloud computing toward balanced delay and power consumption. *IEEE Internet of Things Journal*. 2016;3(6):1171-1181

IntechOpen

Radial Line Slot Array (RLSA) Antennas

Teddy Purnamirza

Abstract

Radial line slot array (RLSA) antenna was initially developed for satellite antenna receivers at a frequency of Ku-band. The success of this development inspired researchers to continue the study to other bands and other applications, such as Wi-Fi at 5.8 GHz. Wi-Fi applications need small antennas that lead to the diminution of RLSA antennas. Small-RLSA antennas experienced high reflection due to the small number of slots. One of the techniques that effectively eliminates the reflection was developed and named as extreme beamsquint technique. Several researches have successfully developed small-RLSA antennas by implementing this technique for Wi-Fi applications. Furthermore, for the future, it is possible to widen the researches to other frequencies and other features of RLSA antennas such as multibeam, multiband, and diminution by cutting off RLSA antennas.

Keywords: RLSA antennas, extreme beamsquint, small RLSA, RLSA for Wi-Fi, future RLSA antennas

1. Introduction

Radial line slot array (RLSA) antennas are a type of cavity or waveguide antennas. These antennas were firstly developed for satellite receivers as an option besides parabolic antennas. Unlike parabolic antennas, RLSA antennas have an advantage of having feeders at the back of the antenna, so that the feeders do not block out incoming signals. The other advantage is their flat shape so that they are more aesthetic compared to parabolic antennas. Nowadays, RLSA antennas are developed for different frequency applications such as Wi-Fi, 5th G, etc.

This chapter discusses briefly all about radial line slot array (RLSA) antennas, especially for the linearly polarized (LP)-RLSA antennas. Firstly, in Section 2, the review of RLSA antennas including the development of RLSA antennas, their applications, their development obstacles and the developed technique to overcome the obstacles are reviewed. Secondly, in Section 3, the theory of RLSA antennas is explained which includes how the antenna works and several equations to calculate antenna parameters. Thirdly, in Section 4, the mechanism of reflections in RLSA antennas, which is due to slot reflections and due to remaining power in antenna perimeter, is discussed. Fourthly, in Section 5, the theory of extreme beamsquint technique is also explained in detail. Lastly, in Section 6, the idea of future research in topic of RLSA antennas is briefly explained, including the idea of cutting off RLSA antennas to smaller size, multibeam RLSA antennas, utilizing background as

radiating element and multiband RLSA antennas. It is hoped that the ideas can inspire researches for the next development of RLSA antennas.

2. Review of RLSA antenna developments

Kelly introduced the concept of RLSA antennas in the 1950s [1]. Although Kelly could produce a high-gain RLSA antenna, the structure of the antenna feeder was still complex, leading it to be costly.

In 1988, Ando et al. proposed a RLSA antenna at a frequency of 12 GHz. This antenna was designed using the technique of slot arrangements. The technique aims to produce a uniform-aperture distribution. This antenna has a double-layer cavity and exhibits a good linear polarization. Ando also proposed a beamsquint technique to improve the poor reflection coefficient in linearly polarized RLSA antennas [2, 3]. In the same year, by applying a reflection coefficient suppression and slot coupling technique, Ando successfully designed a LP-RLSA antenna for satellite applications at 12 GHz. This antenna has the efficiency of 76% and the gain of 36 dB [4–6]. Takada et al. introduced a technique to improve the reflection coefficient using a reflection cancelling slot technique. This technique successfully improved the reflection coefficient of RLSA antennas from -2 to -10 dB [7]. Endo et al. designed an optimum thickness of double-layer RLSA antennas in order to realize the mass production of thinner RLSA antennas [6].

In 1990, Ando et al. furthermore introduced a circularly polarized RLSA (CP-RLSA) antenna. This antenna utilizes a single-layer cavity instead of a double-layer cavity. This simpler cavity structure improves the complexity of RLSA fabrications and can achieve the gain of 35.4 dBi and the efficiency of 65%. Ando used two techniques to improve the antenna performance. The first is the technique of varying the slot length and slot spacing used to event out the aperture illuminations of the antenna. The second is the technique of matching spiral used to reduce the reflection of the residual power at the antenna perimeters [8, 9]. In 1991, Takashi et al. proposed the technique of varying the slot length and spacing. Utilizing this technique Takahashi proposed several high-efficiency single-layer RLSA antennas with the diameter of 25–60 cm. These antennas can achieve efficiencies of between 70 and 84% [10]. Furthermore, Takashi et al. produced and marketed a 78% efficiency, 32.6 dB gain and single-layer RLSA [11–13].

Australian researchers started to investigate RLSA in 1995. They reported several investigations to design LP-RLSA antennas for satellite receivers. These investigations used the combination of the theoretical and experimental approach. The availability of low-cost materials (polypropylene) and low-cost fabrication also become a consideration in these researches. In 1997, Davis reported a 60 cm diameter LP-RLSA prototype designed using the reflection cancelling slot technique. This technique can overcome the inherent poor reflection coefficient of LP-RLSA antennas [4]. Davis and Bialkowski also successfully tested a RLSA antenna designed utilizing the reflection cancelling slot technique and a beamsquint value of 20° [14, 15]. Furthermore, Davis and Bialkowski reported an investigation of LP-RLSA antennas utilizing the beamsquint technique for several squint angles. This technique successfully improved the reflection coefficient under -25 dB [16]. Davis integrated the report of [2, 4, 7, 11] to form a beam synthesis algorithm used to calculate the design parameter of LP-RLSA antennas [17].

Due to the successful development of RLSA antennas for satellite applications, researchers tried to bring RLSA antennas into small antenna application for Wi-Fi devices. However, the design of small-RLSA antennas was not easy since small-size RLSA antennas normally performed high reflection coefficient [18–20]. Hirokawa

et al. used a technique for matching slot pair in order to reduce the remaining power at the antenna perimeter of small-aperture RLSA, so that this technique can minimize the reflection coefficient [21, 22]. Akiyama et al. also used the same technique for matching slot pair [23, 24]. However, the technique for matching slot pair is only used to radiate the remaining power at the antenna perimeter and does not contribute to the antenna gain. Reference [25] introduced the use of long slots in order to increase the ability of slots to radiate power, so that it can reduce the remaining power at the perimeter of small-aperture RLSA antennas, thus reducing the reflection coefficient. However, although this method can reduce the reflection coefficient, this method also can decrease the antenna gain. This is because that the long slots cannot radiate a focus power.

In 2002, Malaysian and Australian researchers started to investigate the application of RLSA antennas for wireless LANs. Tharek and Ayu successfully fabricated a low-profile RLSA antenna at a frequency of 5.5 GHz with a broad radiation pattern of 60° used for indoor wireless LANs [26]. Bialkowski and Zagriatski investigated the design of RLSA antennas for wireless LANs and successfully fabricated a dual-band 2.4/5.2 GHz antenna [27, 28]. Furthermore, Imran et al. reported the design and test of RLSA antennas for outdoor point-to-point applications at the frequency of 5.8 GHz [29–31]. However, this design utilized a beamsquint technique that is similar with the technique used to design RLSA antennas for satellite applications. Hence, the diameter of this antenna is still considered large with a diameter of 650 mm, so that it is not applicable for small Wi-Fi devices. Islam reported the utilization of low-cost FR4 materials to fabricate RLSA antennas at the frequency of 5.8 GHz for wireless LANs. This invention is quite innovative since FR4 materials are a low-cost material and easy to be fabricated [32, 33]. However, there are some drawbacks in designing this antenna, such as a design of overlap slots, a loss cavity due to the use of several FR4 boards and the use of material loss of FR4. These all lead to low gain (only 8 dB) and low bandwidth (75 MHz).

Purnamirza et al., in 2012, introduced a technique called extreme beamsquint technique in order to overcome the problem of high reflection in small-RLSA antennas [34]. This technique uses the beamsquint values higher than 60° . The theory of how the high values of beamsquint can significantly minimize the reflection coefficient is explained. Purnamirza also developed RLSA antennas that mimic the specification of other types of antenna that is available in markets [35–38].

3. Basic theory of RLSA antennas

This section discusses the theory of RLSA antennas including the structure, the theory of how RLSA antennas work as well as several formulas to design RLSA antennas.

3.1 Structure of RLSA antennas

Figure 1 shows the illustration of the structure of a RLSA antenna. The figure shows the structure of RLSA antennas consisting of a radiating element, a cavity, a background and a feeder. The radiating element usually is a circular plate made of metals, such as aluminium, copper or brass. The radiating element consists of many slot pairs. One slot pair acts as one antenna element so that all the slot pairs form an array antenna. The background is a metal plate just like the radiating element, but the background does not have slots. The cavity is a dielectric material that has the form of a tube. Together with the radiating element and the background, the cavity operates as a circular waveguide that guides the signal from the feeder to propagate

in radial direction. The feeder is a part of RLSA antennas used to feed signals from a transmission line into the antenna.

3.2 How RLSA antennas work

Figure 2 shows the wave propagation mechanism including TEM cavity mode and TEM coaxial mode. The feeder placed in the centre of the antenna cavity feeds the electromagnetic power (indicated by the arrows). The feeder is an ordinary SMA feeder, which is modified by adding a head disc. The head disc has a function to convert the electromagnetic power from a TEM coaxial mode into a TEM cavity mode (a radial mode), so that the electromagnetic power fed by the feeder will propagate in a TEM mode and in a radial direction within the antenna cavity.

When the power passes the slot pair, some amount of the power escapes through the slot pair and radiates as illustrated in **Figure 3**. Hence, the slot pair can be considered as one antenna element. Since there are many slot pairs (thousands in normal-size RLSA antennas), all the slot pairs will form an array antenna. Therefore, this is the reason why ‘array’ word is included in the name of RLSA.

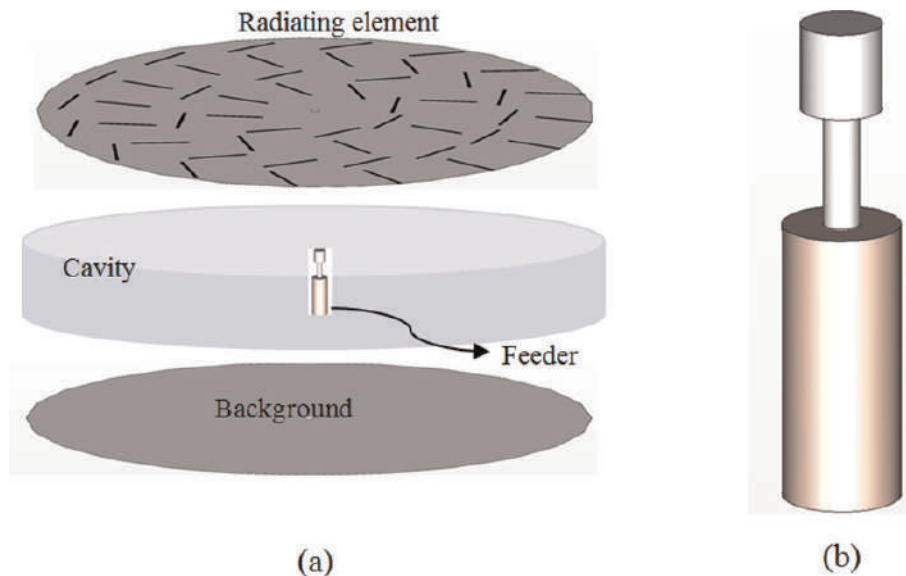


Figure 1. (a) The component of RLSA antennas. (b) The magnified view of the feeder [39].

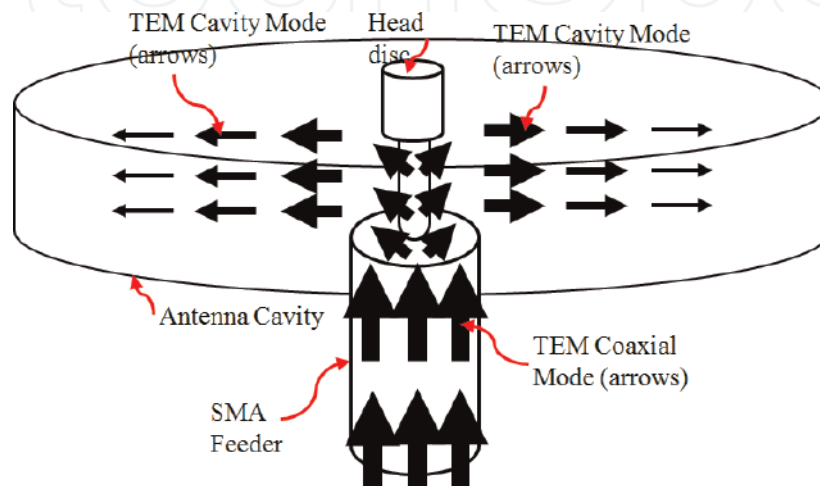


Figure 2. Illustration of the TEM cavity mode and the TEM coaxial mode [39].

3.3 Polarizations

A slot pair, which represents a signal source in RLSA antennas, is located in the top surface of the radiating element of a RLSA antenna. A linear polarization in the RLSA antenna can be produced by combining two signals from the slot pair.

Figure 4a shows the illustration of the slot pair. The signal from Slot 1 and the signal from Slot 2 have a phase difference of 180° or π radians since Slot 1 and Slot 2 have the distance of half wavelength ($0.5\lambda_g$) to each other. Since the orientation of Slot 1 and Slot 2 is perpendicular to each other, the signals from Slot 1 (at y axis) and Slot 2 (at x axis) are also perpendicular to each other, as shown in **Figure 4b**.

Figure 4b shows that when Signal 1 is increasing in positive values, Signal 2 is decreasing in negative values. Since their position is perpendicular to each other, the resulting wave becomes a line in Quadrant II. When Signal 1 is decreasing towards zero and Signal 2 is increasing towards zero, the resulting signal will be a line in Quadrant II but with a shorter length compared to the line in the previous case. When Signal 1 is decreasing in negative values and Signal 2 is increasing in positive values, then the resulting signal will be a line in Quadrant IV. When Signal 1 is increasing towards zero and Signal 2 is decreasing towards zero, then the resulting signal will be a line in Quadrant IV but with the shorter length compared to the line in the previous case. Now, we can understand that the resulting signal of Signal 1 and Signal 2 results in a signal that looks like a straight line where the

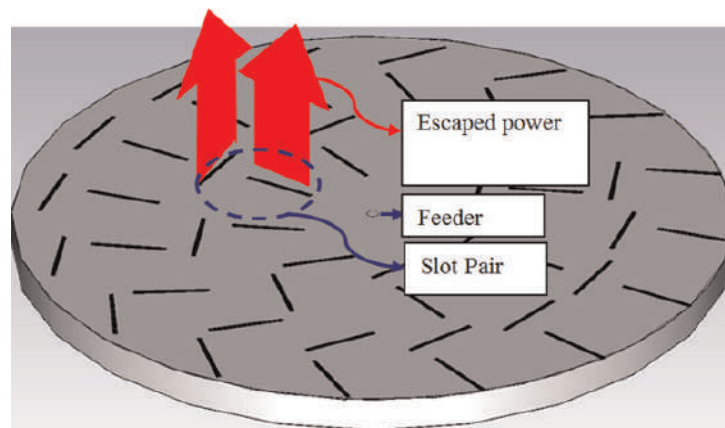


Figure 3.
 Illustration of the power escaping from the slot pairs [39].

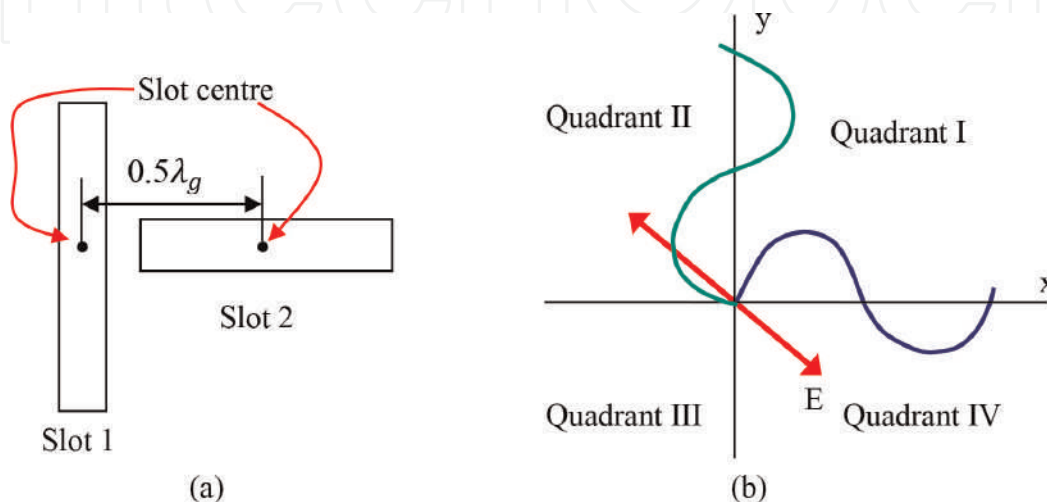


Figure 4.
 Polarization establishment in a linearly polarized RLSA [39]. (a) slot pair position (b) signal of each slot.

length changes as a function of time; this is the reason why its name is ‘linear polarizations’.

3.4 Orientation of the slot in RLSA antennas

Figure 5 shows the position of the slots (indicated by ‘A’ and ‘B’) and the squint of the inclination angles of the slots (indicated by θ_1 and θ_2). The slot pair must be located in the correct position on the radiating surface of RLSA antennas. The slot pair must be located in different and unique positions in order to prevent overlapping between them.

Equations (1) and (2) express the squint of the slots obtained by the beamsquint technique [4, 14–17, 39–43]:

$$\theta_1 = \frac{\pi}{4} + \frac{1}{2} \left\{ \arctan \left(\frac{\cos(\theta_T)}{\tan(\phi_T)} \right) - (\phi - \phi_T) \right\} \quad (1)$$

$$\theta_2 = \frac{3\pi}{4} + \frac{1}{2} \left\{ \arctan \left(\frac{\cos(\theta_T)}{\tan(\phi_T)} \right) - (\phi - \phi_T) \right\} \quad (2)$$

where θ_1 is the inclination angle of Slot 1; θ_2 is the inclination angle of Slot 2; θ_T is the beamsquint angle in elevated direction; ϕ is the azimuth angle of Slot 1 and Slot 2 position; and ϕ_T is the beamsquint angle in azimuth direction.

3.5 Arrangement of slot pairs

Figure 6 shows the geometrical arrangement of a slot pair or also called a unit radiator. The arrangement of the unit radiator in the radiating surface of RLSA antennas must be carefully calculated and drawn since a little deviation of the unit radiator position will rapidly decrease the performance of RLSA antennas.

Based on **Figure 6**, the distance of a particular unit radiator from the centre point of RLSA antennas is expressed in Eq. (3) [4, 14–17, 39–43]:

$$\rho_\rho = \frac{n\lambda_g}{1 - \xi \sin\theta_T \cos(\phi - \phi_T)} \quad (3)$$

Where $\xi = \frac{1}{\sqrt{\epsilon_r}}$

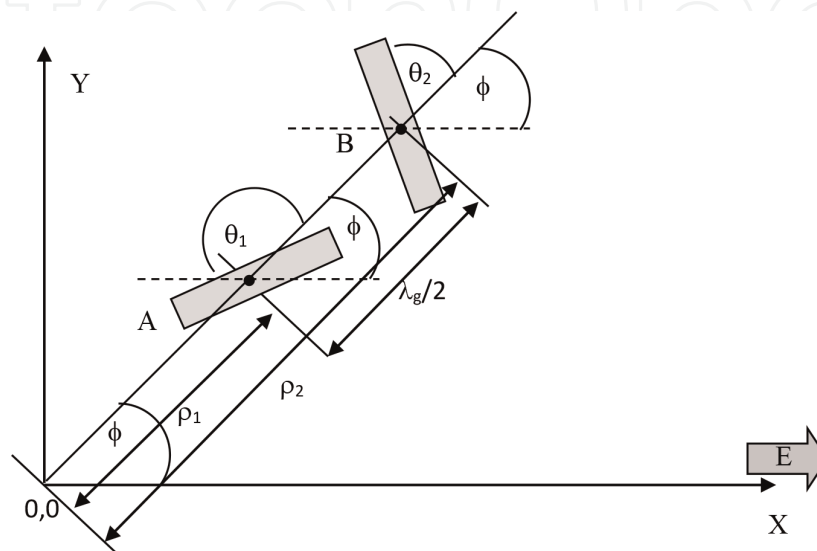


Figure 5.
Slot pair geometry [39].

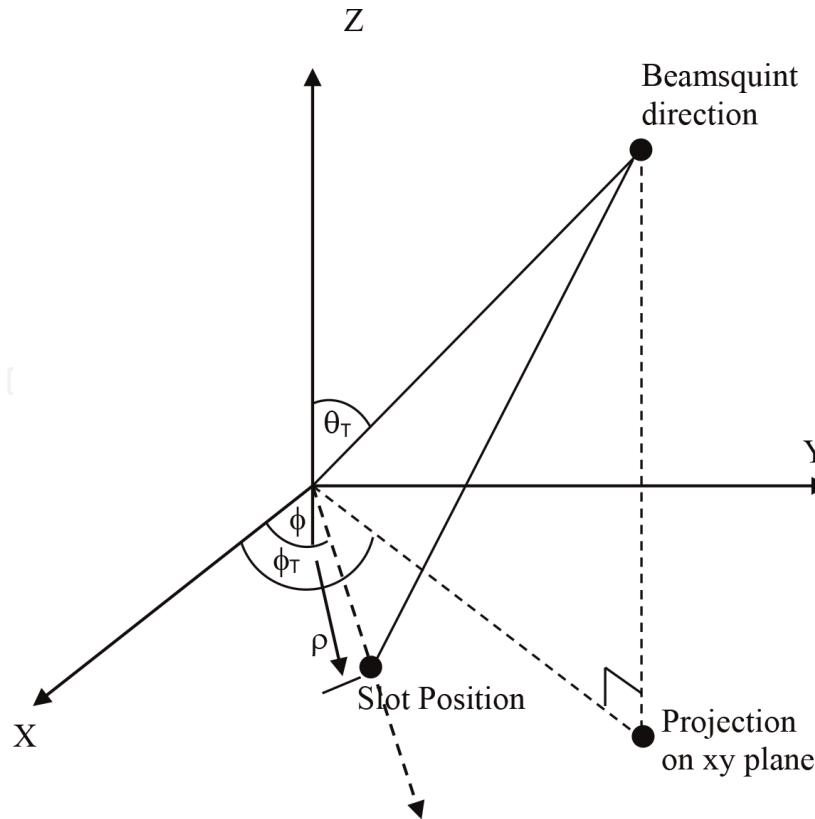


Figure 6.
 Geometrical arrangement of a unit radiator [39].

Equation (4) expresses the distance between two adjacent unit radiators located in two different rings (the distance in the radial direction) [4, 14–17, 39–43]:

$$S_{\rho} = \frac{\lambda_g}{1 - \xi \sin \theta_T \cos (\phi - \phi_T)} \quad (4)$$

Equation (5) expresses the distance between two adjacent unit radiators in a same ring (the distance in the azimuth direction) [4, 14–17, 39–43]:

$$S_{\phi} = \frac{2\pi\lambda_g}{\sqrt{1 - \xi^2 \sin^2 \theta_T}} \frac{q}{p} \quad (5)$$

where λ_g is the length of the wavelength inside the cavity of RLSA antennas; ϵ_r is the relative permittivity of the cavity of RLSA antennas.

n is the ring numbers (1,2,3, etc.); q is the integer numbers (1, 2, 3, etc.) that express the distance of the innermost ring from the centre of RLSA antennas; and p is the number of unit radiators in the innermost ring.

The parameters of S_{ρ} , S_{ϕ} , ρ_{ρ} , ρ_1 , and ρ_2 are shown in **Figure 7**. Since the distance from the centre of the unit radiator to Slot 1 or Slot 2 is ' $\lambda_g/4$ ', Eqs. (5)–(7) express the distance of slots from the centre of antennas [4, 14–17, 39–43]:

$$\rho_{\rho 1} = \frac{(n - 1 + q - 0.25)\lambda_g}{1 - \xi \sin \theta_T \cos (\phi - \phi_T)} \quad (6)$$

$$\rho_{\rho 2} = \frac{(n - 1 + q + 0.25)\lambda_g}{1 - \xi \sin \theta_T \cos (\phi - \phi_T)} \quad (7)$$

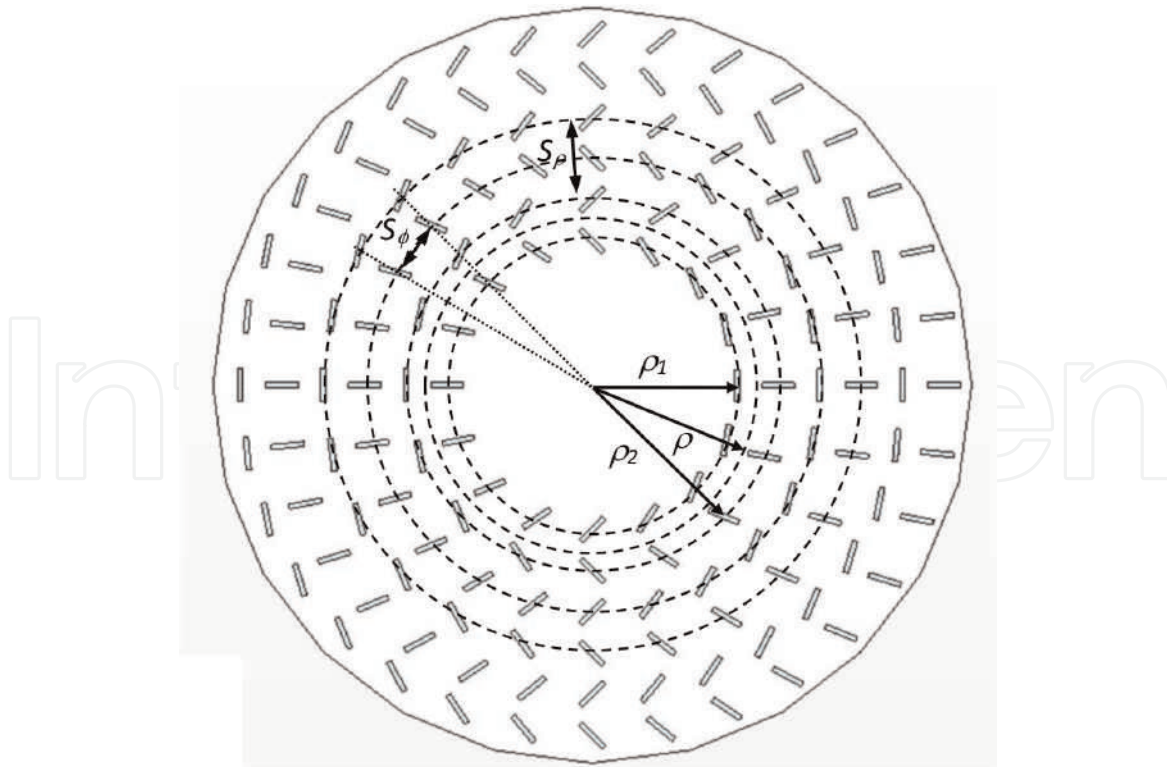


Figure 7.
Definition of some slot parameters [39].

3.6 Length of slots

The length of the slots on the radiating surface of RLSA antennas must be varied in order to achieve a uniform aperture illumination. The farther a slot from the centre of the antenna, the longer the length of the slot will be. The length of the slot is the function of ρ that is the distance of the slot from the centre of the antennas, as expressed by Eq. (8) [42]:

$$L_{rad} = (4.9876 \times 10^{-3} \rho) \frac{12.5 \times 10^9}{f_0} \quad (8)$$

The formula in Eq. (8) is an approximate formula. To get an accurate formula, we need to do some measurements and experiments.

4. Reflection in small-RLSA antennas

4.1 Signal reflection due to remaining power

The power (P) comes from the feeder, which is located at the centre of the antenna, and flows towards the antenna perimeter, as illustrated in **Figure 8b**. When the power passes the slots, some amount of the power radiates through the slots. The power inside the cavity will decrease every time the power passes the slots and will continue to decrease until the power reaches the antenna perimeter. Equation (9) expresses the remaining power (P_R) at the antenna perimeter [42]:

$$(P_R) = P (1 - \alpha)^n \quad (9)$$

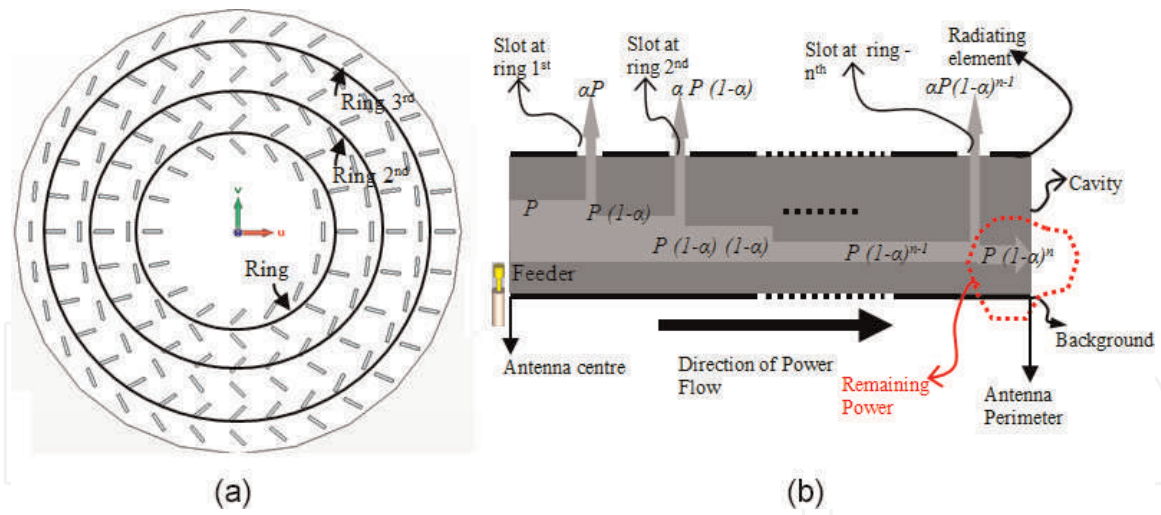


Figure 8.
 (a) Top view of RLSA. (b) Cut view of a RLSA antenna and the power flow mechanism inside the RLSA cavity [39].

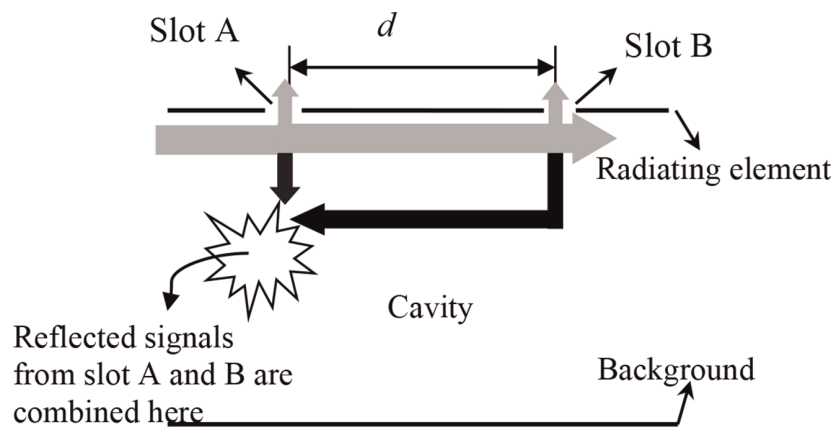


Figure 9.
 Illustration of the reflected signals from the slot [39].

Equation (9) shows that the amount of the remaining power depends on the number of rings (n), which is also proportional to the number of slots. For small-RLSA antennas, which have a small number of slots, the amount of the remaining power at the antenna perimeter will be high. Part of this remaining power will be reflected back to the feeder and result in a high signal reflection, thus increasing the reflection coefficient. For normal-size RLSA antennas, which have thousands of slots, the remaining power at the antenna perimeter is very small so that its effect to the signal reflection is neglected.

4.2 Signal reflection due to the reflected signal from slots

Figure 9 shows the front cut view of a RLSA antenna and the signal flow within the cavity of the RLSA antenna. The grey arrows represent the signals that flow from the centre of the RLSA antenna to the antenna perimeter, and the black arrows represent the reflected signal from the slots. **Figure 9** shows that since the distance between the slots (d) is $\lambda_g/2$, the signal from slot ‘A’ will travel for $\lambda_g/2$ to reach ‘B’. At ‘B’, some of the signal will be reflected back and travel for another $\lambda_g/2$ to reach ‘A’. Therefore, the reflected signal from slot ‘A’ and slot ‘B’ will have a different

phase of $\lambda_g/2 + \lambda_g/2 = \lambda_g$ or 360° (or can be said there is no phase difference), so that they will strengthen each other and result in a high signal reflection [42].

5. Extreme beamsquint technique

The ability of beamsquint technique in minimizing the reflected signal from the slots depends on one condition, that is, the number of ring must be sufficient. As an example, **Figure 10a** and **b** shows the reflected signals of a three-ring RLSA antenna and the reflected signals of a two-ring RLSA antenna, respectively. Since every ring consists of two slots, hence, there are six reflected signals for the three-ring RLSA antenna and four reflected signals for the two-ring RLSA antenna. It is assumed that the amplitude of all reflected signals is the same in order to simplify the analysis. From **Figure 10a**, it can be observed that all the graph space is covered by the reflected signals; hence the combination of all reflected signals will cancel out each other, and the minimum signal reflection is obtained. In contrast, from **Figure 10b**, it can be seen that not all graph space (the area pointed by ‘A’) is covered by the reflected signals; hence the combined signal will be greater than the combined signal in **Figure 10a**.

From the example in the previous paragraph, it can be concluded that a smaller number of ring will decrease the ability of beamsquint technique in cancelling the reflected signal. Therefore, this is the reason why the reflection coefficient of small-RLSA antennas, which have few numbers of rings (less than 2), is high and why the normal beamsquint technique fails to minimize the reflection coefficient of small-RLSA antennas. The next section will explain how the proposed extreme beamsquint technique can reduce the high reflection coefficient of small-RLSA antennas by increasing the number of ring.

The position of the ring in radial direction (S_ρ) can be expressed by Eq. (10) [21]:

$$S_\rho = \frac{r\lambda_g}{1 - \xi \sin \theta_T \cos(\phi - \phi_T)} \quad (10)$$

θ_T is the beamsquint angle, ϕ is the position of slots in azimuth, ϕ_T is the azimuth angle of beamsquint and r is the ring number. **Figure 11a** illustrates the definition of all this parameters.

Based on Eq. (10), by utilizing $r = 1$, $\phi_T = 0$ and $\phi = 0-360^\circ$, the rings for beamsquint angle of 10° , 30° and 60° are plotted as shown in **Figure 11b**.

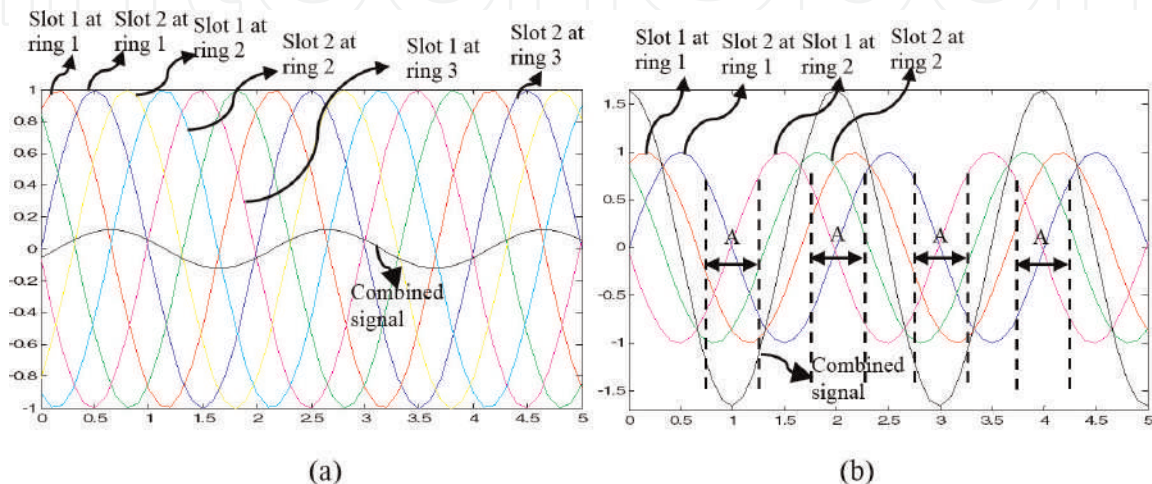


Figure 10. (a) Reflected signal of a three-ring RLSA antenna. (b) Reflected signal of a two-ring RLSA antenna [39].

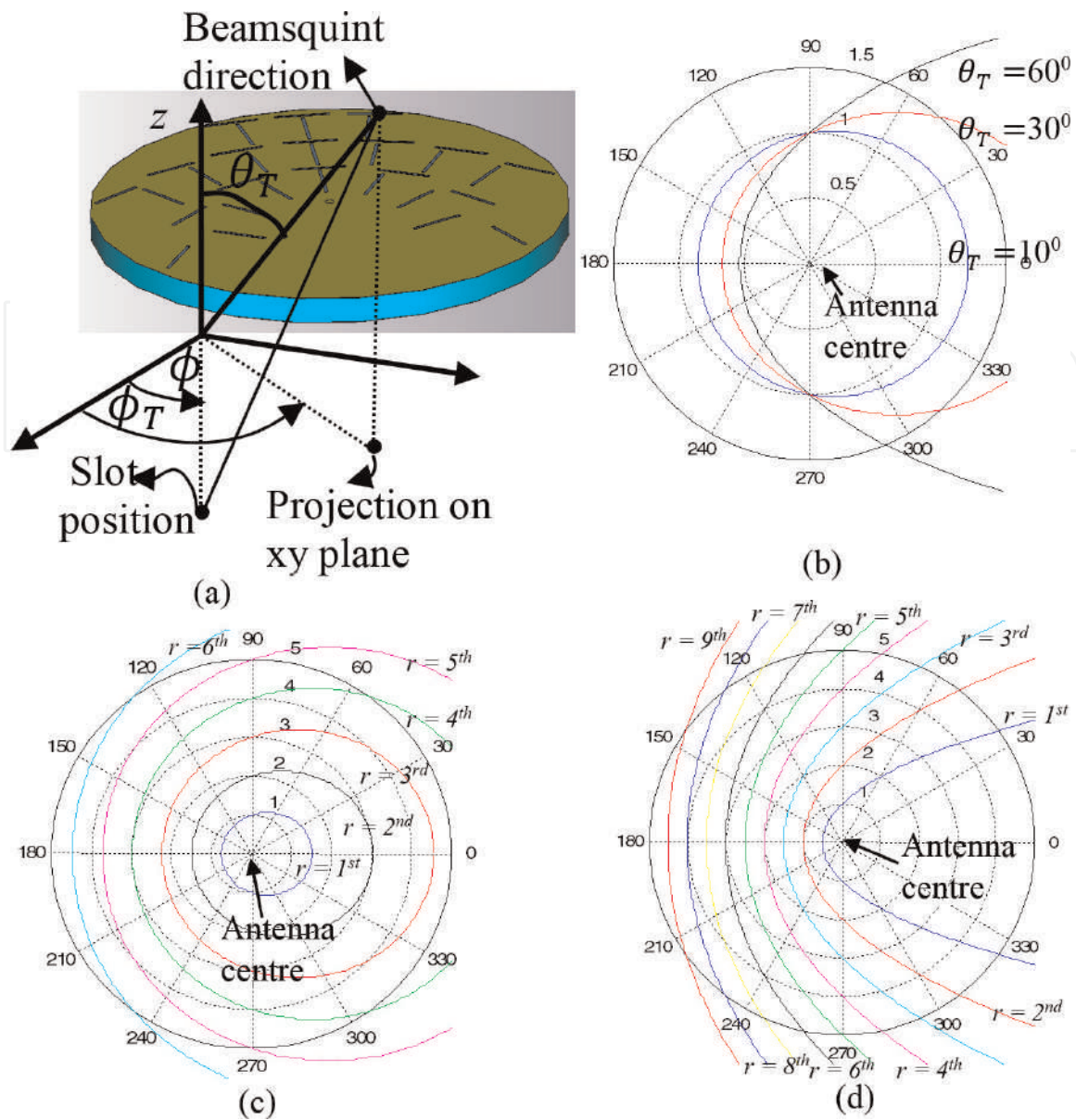


Figure 11.
 (a) Illustration of some parameters of ring position. (b) Plot of the ring for beamsquint of 20, 30 and 60°. (c) Plot of various ring numbers for beamsquint angle of 20°. (d) Plot of various ring numbers for beamsquint angle of 80° [39].

It illustrates that the beamsquint technique performs the ring in the shape of ellipse rather than in the shape of circular. From **Figure 11b**, it can be observed that the position of the ring at the left-hand side will move closer to the centre of the antenna as the beamsquint increases. In contrast, the position of the ring at the right-hand side will move farther from the centre of the antenna as the beamsquint increases.

Still based on Eq. 3, by utilizing $\phi_T = 0$ and $\phi = 0$ to 360° , the rings are plotted for various ring numbers both for the beamsquint angle of 20° and 80° as shown in **Figure 11c** and **d**, respectively. From these figures, it can be observed that at the left-hand side, the distance between rings for beamsquint angle of 80° is shorter than the distance between the rings for beamsquint angle of 20° . Due to the shorter distance between rings, the beamsquint angle of 80° has more rings (nine rings) that can be plotted in the antenna area compared to the beamsquint angle of 20° (six rings). Based on the previous examples and explanations, it can be concluded that the higher beamsquint angle can yield more rings. This fact is very useful to include additional rings for the small-RLSA antenna, which originally has a low number of rings (less than 2). The extra number of rings will have more ability to minimize the

reflection coefficient of small-RLSA antenna. The use of extra high beamsquint angle underlies the naming of extreme beamsquint technique.

6. Future development of RLSA antennas

Space to be explored for RLSA antennas has remained wide, since only few researchers study this topic. This is due to the drawing slots of RLSA antennas that are difficult without using computer programmes. This is unlike microstrip antennas which are easy to draw since their shape is simple. Moreover, it is more difficult to fabricate RLSA antennas compared to microstrip antennas since there is no raw material that is ready to be cut or to be formed. This is unlike microstrip, which can use many types of boards such as FR4. Therefore, due to these reasons, less researchers are interested in studying RLSA antennas than microstrip antennas. Below, several research ideas in the field of RLSA are presented to be explored deeper, especially for doctoral dissertation and master thesis.

6.1 Cutting antennas

6.1.1 Concentrated slot area

The use of extra high beamsquint results in concentrated slots in a certain area of radiating elements, and leaving other areas vacant from slots, as shown in **Figure 12a**.

Our hypothesis is that since the vacant area is not useful, then it can be cut off, thus resulting in a smaller antenna, as shown in **Figure 12b**. We have studied that definitely there will be an effect of the cut, which is a leakage power along the cutting line, shown in **Figure 12c**. This leakage power reduces the antenna gain. However, the antenna gain will not be affected significantly since the power density within the cut antenna will increase, thus also will increase the gain, then counteracting the decrease gain due to the leakage power.

6.2 The use of background as radiating element

Theoretically, only radiating elements that are used as place for slots, as shown in **Figure 13a**. The background always functions as conventional background to

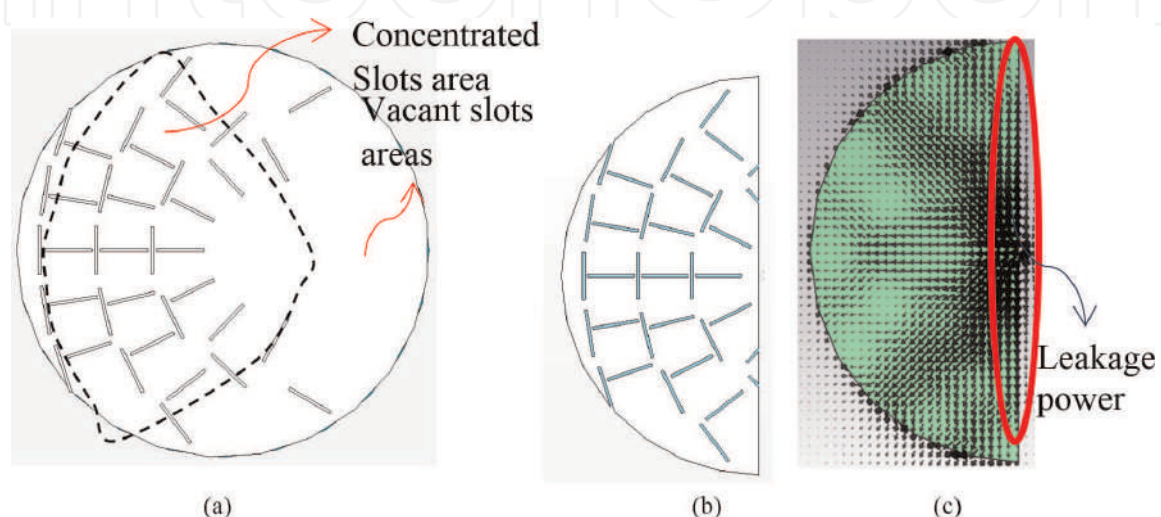


Figure 12.
(a) Concentrated slots. (b) Cut antennas. (c) Leakage power.

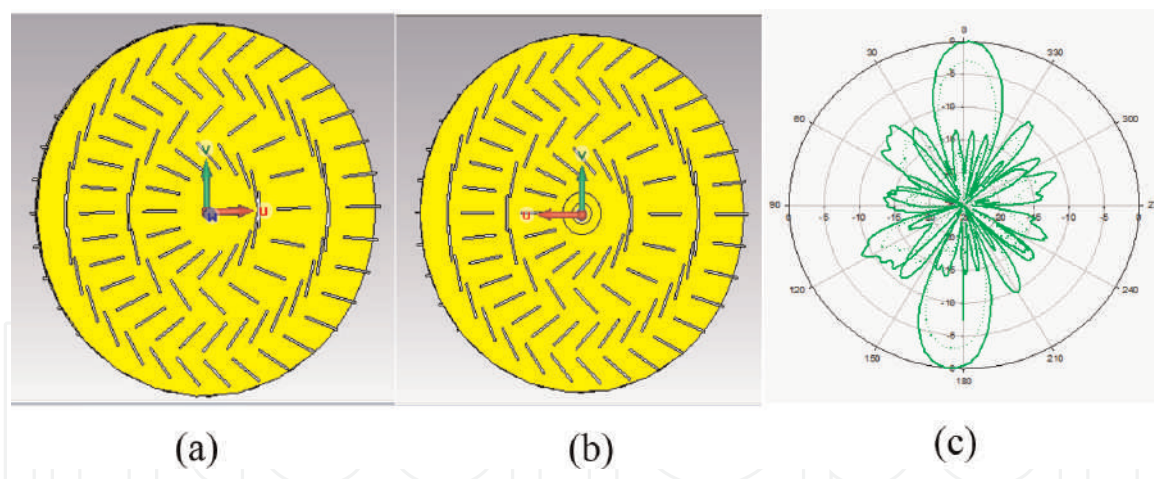


Figure 13.
 (a) Radiating element. (b) Background. (c) Radiation pattern.

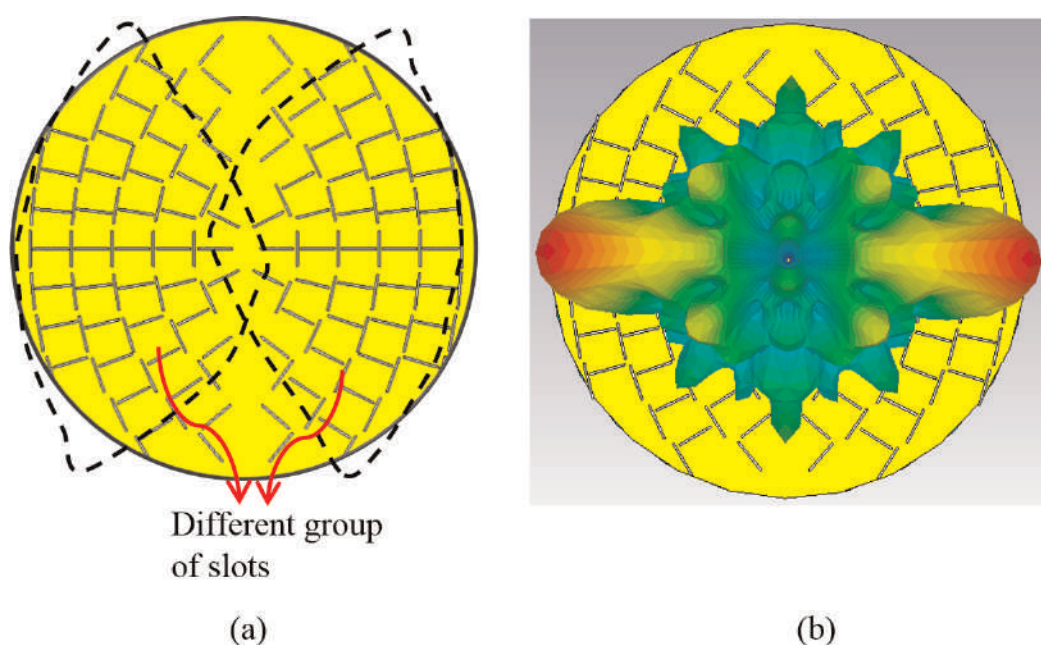


Figure 14.
 (a) Design of dual-beam antenna. (b) Beam result.

radiating elements. Our hypothesis is that the background can be used to draw slots on it, as shown in **Figure 13b**. This will result in a dual-beam antenna as shown in **Figure 13c**. Of course, the gain will decrease by 3 dB compared to the originally single-beam antenna, since the power is divided into two beams.

6.3 Multibeam antennas

Multibeam antennas can be produced by designing slots using different beamsquint values. The slots are grouped and placed based on its beamsquint values. **Figure 14a** shows the slot design of two beams, and **Figure 14b** shows its beams. Things to note are that there will be a slot coupling between adjacent slot groups, which will lessen the sharpness of beams or the gains. Therefore, it is needed to put the slot group not too close together such that we get satisfied gains.

6.4 Multiband antennas

Multiband antennas can be produced by designing slots using different frequencies. **Figure 15** shows the slots that are used for two frequencies. It is noted that we

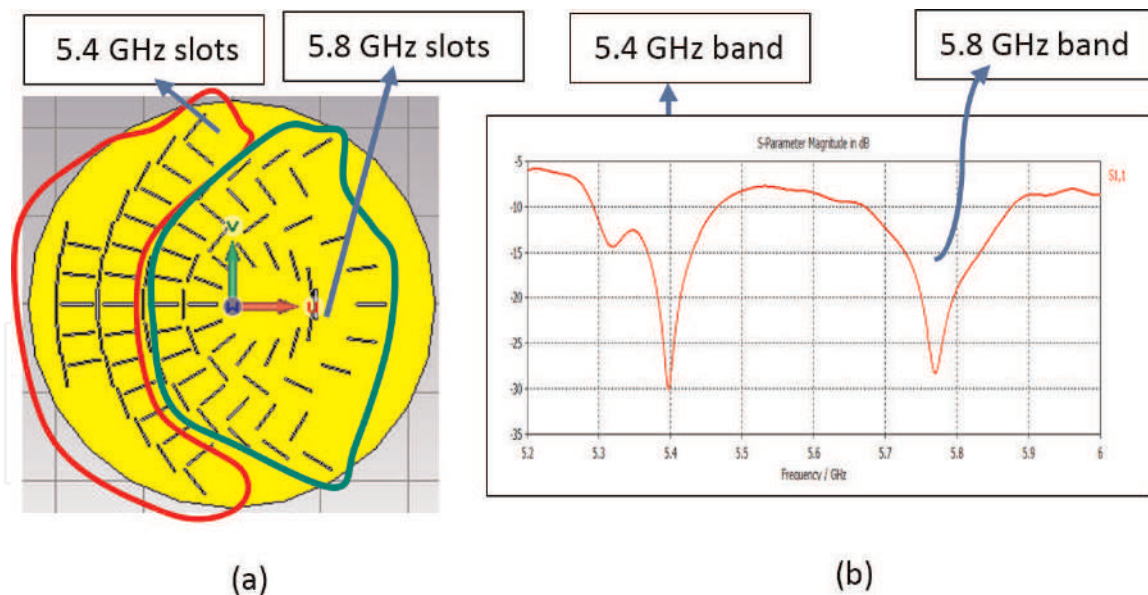


Figure 15.
 (a) Design of dual-band antenna. (b) Band result.

cannot differentiate between the 5.4 and 5.8 GHz slots since they are plotted mixed. This will not effect to the gain since all slots are designed using a same beamsquint value. Research on this topic can be as follows: firstly, a study on how to correctly place different frequency slots, so that the correct placement will not increase antenna reflections. Secondly, a study of how far two different bands or more can be separated since a different band needs a different feeder structure. However in multiband antennas, we use a same feeder structure so that it will effect to the increase of reflection, such that different bands cannot be separated too far.

7. Conclusions

RLSA antennas have been developed since the 1980s until nowadays. They were initially developed for satellite receiver antennas. Due to their advantages, such as high gains and flat shapes, these antennas have been also developed for small device applications at smaller frequencies, such as Wi-Fi, 5th G, 4th G, etc. However developing RLSA antennas for small device applications had been facing the problem of high signal reflections, due to the limited number of slots. Several techniques had been proposed to overcome the problem. Among the techniques, the extreme beamsquint technique is the most effective technique in reducing signal reflections. By resolving the problem of signal reflections, the research areas for RLSA antennas become wide open, especially for multibeam RLSA antennas, multiband RLSA antennas and size minimization by cutting RLSA antennas.

IntechOpen

IntechOpen

Author details

Teddy Purnamirza
Universitas Islam Negeri Sultan Syarif Kasim, Pekanbaru Riau, Indonesia

*Address all correspondence to: tptambusai@uin-suska.ac.id

IntechOpen

© 2019 The Author(s). Licensee IntechOpen. This chapter is distributed under the terms of the Creative Commons Attribution License (<http://creativecommons.org/licenses/by/3.0>), which permits unrestricted use, distribution, and reproduction in any medium, provided the original work is properly cited. 

References

- [1] Kelly KC. Recent annular slot array experiments. In: IRE National Convention Record; Vol. 5; 1957;1. pp. 144-151
- [2] Ando M et al. Linearly polarized radial line slot antenna. IEEE Transactions on Antennas and Propagation. 1988;36:1675-1680
- [3] Ando M et al. Linearly-polarized radial line slot antenna. IEEE Antennas and Propagation Society. 1988;1:836-839. AP-S International Symposium (Digest)
- [4] Davis PW. Experimental investigations into a linearly polarized radial slot antenna for DBS TV in Australia. IEEE Transactions on Antennas and Propagation. 1997;45: 1123-1129
- [5] Ando M et al. Radial line slot antenna for DBS reception. In: Conference Proceedings—European Microwave Conference; 1988. pp. 306-311
- [6] Endo K et al. Waveguide design of a radial line slot antenna. Electronics and Communications in Japan. Part I: Communications. 1990;73:109-115. (English translation of Denshi Tsushin Gakkai Ronbunshi)
- [7] Takada J-i et al. A reflection cancelling slot set in a linearly polarized radial line slot antenna. IEEE Transactions on Antennas and Propagation. 1992;40:433-438
- [8] Ando M et al. Single-layered radial line slot antenna for DBS reception. In: Conference Proceedings—European Microwave Conference; 1990. pp.1541-1546
- [9] Ando M et al. A slot design for uniform aperture field distribution in single-layered radial line slot antennas. IEEE Antennas and Propagation Society. 1990;1:930-933. AP-S International Symposium (Digest)
- [10] Takahashi M et al. High efficiency flat array antennas for DBS reception. In: Conference Proceedings—European Microwave Conference; 1991. pp. 629-634
- [11] Takahashi M et al. A slot design for uniform aperture field distribution in single-layered radial line slot antennas. IEEE Transactions on Antennas and Propagation. 1991;39:954-959
- [12] Takahashi M et al. Characteristics of small-aperture, single-layered, radial-line slot antennas. IEEE Proceedings H: Microwaves, Antennas and Propagation. 1992;139:79-83
- [13] Takahashi M et al. Small aperture single-layered radial line slot antenna for DBS reception. In: IEEE Conference Publication; 1991. pp. 738-741
- [14] Davis PW, Bialkowski ME. Comparing beam squinting and reflection cancelling slot methods for return loss improvement in RLSA antennas. IEEE Antennas and Propagation Society. 1997;3: 1938-1941. AP-S International Symposium (Digest)
- [15] Davis PW, Bialkowski ME. Linearly polarized radial-line slot-array antennas with improved return-loss performance. IEEE Antennas and Propagation Magazine. 1999;41:52-61
- [16] Davis PW, Bialkowski ME. Performance of a linearly polarized RLSA antenna for different beam squint angles. In: Asia-Pacific Microwave Conference Proceedings (APMC); 1997. pp. 653-656
- [17] Davis PW, Bialkowski ME. Beam synthesis in linearly polarized radial line slot array antennas. IEEE Antennas and

- Propagation Society. 2000;1:94-97. AP-S International Symposium (Digest)
- [18] Tong KF et al. Broadband characteristic of an offset aperture-coupled dual circular disk microstrip antenna. *Electronics Letters*. 1994;30: 1728-1729
- [19] Mowlér M, Lindmark B. A matching slot pair for a circularly-polarized slotted waveguide array. *Proceeding in 2006 First European Conference on Antennas and Propagation*; 2006.1
- [20] Haridas N et al. Reconfigurable MEMS antennas. In: *Proceedings of the NASA/ESA Conference on Adaptive Hardware and System*; 2008. pp. 147-154
- [21] Hirokawa J et al. Matching slot pair for a circularly-polarized slotted waveguide array. *IEEE Proceedings H: Microwaves, Antennas and Propagation*. 1990;137:367-371
- [22] Hirokawa J et al. A matching slot 21 pair for a circularly-polarized slotted 22 waveguide array. *Proceeding in International Symposium on Antennas and Propagation Society, Merging Technologies for the 90's*. 1990;1. pp. 926-929
- [23] Akiyama A et al. Numerical optimization of slot parameters for a concentric array radial line slot antenna. *IEEE Proceedings: Microwaves, Antennas and Propagation*. 1998;145: 141-145
- [24] Akiyama A et al. Design of radial line slot antennas for millimeter wave wireless LAN. *IEEE Antennas and Propagation Society*. 1997;4:2516-2519. AP-S International Symposium (Digest)
- [25] Zagriatski S, Bialkowski ME. Circularly polarized radial line slot array antenna for wireless LAN access point. In: *15th International Conference on Microwaves, Radar and Wireless Communications (MIKON—2004)*; 2004. pp. 649-652
- [26] Tharek AR, Ayu IKF. Theoretical investigations of linearly polarized radial line slot array (RLSA) antenna for wireless LAN indoor application at 5.5 GHz. In: *Proceedings of the Mediterranean Electrotechnical Conference—MELECON*; 2002. pp. 364-367
- [27] Bialkowski KS, Zagriatski S. Investigations into a dual band 2.4/5.2 GHz antenna for WLAN applications. In: *15th International Conference on Microwaves, Radar and Wireless Communications (MIKON-2004)*; 2004. pp. 660-663
- [28] Bialkowski KS, Zagriatski S. A dual band 2.4/5.2 GHz antenna including a radial line slot array and a patch. *IEEE Antennas and Propagation Society*. 2004;3:3095-3098. AP-S International Symposium (Digest)
- [29] Imran MI, Tharek AR. Radial line slot antenna development for outdoor point to point application at 5.8 GHz band. In: *2004 RF and Microwave Conference, RFM 2004—Proceedings*; 2004. pp. 103-105
- [30] Imran MI et al. An optimization of beam squinted radial line slot array antenna design at 5.8 GHz. In: *2008 IEEE International RF and Microwave Conference (RFM 2008)*; Sabah; 2008. pp. 139-142
- [31] Imran MI et al. Beam squinted radial line slot array antenna (RLSA) design for point-to-point WLAN application. In: *2007 Asia-Pacific Conference on Applied Electromagnetics Proceedings (APACE-2007)*; 2007
- [32] Islam MRU, Rahman TA. Novel and simple design of multi layer radial line slot array (RLSA) antenna using FR-4 Substrate. In: *2008 Asia-Pacific Symposium on Electromagnetic*

- Compatibility and 19th International Zurich Symposium on Electromagnetic Compatibility (APEMC 2008); 2008. pp. 843-846
- [33] Islam MRU et al. Simple integrated system for wireless backhaul networks. In: Proceedings of the International Conference on Computer and Communication Engineering 2008 (ICCCE08): Global Links for Human Development; 2008. pp. 341-345
- [34] Purnamirza T, Tharek AR, Jamaluddin MH. The extreme beamsquint technique to minimize the reflection coefficient of very small aperture-radial line slot array antenna. *Journal on Electromagnetic Wave and Application*. 2012;**26**: 2267-2276
- [35] Purnamirza T, Kristanto D, Ibrahim IM. A design of compact radial line slot array (RLSA) antennas for Wi-Fi market needs. *Progress in Electromagnetics Research Letter*. 2016; **64**:21-28
- [36] Purnamirza T, Ibrahim IM, Prowadi P, Amillia F. Small radial line slot array (RLSA) antennas for Wi-Fi 5.8 GHz devices. *International Journal on Communications, Antenna and Propagation (IRECAP)*. 2017:397-402
- [37] Purnamirza T, Hasbi S, Ibrahim IM, Mulyono, Amillia F, Rahmi D. A radial line slot array (RLSA) antenna with the specifications of 16 dBi outdoor patch antenna. *TELKOMNIKA (Telecommunication Computing Electronics and Control)*. 2018;**7**:46-52
- [38] Purnamirza T, Budikesuma P, Ibrahim IM, Rahmi D, Susanti R. A small-RLSA antenna utilizing the specification of back fires 17 dBi LAN antennas. *Telkomnika (Telecommunication Computing Electronics and Control)*. 2018;**16**:16
- [39] Purnamirza T. Very small aperture radial line slot array beam steering antennas [thesis]. Johor: Universiti Teknologi Malaysia; 2013
- [40] Bialkowski ME, Davis PW. Predicting the radiation pattern of a radial line slot array antenna. In: *Asia-Pacific Microwave Conference Proceedings (APMC)*; 1999. pp. 162-165
- [41] Bialkowski ME, Davis PW. Design and development of a radial line slot array antenna of arbitrary polarization. In: *Asia-Pacific Microwave Conference Proceedings (APMC)*; 2000. p. 2
- [42] Bialkowski ME, Davis PW. Linearly polarized radial-line slot-array antenna with a broadened beam. *Microwave and Optical Technology Letters*. 2000;**27**: 98-101
- [43] Davis PW. A linearly polarised radial line slot array antenna for direct broadcast satellite services [thesis]. Queensland: University of Queensland; 2000

New High-Speed Directional Relay Based on Wireless Sensor Network for Smart Grid Protection

Ali Hadi Abdulwahid

Abstract

The production of energy from water represents large amounts of clean and renewable energy. However, only 30% of this energy has been developed so far. Hydropower, particularly hydropower plants, is not only environmentally friendly but also economical, and operates more efficiently than any other renewable energy system. Hydropower plants are largely automated and have relatively low operating costs. The main components of the power system must be continuously monitored and protected to maintain the quality and reliability of the power source. This task is provided by the data collection, monitoring and protection system. Turbines must be protected not only by short circuits but also by abnormal conditions. The proposed protection has been designed to avoid damaging the original power (motor or turbine), this usually happens when the generator fails, and the machine operates as a synchronous motor connected to the power system. In this case, the generator becomes an active load, causing a rise in temperature and severe damage to the main turbine, and hence it becomes a need to quickly detect these conditions. This study proposes a new controller for Neuro-Fuzzy to prevent reverse power flow and to keep the quality and reliability of supply. Fuzzy system network has attracted various scientific and engineering researchers. The new feature of this work is to adjust the membership function as a reverse mechanism derived of the Fuzzy Logic Controller. The smart meter network is the basis of the smart grid. In this study, smart grid meters were implemented using ZigBee technology based on wireless sensor networks. The ZigBee network of wireless sensors due to its low battery, low power consumption, become more useful than other wireless communication systems to provide a high-performance measurement. This study shows the ZigBee network using the OPNET simulation. Depending on the performance, parameters were analysed to understand the operating characteristics of the star, tree, and mesh.

Keywords: smart grids, ZigBee IEEE 802.15.4, neuro-fuzzy network, directional relay

1. Summary

Literature reviews play a vital role in improving renewable energy because science is still a cumulative effort in the first place. As with any discipline, the synthesis of rigorous knowledge becomes indispensable to keeping up with the is growing searched pace of smart grid domain, which is developing exponentially by academics and engineers and scientific searched in the content of many papers,

evaluated and synthesized [1–3]. The proposed study could provide a theoretical basis for confirming the need for investigative questions, proving that research methods have increased accumulated knowledge. Besides, high-quality reviews have made researchers look for a lot of literature when conducting empirical research.

In addition, high-quality reviews have made researchers look for a lot of literature when conducting empirical research. To conclude, our main objective in this chapter is to develop solutions to improve the spread of distributed energy and with high-speed synchronisation communication, that is central to the continuous development of the smart grid field. We hope that ours. This chapter will serve as a valuable source for those conducting, evaluating or engineers in this important and growing domain. The future distribution network may include a large-scale distributed power generation penetration into the smart grid. This scenario is aimed at the transition from a passive distribution network to an active distribution. The integration of DG units has a significant impact on the operation of power flow, voltage distribution, and protection systems in the distribution network [1]. (1) Explore issues that drive the demands of future rapid Intelligent protection systems, (2) design and develop a protection strategy that can be applied to any grid equipped DG. The concept of innovative protection must ensure the selectivity of protection in case of failure, (3) apply the new concept of intelligent protection algorithm.

As a result, the performance of the existing distribution network's traditional inverse-time protection system was evaluated. In this way, we have identified the problems faced by the current applicable protection strategies; the results of the simulation prove that the traditional protection system is insufficient to provide a satisfactory level of protection selectivity. This chapter introduces the transformation of the traditional protection strategy to the future intelligent distribution network protection system. This shows how unprecedented advances in sensor technology and the emergence of new communication protocols have stimulated innovation in protection systems. The latest technological advances have enabled existing protection systems based on local information to be transferred to innovative security systems, In Addition; the details of the new communication mechanism for the application of high-speed protection systems were discussed. Clever's protection strategies are fast, flexible and offer a high level of selectivity protection.

This chapter designs and develops a new concept of intelligent protection strategy. This approach applies to any network administered by DG. The proposed intelligent protection system aims to reduce the time to eliminate failures, to ensure the selectivity of protection and to enhance the availability of the units of the DG throughout faults. The new scheme of realising a protection scheme using advanced sensor, neural fuzzy scheme and ZigBee network is expounded. The intelligent algorithm ensures the selectivity of the protection by minimising the time of failure and eliminating the problem of the large time disconnection in the system [1].

2. Introduction

The smart grid (SG) is the next generation of power grids. Its purpose is to overcome the problems that exist in the conventional power grid. Smart grid technology has been used, such as sensors and communication networks, and advanced software and sensors to provide control and enhance the protection and optimisation of all network components, including production, transmission, and distribution.

Although neural networks implement to solve tuning problems, the fuzzy logic controller is intended to use structured knowledge in the form of rules [4, 5].

The combination of Fuzzy Logic and neural networks provides the ability to solve optimisation problems. This new method consolidates the established advantages of both approaches and avoids the limitations of both approaches. Control algorithms are used to prevent unexpected fluctuations in voltage and frequency. Smart grids use energy storage systems and communication networks to ensure total coordination between power generation and energy use. Reduce the energy loss of the network to minimise demand and energy costs [6–8]. A reliable, real-time information flow among parts of the network is critical to the success of the smart grid self-regulation process. There are many wireless standards for technical applications [9]. One of the most popular technologies is ZigBee wireless sensor network (WSN), which is distributed on the smart grid structure, which has a lot of equipment to communicate with each other through the wireless network. These electronic devices are called Sensors/Detectors/Transducers [9]. Sensors are devices that can recognise several of the physical units, such as current, voltage, impedance, etc. Also, the ZigBee system is featured by low energy consumption. It is also more economical than other communications because it provides flexibility and scalability [10–12].

The construction of this chapter is as follows: Section 2 confers a study of the SG communication system. The proposed protection system and results are analysed in Section 3; Section 4 the wireless sensor network using OPNET and simulation results; In Section 5, the conclusions are discussed.

3. The smart grid communication network architecture

The old communication system is characterised by limited efficiency and limited information exchange; the intelligent metering network is the backbone of a smart distribution network. It is essential to select the appropriate communications to facilitate the real-time flow of bi-directional information. It is mainly used by the main transmission point and a limited number of sensors on the transmission line for control and fault detection. Compared with the traditional network, an intelligent system contains a much larger number of sensors. Sensors are used to exchange information between terminals devices and data centres to handle such a large data stream, the SG must-have reliable communications and security infrastructure. The communication infrastructure must be self-managed and configured to change automatically [13].

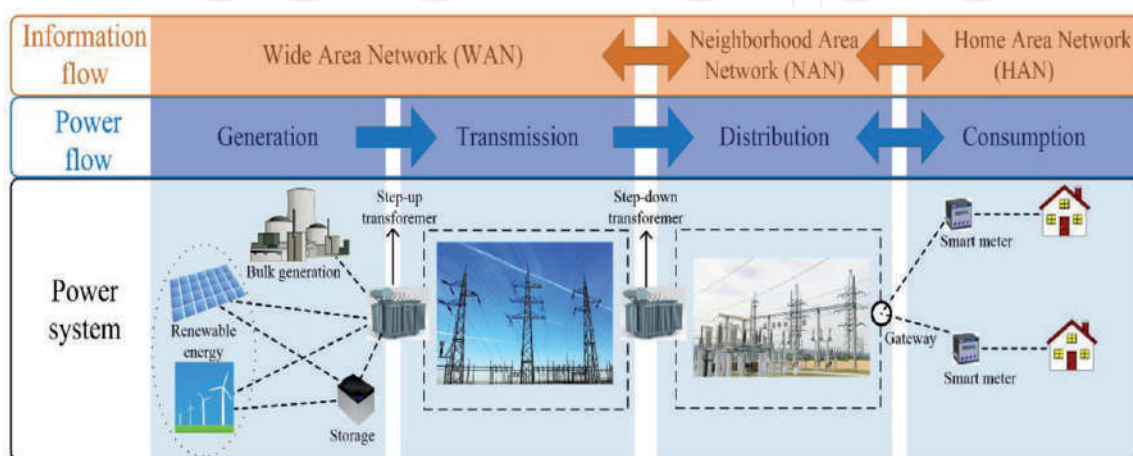


Figure 1.
 Communication network architecture [14].

Figure 1 shows the smart grid communication architecture, including the neighbourhood network (NANs), home LAN (HANs), wide area network (WANs), substation and data centre. These networks as follows will be displayed briefly [14–16].

3.1 Wireless area network (WAN)

It serves as backbones that help the power grid that provides communication between utility systems and substation systems. The can help prevent power outages by providing real-time information from the electricity grid. It supports real-time control and protection. This system is useful when dealing with unforeseen contingencies, and it is essential to avoid interruptions and failures [17–20]. This application helps in performing a generator process and provides support for large power systems. The main disadvantage of this kind of WLAN is the possibility of devices interfering at the same frequency is high. The network operates between 2.4 and 3.5 GHz. Among its advantages are low-cost equipment, the use of which has spread across a wide range of applications.

3.2 Network home area (HAN)

Some technologies introduced in the Home Network System are ZigBee, WLAN with PLC. The construction of a Building Area Network (BAN) is considered to be more complicated than the Home Area Networks (HAN). The HAN can be classified as a part of the customer network structure; HAN is often used by consumers in the housing and business sectors, using power tools to communicate [21]. It is a combination of connected devices, management software and dedicated LAN. HAN supports communication between smart meters and appliances used in homes, industries or buildings. It supports several other services, including Demand Response, pre-payment, real-time pricing and load control. The essential of the HAN communication system is to include low-cost, low power consumption with secure communication [6, 10, 22].

3.3 Neighbourhood area network (NAN)

NAN is best described as a bridge between WAN and HAN and used in a NAN to collect data of points adjacent with the help of intelligent electronic devices (IEDs), which are widely deployed in the whole area. It is a two-way communication technology developed that give information about the control system for smart grids. Compared to WAN, the data rate is not high, and the transmission power is low for short-range transmission. WLAN, PLC and ZigBee are some of the techniques on which the NAN network can be implemented [23].

4. Proposed protection system simulation and modelling

In some cases, the generator starts to behave like a motor when the prime mover does not provide enough torque to keep the generator rotor rotating at the same frequency as the line of the parallel power source, and instead of giving power; it draws power from the parallel power source. Also, if the synchronisation ranges process rotates slowly, also both the loss of the alternator excitation. The governor is the fault of the original sender. Similarly, the generator will also extract the current from the source line [24]. When the rotating part of the generator fails, the generator stops generating electricity and starts drawing electricity from the parallel power source [25]. This situation may damage the drive

unit and is not desirable. It should be detected as soon as a possible problem, and quickly disconnect the equipment from the parallel power supply, thereby protecting the generator from damage. In exceptional turbine cases, the power supply direction is changed from line to generator. It usually uses a directional protection relay to monitor the current flow and take appropriate action to prevent all outage case. The directional protection relay is working when the reverse power exceeds a certain percentage of the rated power output; it will trip the circuit breaker of the generator, disconnect the generator from the line under not normal circumstances, the relay setting is about 5% of the power generator [26]. The directional protection relay is located on the generator latch cabinet and is an integral part of the circuit breaker. The structure of the relay is designed to limit the reverse current flow depending on the amount of current and voltage between the two phase angles. If the line power is inverted, the current through the relay current coil will be inverted concerning the polarisation voltage and provide directional torque [27]. This technique compares the relative phase angle between the (current and voltage), as shown in **Figure 2**.

Typically, the phase angle is used to define the fault compares to the reference value. The voltage is usually applied as a reference amount. By comparing the operating voltage and current phase angle, can be inferred the fault occurs. Therefore, the fault current can be described with the phase relationship with the voltage line -90 for the forward fault, 90 for reverse fault. The relay wills response to the phase angle difference between the two quantities to come out trip signal [28]. In cases where optimal protection is required, Rogowski coil current sensors are used as CT and PT to avoid faults in conventional AC Transformers and must set a certain amount of delay during operation, to prevent power fluctuations, the transient effect during synchronisation. If the angle between the current vector and the voltage is Δ , the power flow is $-900 < \Delta < 900$ [29]. Under normal conditions, the voltage overlaps with the current range is more significant than their non-overlapping interval. However, in the case of reversing energy flow, this overlap is reduced to a lower level. **Figure 3** shows this assembly and implementation. The low signal of the current and voltage of RC sensors changes to form a square wave having a value of “ ± 1 ” and then multiplying these level signals to produce a positive number in the overlap interval, in the negative numbers are generated in the non-overlap interval [30].

The integration limit of the scheme is set to zero, therefore the integration of the load is perpetually < 0 under normal conditions. However, in the opposite trend, the production condition system as a whole tends to decline until the threshold constant

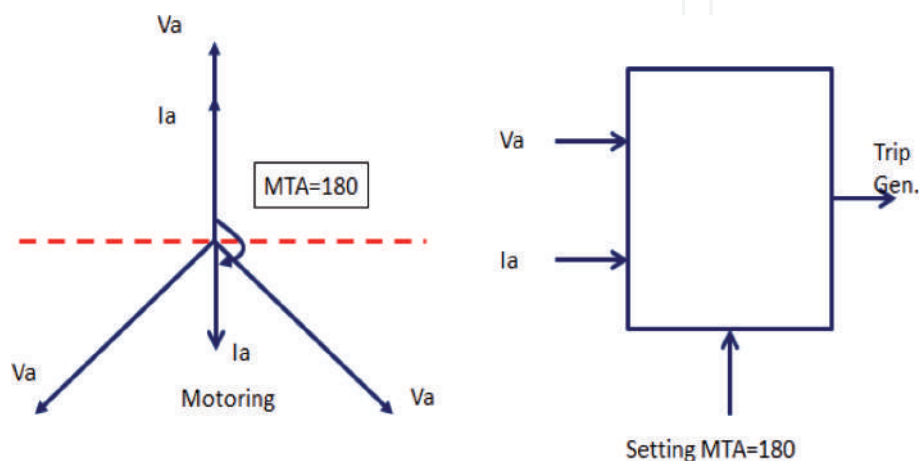


Figure 2.
 According to the reverse power relay current with a voltage vector diagram.

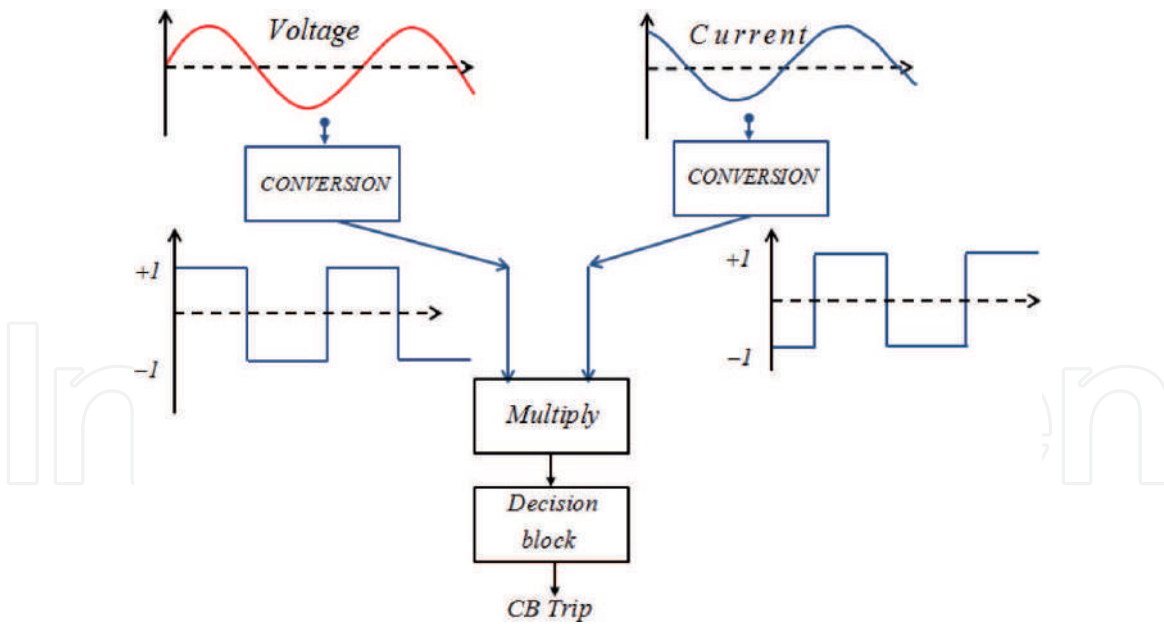


Figure 3.
Diagram of implementing a directional component.

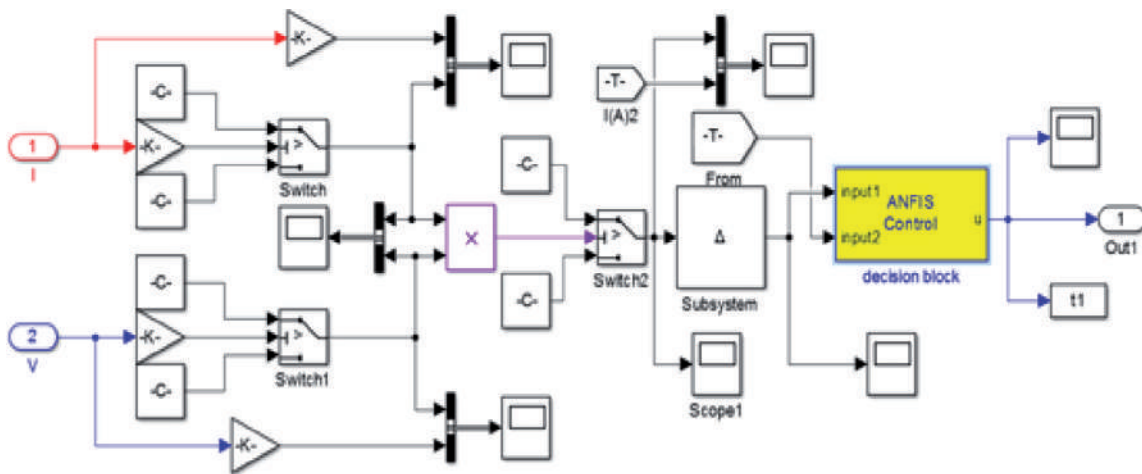


Figure 4.
Modelling of a directional relay component.

is reached. In this situation, the constant is set to 0.01 and the select value based on the amount of reverse power [23]. The output of the reverse power relay (RPR) is transferred to a decision where the production is one for normal operation, zero for abnormal conditions, as displayed in **Figure 4**.

Figure 5(a) presents the 3ϕ current directions, $\cos \phi$, and power factor, and **Figure 5(b)** the same ideas of the P and Q expansion.

4.1 The adaptive neuro-fuzzy approach

The selection of the membership function dramatically affects the quality of the fuzzy controller. Therefore, the method requires a more fuzzy logic controller. In this paper, a new method of neural networks is used to solve the adjustment problem of a fuzzy logic controller. We consider a dynamic system of multiple entrances, a single exit. The system is exported to the desired state of the control action can be described by the concept of the well-known “if-then” rule, where the input variables are first converted to their respective linguistic

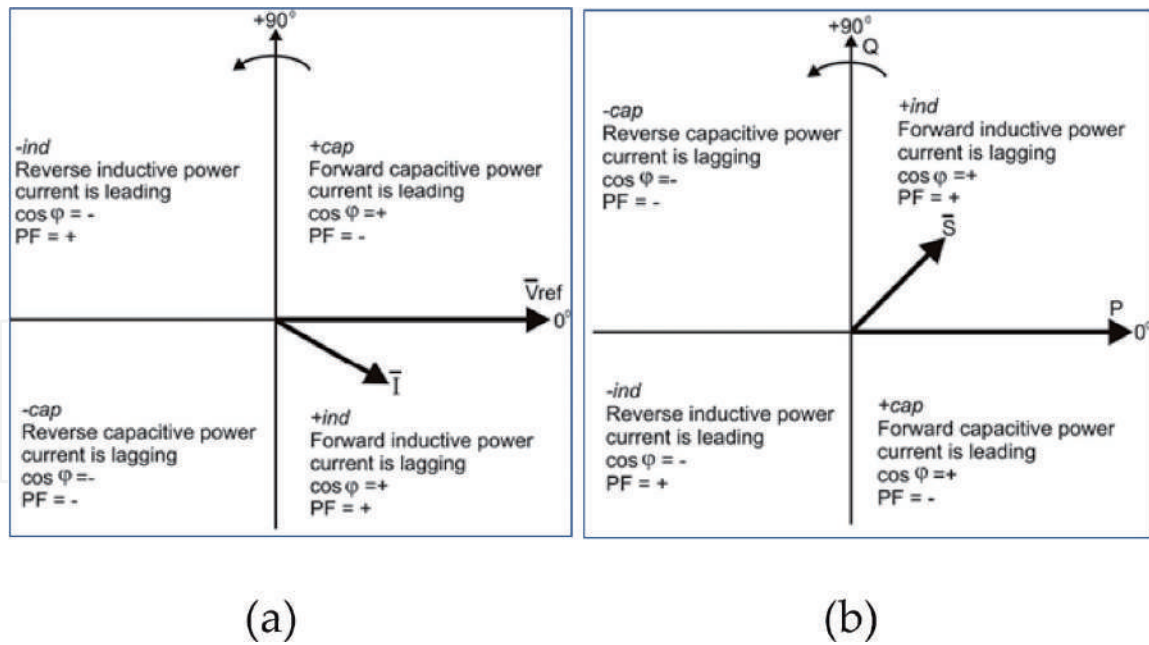


Figure 5.
 (a) Quadrants of current/voltage. (b) Quadrants of a power.

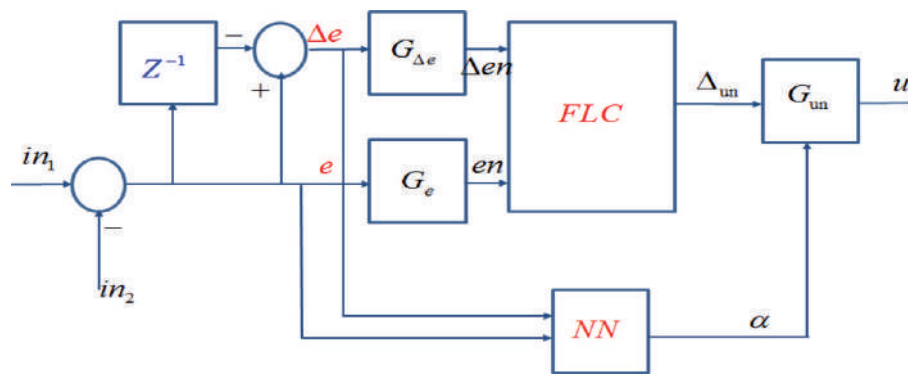


Figure 6.
 Control method using adaptive neuro-fuzzy.

variables, also known as fuzzification. The value of these rules certainly output. Then use defuzzification to convert the output to a precise value. For simplicity, we used a modified centre of area method, and the Triangle fuzzy set will be used for input and output.

The linguistic form of the control rules is the basis of the designed fuzzy unit. It depends on the accuracy of the choice of parameters, which is the translation of the linguistic rules of the fuzzy set theory. The neural network (NN) is used to improve the selection of these parameters. In this scenario, the neural network is combined with the fuzzy logic unit. As shown in **Figure 6**, it uses the first fuzzy logic rule and then uses the neural network to generate the automatic adjustment output. References input [in (1)] related to the existing input [in (2)], product $e(t)$, and incremental changes $\Delta e(t)$ [31, 32]:

$$\Delta e(t) = e(t) - e(t - 1) \tag{1}$$

The proposed unit has two input factor gain measures of control, G_e and $G_{\Delta e}$, and one scaling gain $G_{\Delta u}$. The output-input scale factors are expressed as follows:

$$\Delta e_N(t) = \Delta e(t).G_{\Delta e}, \tag{2}$$

$$e_N(t) = e(t).G_e \tag{3}$$

In the same e_N and Δe_N scaling factor system to identify the fuzzy logic controller input signal product [33, 34]. Fuzzy logic controller output signal is Δu_N , it is the scale factor input. The neural network has two inputs, $e(t)$ and $\Delta e(t)$, and the neural network signal output α , which is used to fine-tune the product control of the operator. The output signal of the scale factor can be expressed by the formula:

$$\Delta u(t) = \Delta u_N(t)\alpha.G_{\Delta u} \tag{4}$$

The output signal can be written as follows:

$$u(t) = \Delta u(t) + u(t - 1) \tag{5}$$

The results are displayed in **Figure 7**, which illustrates the specified fuzzy rules. We have selected fuzzy set and membership functions, **Table 1** summarizes the development of the rules used in this study [1].

Forming a neural network composed of three layers (two input layers, three hidden layers and one output layer). Neural network input (NN) is including the same number of output of fuzzy logic. The activated function has a value from -1 to $+1$ for the output signal, as shown in **Figure 8** [35–37].

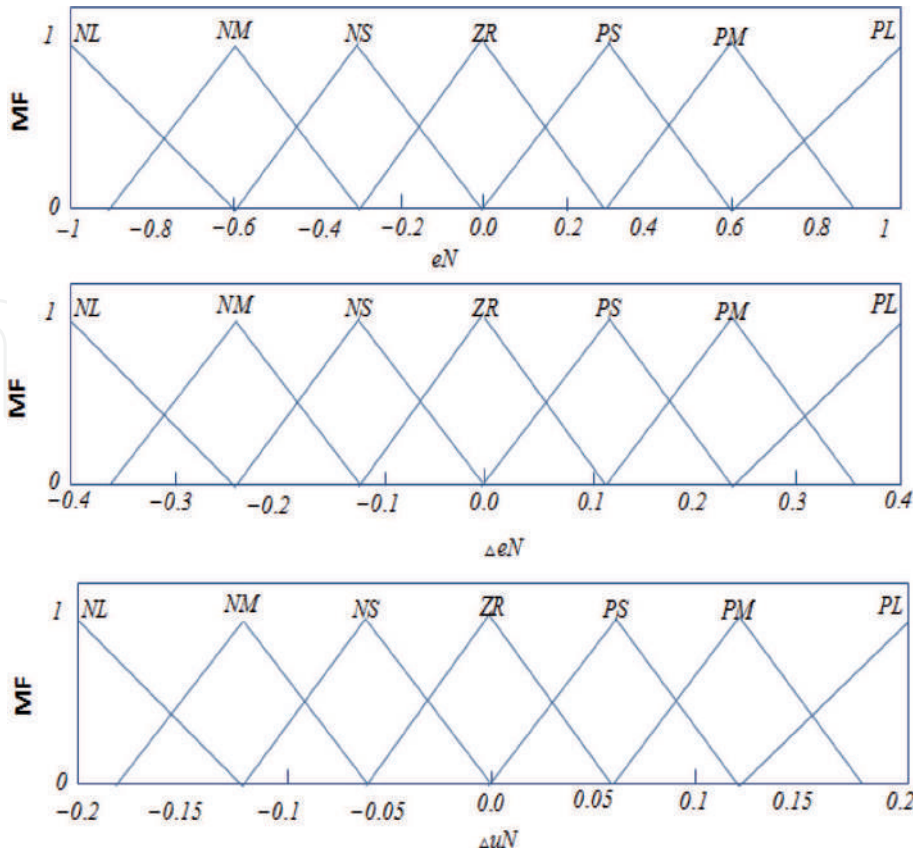


Figure 7.
Fuzzy logic membership functions.

$$e_N$$

| | NL | NM | NS | ZR | PS | PM | PL |
|----|----|----|----|----|----|----|----|
| NL | PL | PL | PM | PM | PS | PS | ZR |
| NM | PL | PM | PM | PS | PS | ZR | NS |
| NS | PM | PM | PS | PS | ZR | NS | NS |
| ZR | PM | PS | PS | ZR | NS | NS | NM |
| PS | PS | PS | ZR | NS | NS | NM | NM |
| PM | PS | ZR | NS | NS | NM | NM | NL |
| PL | ZR | NS | NS | NM | NM | NL | NL |

Table 1.
 Rules of FL.

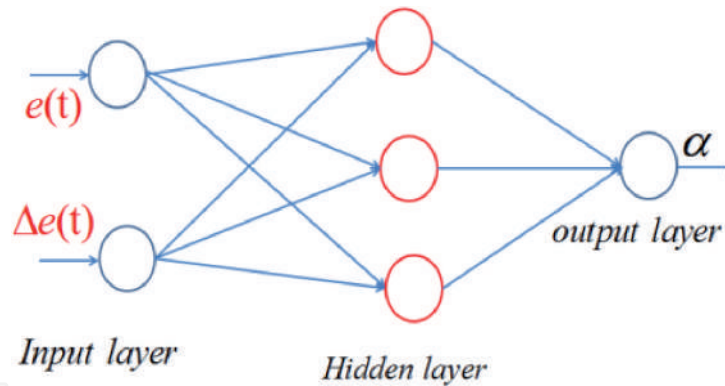


Figure 8.
 The description of the neural network compositions.

$$f(x) = \frac{1 - e^{-x}}{1 + e^{-x}} \quad (6)$$

The activation function neuron in the output layer is:

$$h(x) = \frac{1}{1 + e^{-x}} \quad (7)$$

Control Unit based on the measured output signal $u(t)$ from neuro-fuzzy circuit to adjust the trip circuit:

$$\theta_{new} = \theta_{initial} - k.u \quad (8)$$

where the θ initial is the initial switching output and k is a constant.

4.2 Simulation results

As shown in **Figure 9**, the simulation design uses 200 MVA /11 kV, with a synchronous generator connected to a transmission line 25 kV through an 11/25 transformer, 60 Hz, Load 10 MW, and 3 Mvar. Relays are tested in a variety of situations. The conditions and results of the discussion are as follows.

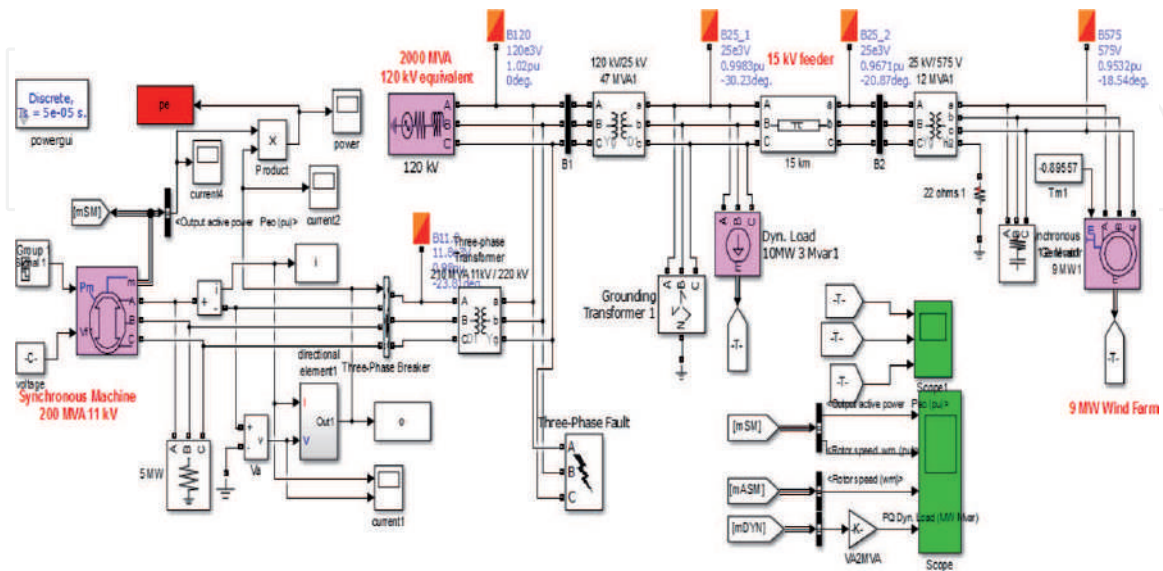
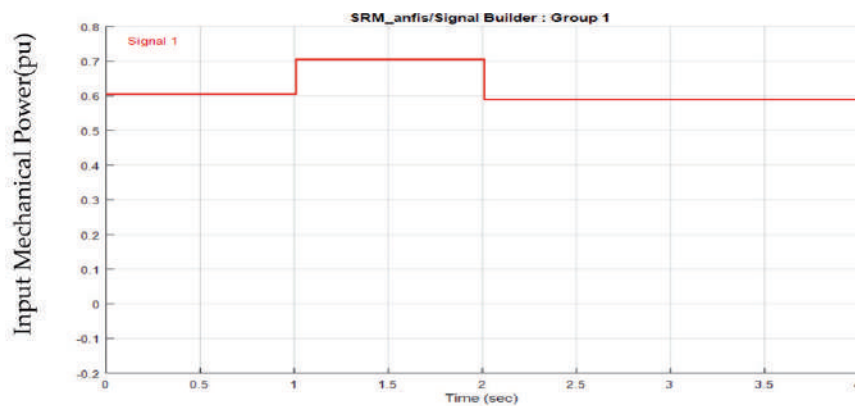
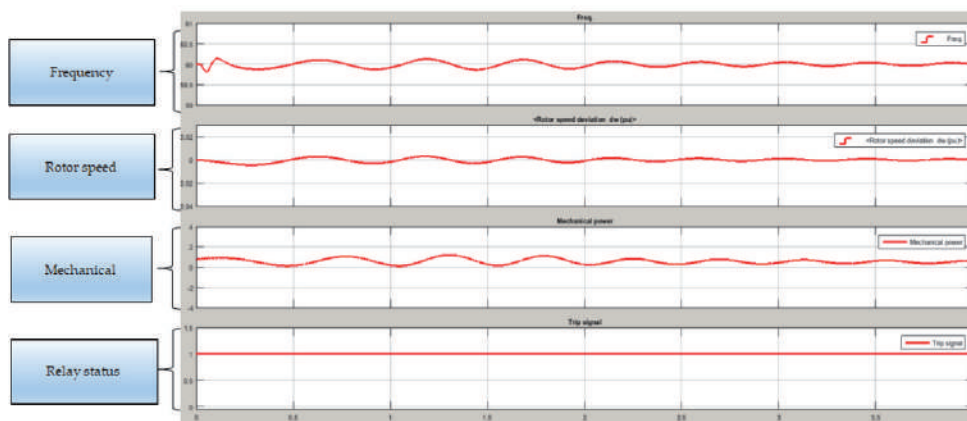


Figure 9.
Model of a reverse power relay in an electrical power system.



(a)



(b)

Figure 10.
(a) Performance of input-output power; and (b) relay status.

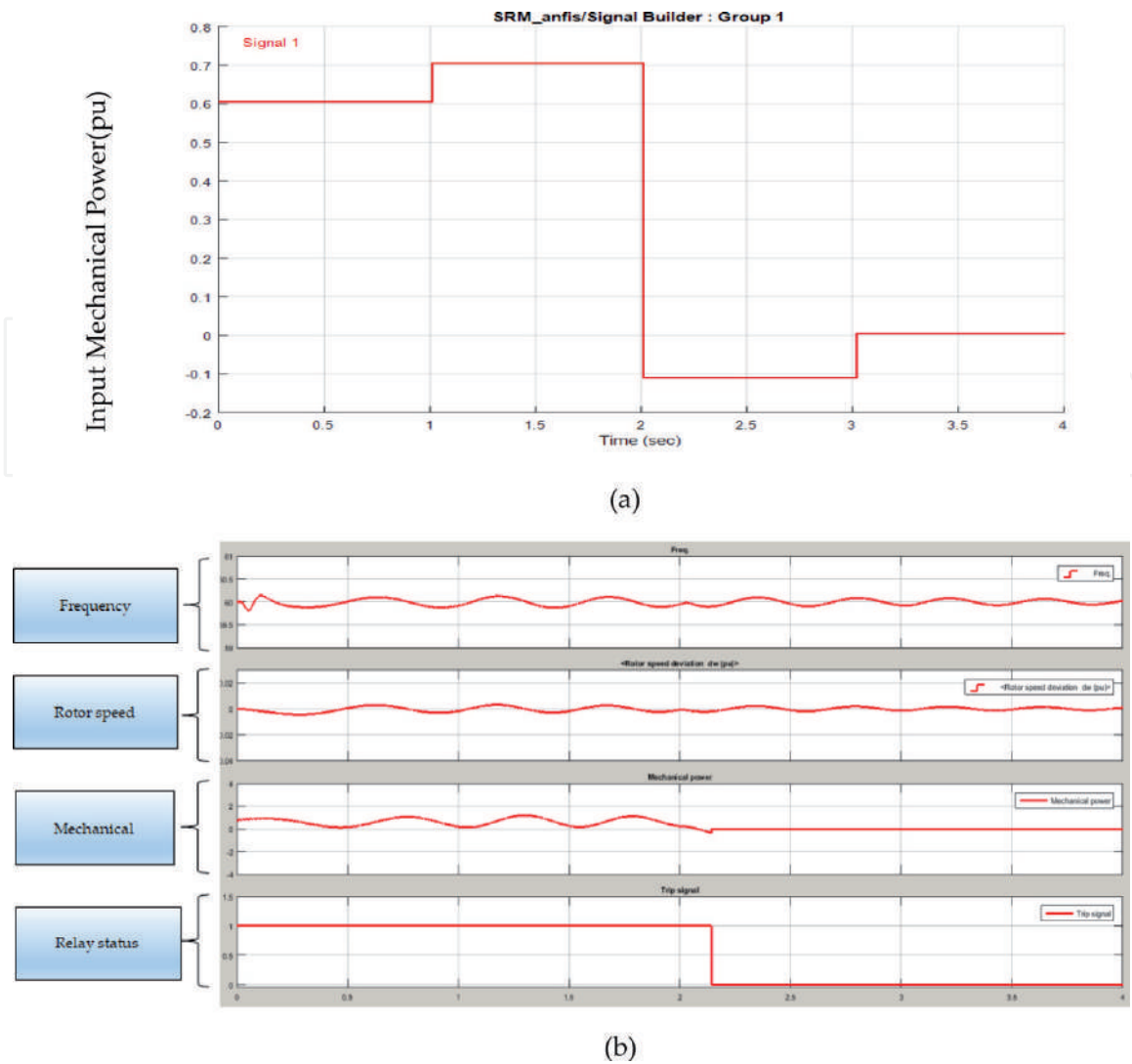


Figure 11.
 (a) Performance of the input-output power; and (b) relay status.

The structure of propose protection is shown in **Figure 4**. The nodes of in_1 and in_2 represent the input variables and pass their values to the blocks that contain the respective membership functions in Neuro-Fuzzy controller. The relays are tested under a variety of conditions. We have provided the details of the system in **Table A1** [1].

4.2.1 Simulation results under the normal condition

In this case, the mechanical power input of the generator within 1–2 seconds differs from 0.6 to 0.7 pu, at the under normal circumstances the observed state is shown in **Figure 10**, and the relay does not trip.

4.2.2 Simulation results under the faulty condition

In this case, the mechanical power input in 2–3 seconds from 0.7 to –0.1 pu. Relay responds to this change after 0.15 second for safe, and the relay is triggered, where the fault occurred at 2 seconds as shown in **Figure 11**. Input Mechanical Power (pu).

The reverse current adjustment knob and the delay time are shown in **Table A2** of the Appendix, and then the trip is confirmed with the minimum reverse current in the range of 2–20%. The trip time delay setting range is 0–20 seconds.

5. Wireless sensor network using OPNET simulator

5.1 Zigbee network method

The OPNET modeller is one of the most important simulation tools for communication network inspection. ZigBee networks are known for their low power consumption, low cost, low data rate, and high battery life.

The current work as shown in **Figure 12**, consists of the workstation featuring a coordinated connection to six routers, with eight nodes installed at a range (200 meters) from each other. To participate in the calculation of system variables, the OPNET collected a large number of variables. The indicators relate to two types of statistical data for the agreement: local and global statistics. However, in terms of network performance, this study is more occupied in collecting quantitative information for the system. As a result, current research is based on data obtained from global statistics [1].

The values of the design parameters are shown in **Figure 13**, and the values of the parameters on the router are shown in **Figure 14**. Transmission power is estimated to be 0.1 w.

The ZigBee coordinator parameter is illustrated in **Figure 15**.

5.2 Simulation results

The simulation results are simulated under different topologies of the wireless sensor network, and the effects of different topologies on network efficiency are discussed.

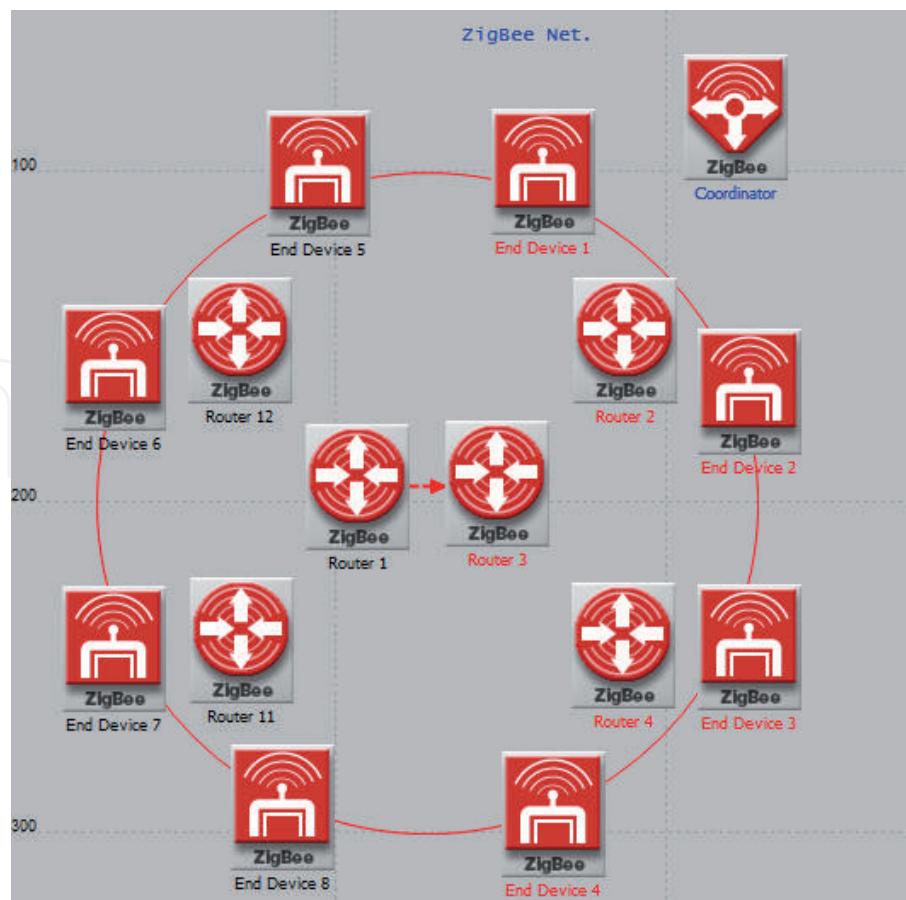


Figure 12.
Basic scenario consisting of one coordinator, (6) routers and (8) end devices.

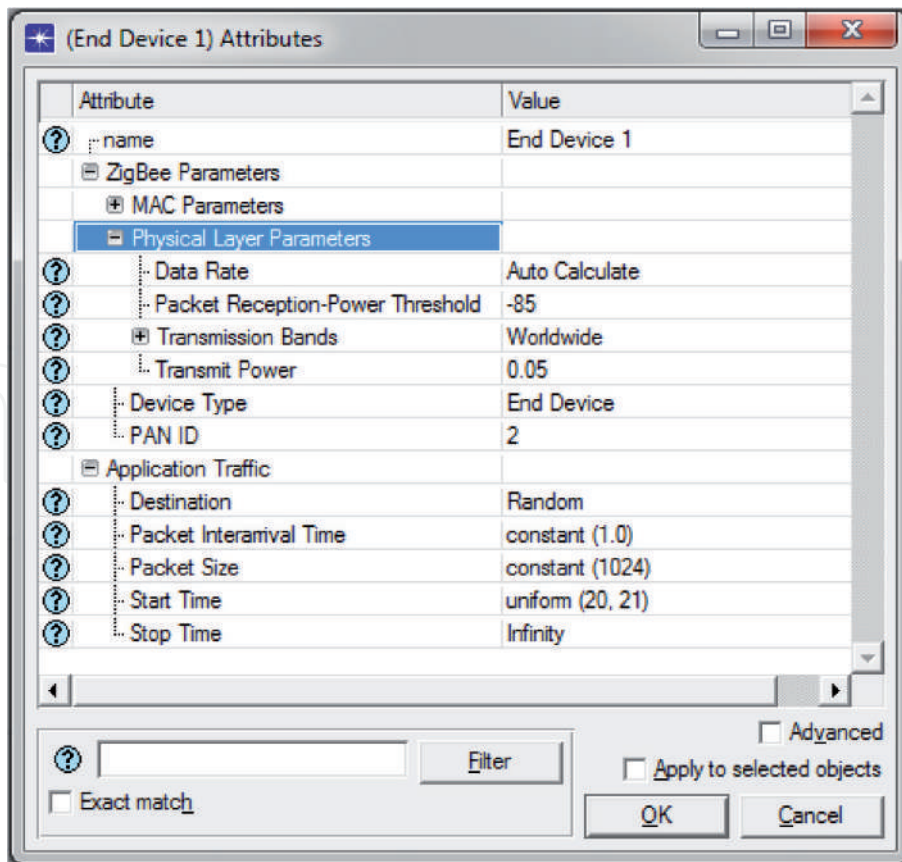


Figure 13.
 End-device parameters.

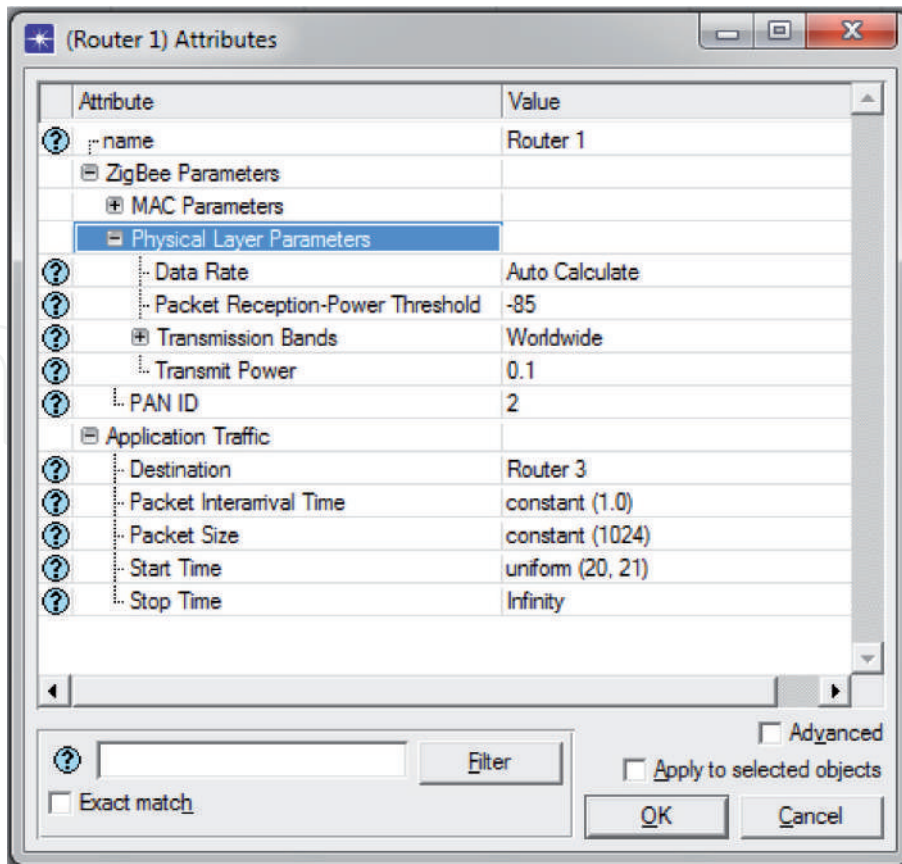


Figure 14.
 Router parameters.

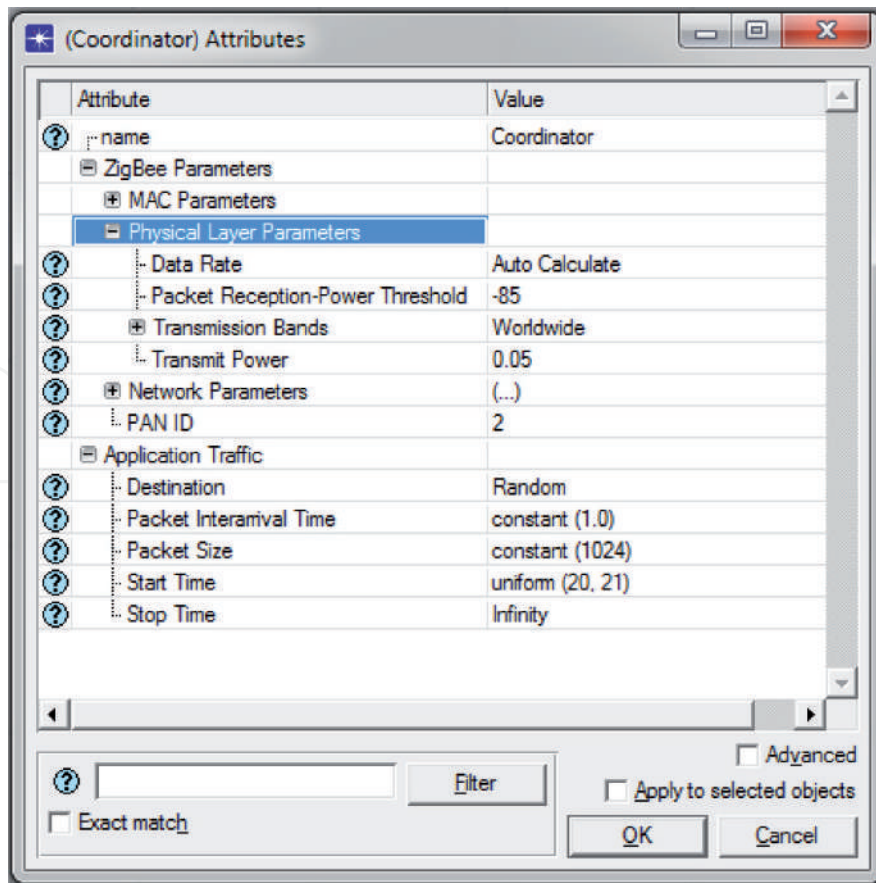


Figure 15. ZigBee coordinator parameter.

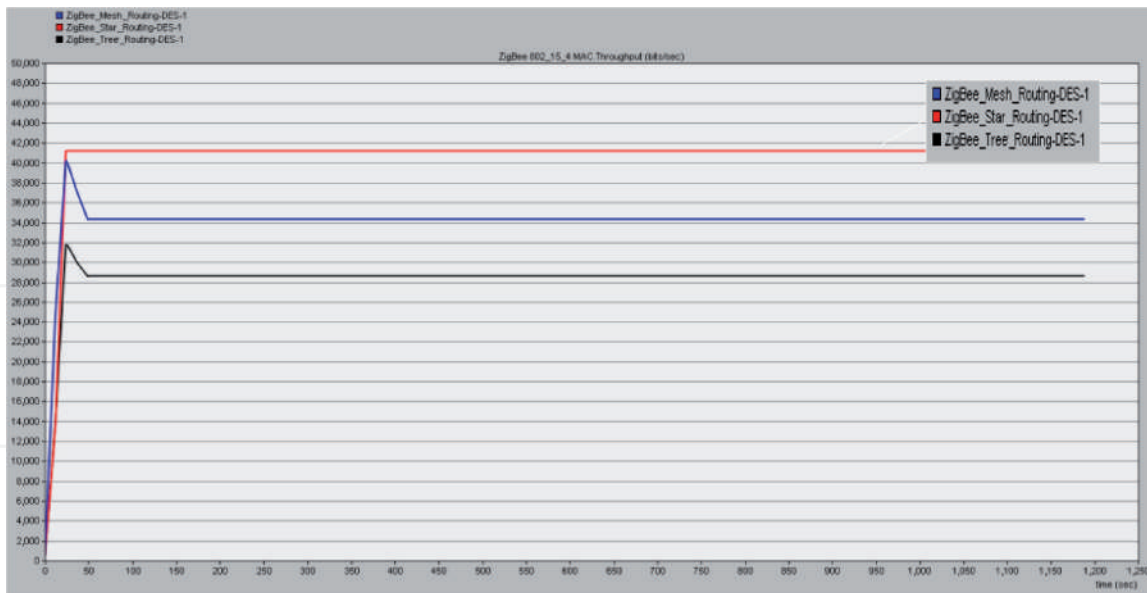


Figure 16. Throughput case.

5.2.1 Throughput

Defined as the average number of bits or packets that are successfully transferred from source to destination. The steady-state results for the star, mesh and tree topology are 0.041, 0.034, and 0.028 Mbit/s, In the star topology, can achieve maximum throughput, this finding is that the star topology interacts with the personal area network (PAN) coordinator, (Figure 16).

5.2.2 Data traffic sent

As shown in **Figure 17**, and finding indicates that the maximum data traffic is in a star topology because this topology type allows communication with the coordinator. The data traffic sent was 0.1465, 0.0385, and 0.0325 Mbit/s, for a star, mesh and tree topology [1].

5.2.3 Data traffic received

Data traffic is defined as the number of data bits received per unit of time. **Figure 18** shows that the received data traffic for (star, mesh, and tree) topology is 0.650, 0.650, and 0.3805 Mbit/s.

This discovery means that the traffic received in the star topology is the largest because all devices communicate via the PAN coordinator and are responsible for generating traffic and routing [1].

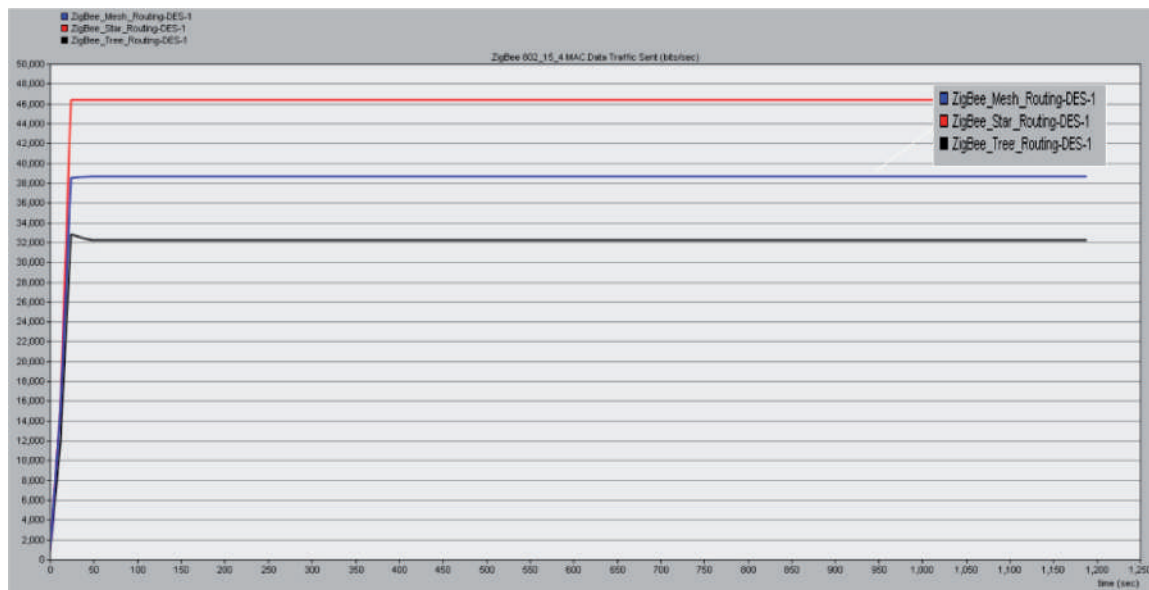


Figure 17.
The total number of data bits transmitted.

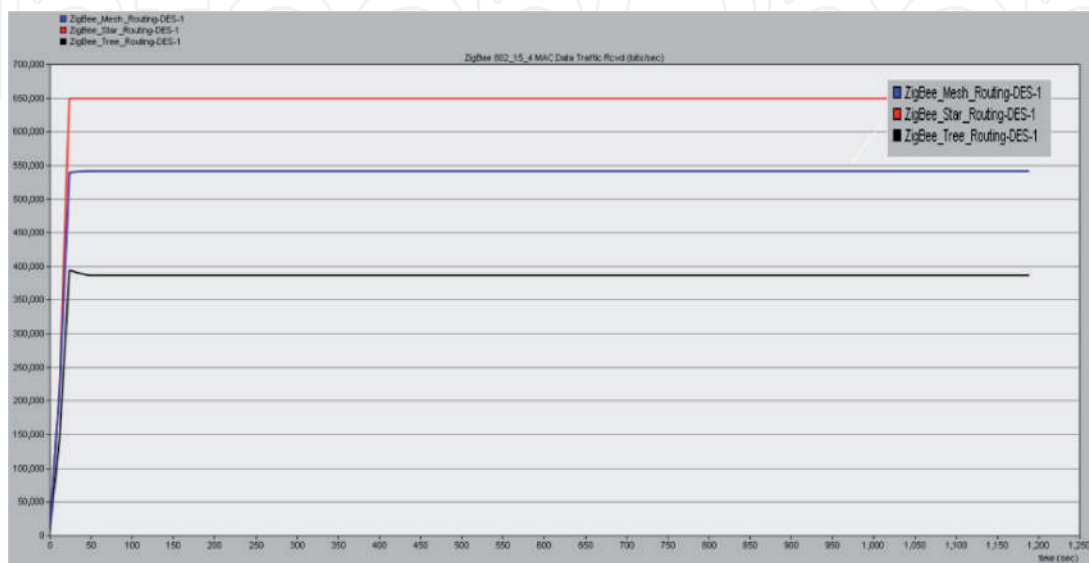


Figure 18.
Data traffic received.

5.2.4 End-to-end delay

It is the time it takes for a home target application to get the package generated by the source application. The results show the mesh/tree, and star topology delays are 9.6 and 7.9 ms. And the delay time of the mesh/tree topology is longer than that of the star topology, as shown in **Figure 19**. In a star topology, only one parent object is represented by a ZigBee coordinator. Therefore, the final mobility of the device may cause some delay.

5.2.5 Medium access control (MAC) load

As shown in **Figure 20**, MACload is used for forwarding the load for each PAN in the transmission of packets in the IEEE 802.15.4 MAC, that is, the physical layer, in the upper layers. The performance of the MACload presents similar results to the throughput performance. In other words, this result confirms the conclusion that

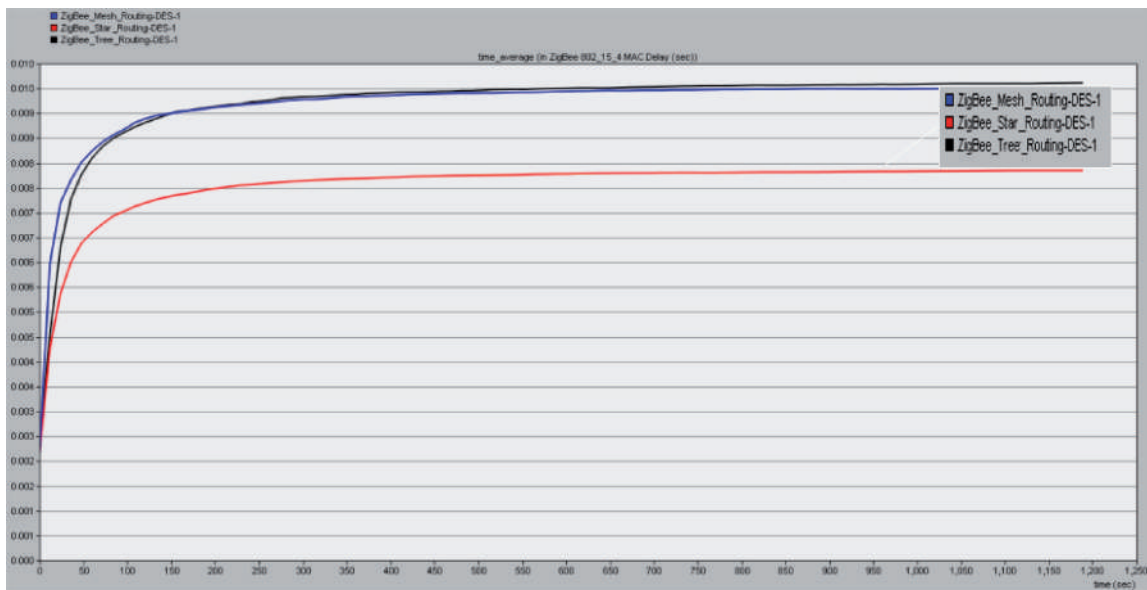


Figure 19.
Data arrival rate against delay.



Figure 20.
Simulation scenario against a MAC load.

| Definition | Value |
|------------------------|-------------|
| Test zone (radius) | ~100 meters |
| Number of end devices | 8 |
| Number of routers | 6 |
| Number of coordinators | 1 |
| Mobility model | Random |
| Simulation duration | 1200 s |

Table 2.
Summary of the simulation parameters.

the faster the load transfer to the upper layers from the physical level is, the more efficient the network. As shown in **Table 2** the local routing information covers only a small area (the diameter of the test distance is about 250 meters) [1].

6. Conclusions

The difference between the ZigBee and the WiMAX mobile networks is the distinction in their technology standard. The WiMAX mobile networks used in the simulation employ the IEEE 802.16 standard technology, whereas ZigBee follows the 802.15.4 standard. Mobile WiMAX seems to have better functionality than ZigBee, but taking into account the scalability of the latter, the former can install additional ZigBee devices because of its low-cost features and the possibility of reducing the battery size and operation hours. However, ZigBee may be more effective in certain areas because of its low energy consumption rate. The advantages of proposed protection are as follows:

(1) To prevent the flow in the opposite direction, and damage to the generator or the main engine. (2) To avoid the occurrence of explosion or fire, this is mostly caused by unburned fuel in the generator.

The existing power system is undergoing significant changes. Smart grid technology is the method used in the future power system framework, the integration of energy and communications infrastructure is inevitable. Intelligent network technology is characterised by the realisation of a complete dual communications infrastructure, automatic measurement, renewable energy integration, distribution automation and network monitoring. Wireless network to achieve the collection and transmission of real-time data. With flexibility in a wireless sensor network, high detection accuracy, low cost and excellent performance. Therefore, it can be used to develop interesting remote sensing applications. Implementation of sensor networks must meet the flexibility, scalability, cost, equipment, changes in the topology of the environment and energy consumption and other factors and limitations. Wireless sensor network has the flexibility, with high precision sensing, low cost and other excellent characteristics. Therefore, the sensor network must meet the flexibility, scalability, cost, environmental topology changes and energy consumption and other factors. The performance analysis of the topology of the ZigBee wireless network was carried out by using OPNET 14.5 simulators. The network topology of the star, tree and mesh is compared according to the end-to-end delay, throughput, Mac traffic load, and the four parameters of the transmit and receive traffic parameters. In terms of star topology throughput, the MacLoad is higher than the resulting value of the mesh topology, so the use of star topology is considered to be very important. The network types of the star, tree, and grid are

compared according to the end-to-end delay, throughput, MAC traffic load, and the four parameters of the transmit and receive traffic parameters. The star topology is the best in terms of performance and has a MAC load that is similar to the mesh topology. Since the ZigBee network has a large number of nodes, so the use of star topology is considered to be very important.

Acknowledgements

The author would wish to thank the editors and critics for their constructive comments and suggestions. The project was supported by the BETC/Southern Technical University.

Author contributions

I would like to thank Ms. Janan Abd-Ali and Dr. Shaorong Wang for overseeing my studies. Thank you very much, Dear Ms. Sandra Maljavac, and all the staff who have cooperated with you, and I wish you all the best.

A. Appendix

| Set point | Value |
|------------|-------------------------|
| Range | ~2–20% reverse current |
| Time delay | Adjustable 0–20 seconds |

Table A1.
Technical data for reverse power monitoring.

| Microgrid | Parameters | Value |
|-------------|----------------|---|
| Generator | Voltage | 11 k V L-L, S = 200 MVA |
| Transformer | Voltage | V_P/V_S (L-L) = 11 kV/220 kV |
| | Frequency | 60 Hz |
| Feeders | Line impedance | R = 0.02 X, L = 0.64 mH |
| | 15 km feeder | R/km = 0.4 Ω , X/km = 0.3 Ω |
| Load | Dyn load | 10 MW, 3 Mvar |

Table A2.
Microgrid simulator parameters [1].

IntechOpen

Author details

Ali Hadi Abdulwahid^{1,2}

1 Engineering Technical College, Southern Technical University, Basra, Iraq

2 School of Electrical and Electronic Engineering, Huazhong University of Science and Technology, Wuhan, Hubei Province, China

*Address all correspondence to: dr.alhajji_ali@yahoo.com

IntechOpen

© 2019 The Author(s). Licensee IntechOpen. This chapter is distributed under the terms of the Creative Commons Attribution License (<http://creativecommons.org/licenses/by/3.0>), which permits unrestricted use, distribution, and reproduction in any medium, provided the original work is properly cited. 

References

- [1] Abdulwahid AH, Wang S. A novel method of protection to prevent reverse power flow base on neuro-fuzzy network for smart grid. MDPI, Sustainability. 2018;**10**:1059. DOI: 10.3390/su10041059
- [2] Abdulwahid A, Wang S. Application of differential protection technique of domestic solar photovoltaic based microgrid. International Journal of Control and Automation. 2016;**9**:371-386
- [3] Khan MS, Woo M, et al. Smart city and smart tourism: A case of Dubai. Sustainability. 2017;**9**(12):2279. DOI: 10.3390/su9122279
- [4] Baronti P, Pillai P, Chook VSC, Gotta SA, Hu YF. Wireless sensor networks: A survey on the state of the art and the 802.15.4 and ZigBee standards. Computer Communications. 2007;**30**:1655-1695
- [5] Akram U, Khalid M, Shafiq S. Optimal sizing of a wind/solar/battery hybrid grid-connected microgrid system. IET Renewable Power Generation. 2018;**12**(1):72-80
- [6] Leccese F. Remote-control system of high efficiency and intelligent street lighting using a ZigBee network of devices and sensors. IEEE Transactions on Power Delivery. 2013;**28**(1):21-28. DOI: 10.1109/TPWRD.2012.2212215. ISSN: 0885-8977
- [7] Cagnetti M, Leccese F, Proietti A. Energy saving project for heating system with ZigBee wireless control network. In: 11th International Conference on Environment and Electrical Engineering; 2012. pp. 580-585. DOI: 10.1109/EEEIC.2012.6221443
- [8] Mishra BC, Panda AS, Rout NK. A novel efficient design of intelligent street lighting monitoring system using ZigBee network of devices and sensors on embedded internet technology. In: 14th International Conference on Information Technology; 2015. pp. 200-205. DOI: 10.1109/ICIT.2015.37
- [9] Kaleem Z, Ahmad I, Lee C. Smart and energy efficient led street light control system using ZigBee network. In: 12th International Conference on Frontiers of Information Technology; 2014. pp. 361-365. DOI: 10.1109/FIT.2014.74
- [10] Qin H, Zhang W. ZigBee-assisted power saving for more efficient and sustainable ad hoc networks. IEEE Transactions on Wireless Communications. 2013;**12**(12):6180-6193. DOI: 10.1109/TW.2013.110813.130035
- [11] Leccese F, Leonowicz Z. Intelligent wireless street lighting system. In: 11th International Conference on Environment and Electrical Engineering; 2012. pp. 958-961. DOI: 10.1109/EEEIC.2012.6221515
- [12] Chen K-L, Chen Y-R, Tsai Y-P, Chen N. A novel wireless multifunctional electronic current transformer based on ZigBee-based communication. IEEE Transactions on Smart Grid. 2017;**8**(4):1888-1897
- [13] Berger LT, Schwager A, Escudero-Garzás JJ. Power line communications for smart grid applications. Journal of Electrical and Computer Engineering. 2013;**2013**:1-16
- [14] Kumar S, Bhattacharyya B, Gupta VK. Present and future energy scenario in India. Journal of The Institution of Engineers (India). 2014;**95**(3):247-254
- [15] Maw HA, Xiao H, Christianson B. A survey of access control models in wireless sensor networks. Journal of Sensor and Actuator Networks.

2014;**3**(2):150-180. DOI: 10.3390/jsan3020150

[16] Callaway E, Gorday P, Hester L. Home networking with IEEE 802.15.4: A developing standard for low-rate wireless personal area networks. *IEEE Communications Magazine*. 2002;**40**:70-77

[17] Youn M, Lee J. Topology control algorithm considering antenna radiation pattern in three-dimensional wireless sensor networks. *International Journal of Distributed Sensor Networks*. 2014;**11**:1-11

[18] Leccese F, Cagnetti M, Trinca D. A Smart City application: A fully controlled street lighting isle based on raspberry-pi card, a ZigBee sensor network and WiMAX. *Sensors*. 2014;**14**(12):24408-24424. DOI: 10.3390/s141224408

[19] Pešović U, Mohorko J. Hidden node avoidance mechanism for IEEE 802.15.4 wireless sensor networks. *Electronic Components and Materials*. 2013;**43**:14-21

[20] Ajay ML. *Fundamentals of Cellular Network Planning and Optimization*. Canada: Willey-Interacience Publication; 2004

[21] Leccese F, Cagnetti M, Calogero A, Trinca D, di Pasquale S, Giarnetti S, et al. A new acquisition and imaging system for environmental measurements: An experience on the Italian cultural heritage. *Sensors*. 2014;**14**(5):9290-9312. DOI: 10.3390/s140509290

[22] Shi JF, Chen M, Yang Z. Power control and performance analysis for full-duplex relay-assisted D2D communication underlying fifth-generation cellular networks. *IET Communications*. 2017;**11**(18):2729-2734

[23] Sharaf H, Zeineldin H, El-Saadany E. Protection coordination for microgrids

with grid-connected and islanded capabilities using communication assisted dual setting directional overcurrent relays. *IEEE Transactions on Smart Grid*. 2018;**9**(1):143-151

[24] Ibrahim ME, Abd-Elhady AM, Power frequency AC. Voltage measurement based on double wound Rogowski coil. *IET-High Voltage*. 2017;**2**(2):129-135. DOI: 10.1049/hve.2016.0091

[25] Farjah E, Givi H, Ghanbari T. Application of an efficient Rogowski coil sensor for switch fault diagnosis and capacitor ESR monitoring in nonisolated single-switch DC-DC converters. *IEEE Transactions on Power Electronics*. 2017;**32**(2):1442-1456. DOI: 10.1109/TPEL.2016.2552039

[26] Leccese F, Cagnetti M, Di Pasquale S, Giarnetti S, Caciotta M. A new power quality instrument based on raspberry-pi. *Electronics*. 2016;**5**:64. DOI: 10.3390/electronics5040064

[27] Abdulwahid A, Wang S. A Busbar differential protection based on fuzzy reasoning system and Rogowski-coil current sensor for microgrid. In: *IEEE PES Asia-Pacific Power and Energy Engineering Conference*. 2016. pp. 194-199. DOI: 10.1109/APPEEC.2016.7779496

[28] Ibrahim M, Abd-Elhady AM. Differential reconstruction method for Power frequency AC current measurement using Rogowski coil. *IEEE Sensors*. 2016;**16**(23):8420-8425. DOI: 10.1109/JSEN.2016.2614352

[29] Aman MM, Jasmon GB, and Khan QA, et al. Modeling and simulation of reverse power relay for generator protection. In: *Power Engineering and Optimization Conference (PEDCO) Melaka, Malaysia, IEEE International*. 2012. pp. 317-322

[30] Ehrenberger J, Svec J. Directional overcurrent relays coordination

problems in distributed generation systems. *Energies*. 2017;**10**(10):1452. DOI: 10.3390/en10101452

[31] Cervantes J, Salazar S, Chairez I. Takagi-Sugeno dynamic Neuro-fuzzy controller of uncertain nonlinear systems. *IEEE Transactions on Fuzzy Systems*. 2017;**25**(6):1601-1615

[32] Kermany SD, Joorabian M, Deilami S, Mohammad ASM. Hybrid islanding detection in microgrid with multiple connection points to smart grids using fuzzy-neural network. *IEEE Transactions on Power Systems*. 2017;**32**(4):2640-2651

[33] Abdulwahid A, Wang S. A novel approach for microgrid protection based upon combined ANFIS and Hilbert space-based Power setting. *Energies*. 2016;**9**(12):1042. DOI: 10.3390/en9121042

[34] Shahgoshtasbi D, Jamshidi MM. A new intelligent Neuro-fuzzy paradigm for energy-efficient homes. *IEEE Systems Journal*. 2014;**8**(2):664-673. DOI: 10.1109/JSYST.2013.2291943

[35] Lin WM, Hong CM, Cheng FS. Fuzzy neural network output maximization control for sensorless wind energy conversion system. *Energy*. 2015;**35**:592-601

[36] Garcia P, Garcia CA, Fernandez LM, Llorens F, Jurado F. ANFIS-based control of a grid-connected hybrid system integrating renewable energies, hydrogen and batteries. *IEEE Transactions on Industrial Informatics*. 2014;**10**:1107-1117

[37] Koraz Y, Gabbar HA. Fault diagnosis of micro energy grids using Bayesian belief network and adaptive neuro-fuzzy interference system. In: *IEEE International Conference on Smart Energy Grid Engineering (SEGE)*; 2017. pp. 14-17. DOI: 10.1109/SEGE.2017.8052790